UNIVERSITY OF TWENTE.

MANGROVE MANIACS
LAC RESTORATION PROJECT

The role of creeks for tidal exchange in the mangrove forest of Lac Bay, Bonaire

Master thesis by Rob van Zee

University of Twente

July 2020

The role of creeks for tidal exchange in the mangrove forest of Lac Bay, Bonaire

MSc thesis

Civil Engineering, Water Engineering and Management group

University of Twente

Rob van Zee

Supervisors:

Ir. R. Gijsman (Rik)	- University of Twente
Dr. Ir. E.M. Horstman (Erik)	- University of Twente
S. Engel (Sabine)	- Mangrove Maniacs
Prof. Dr. D. Van der Wal (Daphne)	- University of Twente

July 2022

Abstract

The mangrove forest in Lac Bay, Bonaire, experiences a die-off of trees in its northern area (Awa di Lodo). This die-off is caused by a combination of hypersaline conditions, long inundation periods and excess sedimentation. It is expected that an increase in the tidal exchange between Lac Bay and Awa di Lodo will decrease the mangrove stressors in Awa di Lodo creating improved environmental conditions for mangroves to grow. The tidal exchange consists of flow through the vegetated forest (sheet flow) and through the creeks (creek flow). Awa di Lodo has two main creeks connections to the forest fringe, the eastern and the western creek system. Due to mangrove roots growing into the creeks in combination with sedimentation, the creeks eventually close off and thereby reduce the creek flow. The Mangrove Maniacs are restoring the creeks in Lac Bay to improve environmental conditions for mangroves and they want a better understanding of the impacts of their work. This study aims to create more insight into the tidal-induced hydrodynamic processes in Lac Bay and the contribution of creeks in the mangrove forest to the tidal exchange.

During a field campaign from January to March 2022 field data were collected on flow velocities, water levels and topographic characteristics of Lac Bay. The field campaign spanned three spring-neap tidal cycles. The analysis of the gathered data was combined with a literature study to investigate the hydrodynamic characteristics in the area. Based on the data from the field campaign, a hydrodynamic model (Delft3D) was built to analyse the effects of tidal creeks restoration on flow velocities, tidal exchange and water levels of Awa di Lodo.

The field measurements show that the tidal wave is diurnal and has a negligible delay propagating through the open water of Lac Bay. In Awa di Lodo, high water is reached on average more than four hours later than in the open bay. During spring tide, the tidal range in the open water is sufficiently large to create an increasing trend in the water level in Awa di Lodo. The water level lowers again when the tidal range decreases during neap tide. Flow velocities in the creeks mainly depend on the water level difference between the open water and Awa di Lodo, meaning that larger water level differences induce larger flow velocities. In addition, the western creek connecting the bay with Awa di Lodo shows a strong flood dominant peak velocity asymmetry, while the eastern creek varies from marginally flood dominant during spring tides, to strongly ebb-dominant during neap tide. A flood dominant tidal duration asymmetry in Awa di Lodo indicates that sheet flow during high tides is responsible for the fast increase of the water level in Aw di Lodo while during low tides the creeks are responsible for the outflow.

The hydrodynamic model simulations of the tidal dynamics in Lac Bay replicate the magnitude of the measured flow velocities in the creeks of Lac Bay. The model does not show the measured ebb flow in the western and centre creek. Water levels in Awa di Lodo are modelled well, except for an overestimation of low water levels and an overestimation of the water level increase. It was found that creeks have a significant influence on the tidal exchange between the open water and Lac Bay. The model showed that the creation of a new creek connection to Awa di Lodo, either by extending the centre creek or by creating a new creek, is found to be the most efficient to increase the tidal exchange. It was concluded that the widening of the creeks, deepening of the creeks or extension of the eastern creek system would have a limited effect on the tidal exchange. Creek restoration is shown to be an effective measure to increase the tidal exchange in the mangrove forest of Lac Bay.

Keywords: Mangroves, Lac Bay, Hydrodynamics, Tidal Exchange, Tidal Asymmetry, Creek

Table of contents

ABSTRACT **3**

LIST OF TABLES **6**

LIST OF FIGURES **6**

1. INTRODUCTION **9**

1.1 PROBLEM DEFINITION 10
1.2 RESEARCH OBJECTIVE 10
1.3 RESEARCH QUESTIONS 11
1.4 RESEARCH METHODOLOGY 11

2. LAC BAY **12**

2.1 TOPOGRAPHIC DESCRIPTION OF LAC BAY 12
2.2 MANGROVE POPULATION 14
2.3 PRECIPITATION AND EVAPORATION 16
2.4 INFLUX IN THE BACKWATER 16

3. DATA COLLECTION **18**

3.1 BATHYMETRY AND TOPOGRAPHY 19
3.2 WATER LEVELS 20
3.3 FLOW VELOCITIES 21
3.4 VEGETATION CHARACTERISTICS 22

4. HYDRODYNAMIC PROPERTIES OF LAC BAY **24**

4.1 SMOOTHENING OF FIELD DATA 24
4.2 TOPOGRAPHY, BATHYMETRY AND HYPSOMETRY 24
4.3 TIDAL CONSTITUENTS 27
4.4 PROPAGATION OF THE TIDAL WAVE THROUGH LAC 28
4.5 CONVERTING PRESSURE DATA INTO WATER LEVELS 32
4.6 THE BATHTUB EFFECT 32
4.7 TEMPORAL AND SPATIAL VARIABILITY IN VELOCITIES 34
4.8 THE RELATION BETWEEN VELOCITY AND WATER LEVEL 36
4.9 TIDAL ASYMMETRY 42

5. DELFT3D MODEL SET-UP **46**

5.1 BOUNDARY CONDITIONS 46
5.2 GRID 47
5.3 RUNTIME 48
5.4 MODEL PARAMETERS, VEGETATION CHARACTERISTICS AND CALIBRATION 48
5.5 MODEL VALIDATION 49

6. CONTRIBUTION OF CREEKS TO THE TIDAL EXCHANGE **51**

6.1 RESIDENCE TIME 53
6.2 REFERENCE SCENARIO 53
6.3 EFFECT OF NO CREEKS 54
6.4 EFFECT OF INCREASING AND DECREASING THE DEPTH OF CREEKS 57
6.5 EFFECT OF INCREASING AND DECREASING THE WIDTH OF CREEKS 58
6.6 EFFECT OF EXTENDING THE CENTRE CREEK 60
6.7 EFFECT OF A NEW CREEK THROUGH THE MANGROVE FOREST 62
6.8 EFFECT OF EXTENDING THE EASTERN CREEK 65
6.9 OVERVIEW OF THE DIFFERENT SCENARIOS 67

7. DISCUSSION 69

7.1 CURRENT SITUATION 69
7.2 MODEL SETUP 71
7.3 CREEK RESTORATION SCENARIOS 74
7.4 FIELD MEASUREMENTS 75

8. CONCLUSIONS 77

9. RECOMMENDATIONS 79

10. REFERENCES 81

List of tables

Table 1: Information on the deployed instruments during the field study 18
Table 2: Data on the mangrove root characteristics for the 14 1-by-1 plots 22
Table 3: Dominant tidal constituents per measurement location 28
Table 4: Median and mean delay of the tidal wave with respect to Cai including the standard deviation 30
Table 5: Water level corrections for CF and EF, based on the water levels of WF for all three spring-neap cycles .. 32
Table 6: Interval of the ebb and flood direction in the creeks 37
Table 7: Vegetation characteristics as used in the model 49
Table 8: Overview of flow speeds for the 'deep creek' and 'shallow creek' scenario for ebb and flood at WC, CC and EC 58
Table 9: Overview of maximum flow speeds for the 'wide creek' and 'narrow creek' scenario for ebb and flood at WC, CC and EC 60
Table 10: Tidal exchange, residence time and the ratio of the residence time compared to the reference scenario of each modelled scenario. Red coloured rows indicate a decrease in tidal exchange and blue coloured rows indicate an increase in tidal exchange. A darker shade implies a greater decrease/increase. 67
Table 11: Average mangrove root characteristics for the red and black mangrove 72

List of figures

Figure 1: Satellite image of Lac Bay, Bonaire 9
Figure 2: Overview of the order of the report 11
Figure 3: Naming of locations in Lac Bay with the grey areas representing the mangrove population, adjusted from van Moorsel & Meijer (1993) 12
Figure 4: Windrose of Bonaire measured from November 2016 till April 2022 (Data from KNMI (2022)) 13
Figure 5: Healthy mangrove trees in the forest fringe (left) and dead mangrove trees on the northern side of Lac Bay (right) 14
Figure 6: The stilt roots of the Rhizophora mangle (red mangrove) in Kreek di Pedro (left) and the pneumatophore roots of the Avicennia germinans (black mangrove) in Awa di Lodo (right) 14
Figure 7: Map of change in mangrove vegetation cover in Lac Bay between 1961 and 1996 (Erdmann & Scheffers, 2006) 15
Figure 8: Catchment area of Lac Bay with an indication of the water streams (Wentink & Wulfsen, 2011) 16
Figure 9: Placement of instruments over Lac Bay, the naming of the locations and the marked mangrove area based on own observations 19
Figure 10: Gathering water depth data with the ADCP in the creeks of Lac Bay 20
Figure 11: A Tilt Current Meter (TCM) attached to a paver near Cai 21
Figure 12: Locations of the vegetation plots 22
Figure 13: Interpolated creek profile from ADCP field measurements 25
Figure 14: Full hypsometry of Lac Bay 25
Figure 15: Zoomed-in hypsometry of Lac Bay 26
Figure 16: Bathymetry of Lac Bay ranging from -1.1m to 0.5m+LVD (left) and -20m to 1m+LVD (right) 27
Figure 17: Differences in moment of high tide (green dots) between the forest fringe (WF) and Awa di Lodo (BW) .. 29
Figure 18: Spatial representation of the median delays of the tidal wave with respect to Cai 31
Figure 19: Boxplot of the tidal wave delay data per location with respect to Cai 31
Figure 20: Overview of heights and depth used to calculate water level 32
Figure 21: Water levels of the forest fringe (WF) and Awa di Lodo (BW) during the field study (21 January – 7 March) 33
Figure 22: Maximum water level of Awa di Lodo plotted against the maximum water depth at Cai per tidal cycle for period 1 (left), period 2 (middle) and period 3 (right) with dots indicating periods in the spring-neap cycle (dark blue – start of the cycle; standard blue –spring tide; light blue – end of the cycle) 34
Figure 23: Velocity rose of Cai 34
Figure 24: Velocity roses of WF (left) and Kreek di Taco (WC)(right) 35
Figure 25: Velocity roses of CF (left) and CC (right) 35
Figure 26: Velocity roses of EF (left) and Kreek di Taco (EC) (right) 36

Figure 27: Water levels of the forest fringe (WF) and Awa di Lodo (BW) for the period 28 January – 3 February.... 37
Figure 28: Water level difference between the forest fringe (WF) and Awa di Lodo on the left axis and the velocity in Kreek di Taco (EC) on the right axis 38
Figure 29: Water level difference between the forest fringe (WF) and Awa di Lodo on the left axis and the velocity in Kreek di Pedro (WC) on the right axis..... 38
Figure 30: Water level difference between the forest fringe (WF) and Awa di Lodo (BW) (upper figure), the flow velocities in Kreek di Taco (EC) (middle figure) and the flow velocities in Kreek di Pedro (WC) (lower figure).. 40
Figure 31: Tidal stage-flow speed curves of WC during spring tide for all three spring-neap cycles with the blue dots being the maximum ebb velocities and the red dots the maximum flood velocities of a tidal cycle..... 41
Figure 32: Tidal stage-flow speed curves of EC during spring tide for all three spring-neap cycles with the blue dots being the maximum ebb velocities and the red dots the maximum flood velocities of a tidal cycle..... 42
Figure 33: Flow velocities at Kreek di Pedro (WC) and Kreek di Taco (EC) 43
Figure 34: Peak velocity asymmetry of Kreek di Taco (EC)..... 44
Figure 35: Peak velocity asymmetry at Kreek di Pedro (WC) 44
Figure 36: Tidal duration asymmetry as observed in Awa di Lodo (BW) between 31 January and 1 February with the grey circle and arrow depicting the duration of flood and the yellow circle and arrow depicting the duration of ebb..... 45
Figure 37: Model domain of Lac Bay with the landward boundary in yellow and the seaward boundary in blue..... 46
Figure 38: Comparing the water level data of the measurement stations Sea and WF 47
Figure 39: Grid of the Delft3D model going from 20-by-20 meters on the left and right side, to 2.5-by-2.5 meter inside the creeks..... 47
Figure 40: Water level in Awa di Lodo per grid refinement in model runs without vegetation and a Manning bottom roughness value of 0.023 48
Figure 41: Water level in Awa di Lodo per grid refinement in model runs with vegetation and a Manning bottom roughness value of 0.030 49
Figure 42: Water levels in Awa di Lodo for the reference situation and the measured water level (left); and the tidal exchange for the reference scenario (right) for three spring-neap cycles..... 50
Figure 43: Measured and modelled water velocities of WC (left), CC (middle) and EC (right)..... 50
Figure 44: The reference creek profile with the adjusted creek profiles for the creek restoration scenarios 51
Figure 45: Manually drawn transect in blue over which the modelled tidal exchange is calculated 52
Figure 46: A comparison between the water level in Awa di Lodo and the cumulative discharge of the reference scenario 52
Figure 47: Water levels in Awa di Lodo for the reference situation and the measured water level (left); and the tidal exchange for the reference scenario (right) 54
Figure 48: Snapshot of the bed level elevation in the 'no creeks' scenario 55
Figure 49: Water levels in Awa di Lodo for the reference situation, the 'no creeks' scenario and the measured water level (left); and the tidal exchange for the reference scenario and the 'no creeks' scenario (right) 56
Figure 50: Water velocities of the reference scenario, measured in the field and of the 'no creeks' scenario for WC (left), CC (middle) and EC (right) 56
Figure 51: Water levels in Awa di Lodo for the reference situation, the 'deep creeks' scenario, the 'shallow creeks' scenario and the measured water level (left); and the tidal exchange for the reference scenario, the 'deep creeks' scenario and the 'shallow creeks' scenario (right)..... 57
Figure 52: Water velocities of the reference scenario, measured in the field, of the 'deep creeks' scenario and of the 'shallow creeks' scenario for WC (left), CC (middle) and EC (right)..... 58
Figure 53: Water levels in Awa di Lodo for the reference situation, the 'wide creeks' scenario, the 'narrow creeks' scenario and the measured water level (left); and the tidal exchange for the reference scenario, the 'wide creeks' scenario and the 'narrow creeks' scenario (right) 59
Figure 54: Water velocities of the reference scenario, measured in the field, of the 'wide creeks' scenario and of the 'narrow creeks' scenario for WC (left), CC (middle) and EC (right) 59
Figure 55: Bed level elevation of the Delft3D model in the 'extended centre creek' scenario..... 60
Figure 56: Water levels in Awa di Lodo for the reference situation, the 'extended centre creek' scenario and the measured water level (left); and the tidal exchange for the reference scenario and the 'extended centre creek' scenario (right) 61

FIGURE 57: WATER VELOCITIES OF THE REFERENCE SCENARIO, MEASURED IN THE FIELD AND OF THE 'EXTENDED CENTRE CREEK' SCENARIO FOR WC (LEFT), CC (MIDDLE) AND EC (RIGHT) 62
FIGURE 58: BED LEVEL ELEVATION OF THE DELFT3D MODEL IN THE 'NEW CREEK' SCENARIO 62
FIGURE 59: WATER LEVELS IN AWA DI LODO FOR THE REFERENCE SITUATION, THE 'NEW CREEK' SCENARIO AND THE MEASURED WATER LEVEL (LEFT); AND THE TIDAL EXCHANGE FOR THE REFERENCE SCENARIO AND THE 'NEW CREEK' SCENARIO (RIGHT) 63
FIGURE 60: WATER VELOCITIES OF THE REFERENCE SCENARIO, MEASURED IN THE FIELD AND OF THE 'NEW CREEK' SCENARIO FOR WC (LEFT), CC (MIDDLE) AND EC (RIGHT) 64
FIGURE 61: FLOW VELOCITIES IN THE CREATED CREEK IN THE REFERENCE SITUATION AND IN THE 'NEW CREEK' SCENARIO 64
FIGURE 62: BED LEVEL ELEVATION OF THE DELFT3D MODEL IN THE 'EASTERN CREEK EXTENSION' SCENARIO 65
FIGURE 63: WATER LEVELS IN AWA DI LODO FOR THE REFERENCE SITUATION, THE 'EXTENDED EASTERN CREEK' SCENARIO AND THE MEASURED WATER LEVEL (LEFT); AND THE TIDAL EXCHANGE FOR THE REFERENCE SCENARIO AND THE 'EXTENDED EASTERN CREEK' SCENARIO (RIGHT) 66
FIGURE 64: FLOW VELOCITIES OF THE REFERENCE SCENARIO, OF THE 'EXTENDED EASTERN CREEK' SCENARIO AND MEASURED IN THE FIELD FOR WC (LEFT), CC (MIDDLE) AND EC (RIGHT) 66
FIGURE 65: WATER LEVELS IN AWA DI LODO FOR THE REFERENCE SITUATION, ALL SCENARIOS AND THE MEASURED WATER LEVEL (LEFT); AND THE TIDAL EXCHANGE FOR THE REFERENCE SCENARIO AND ALL SCENARIOS (RIGHT) 67
FIGURE 66: WATER LEVELS IN AWA DI LODO FOR 31 JANUARY AND 1 FEBRUARY FOR THE REFERENCE SITUATION, ALL SCENARIOS AND THE MEASURED WATER LEVEL (LEFT); AND THE TIDAL EXCHANGE FOR THE REFERENCE SCENARIO AND ALL SCENARIOS (RIGHT) . 68

1. Introduction

Mangroves are increasingly being recognised as a cost-effective and sustainable addition to coastal safety (Gijsman et al., 2021). Next to their contribution to coastal safety, mangrove forests are highly productive ecosystems that function as carbon sinks and are home to a variety of species. Mangroves promote ecological diversity while also being economically valuable to humanity (Ashton & Macintosh, 2002; Bennett & Reynolds, 1993; Senger et al., 2021). The number of ecosystem services mangroves provide outnumbers their disservices and by doing so, mangrove forests contribute to the United Nations' Sustainable Development Goals (SDGs) (Friess et al., 2020; Gijsman et al., 2021). They can help in achieving SDG 1 (End Poverty), SDG 2 (End Hunger), SDG 8 (Economic Prosperity), SDG 13 (Climate Action) and SDG 14 (Life Below Water). However, mangrove forests are being converted on a global scale, mainly to make way for agriculture and aquaculture (Adame et al., 2021; Lee, 1999). By removing mangrove forests the services they provide to humanity and nature vanish as well. Other threats like sea-level rise, erosion, changes in sediment fluxes, and hydrological regime changes can also have severe impacts on mangrove forests (Jennerjahn et al., 2017; Lucas et al., 2017).

To maintain and restore mangrove forests, so their ecosystem services remain intact, an understanding of how to restore these systems must be obtained. Hydrodynamics play a major role in mangrove habitat suitability and is therefore important to consider by coastal managers (Cannon et al., 2020). Van Loon et al. (2016) mention that many restoration projects partly fail because the local hydrodynamics are not taken into consideration. Not considering the hydrodynamics in these projects can partly be due to ignorance, but also an important reason is that the hydrodynamics are hard to monitor, quantify and modify.

Figure 1: Satellite image of Lac Bay, Bonaire

This thesis investigates a mangrove forest in Bonaire, located in the southern Caribbean, 90 km off the Venezuelan coast. This tropical island is home to several RAMSAR sites of which Lac Bay is the largest. Figure 1 displays Lac Bay: a clear water lagoon located on the southeast side of Bonaire. Lac Bay is an 824 hectares shallow inland bay surrounded by a buffer zone of 500 m (726 ha), including 183 ha of

Caribbean sea (Ramsar, 2022). Combined, Lac and the buffer zone make up 1550 hectares of protected area containing multiple connected ecosystems such as coral reefs, seagrasses, and mangroves.

On the northern side of Lac, the mangrove forest experiences a die-back (Debrot et al., 2010). High evaporation rates and limited water inputs cause the water in the back of the forest to become hypersaline while excess sedimentation also occurs in the area (Slijkerman et al., 2011). To prevent further die-back and to increase the chances of mangroves repopulating in the backwater of Lac, channels are being opened by the Mangrove Maniacs to reconnect the backwater with the bay. This is done to keep the water flowing through the forest and to increase the tidal exchange with the backwater. However, the hydrodynamic behaviour of Lac Bay is not yet fully understood, let alone the effects the clearing of (new) creeks will have. This research looks into the hydrodynamics of the tides in Lac Bay and how the clearing of (new) channels could increase the tidal exchange in the area.

1.1 Problem definition

The catchment of Lac is prone to non-sustainable overgrazing by livestock (Debrot et al., 2012). Overgrazing has depleted the area of ground cover vegetation resulting in the wind, vehicle traffic, and rainwater mobilizing and transporting sediment into the backwater of Lac, clogging creeks and lagoons and negatively affecting the tidal exchange (Slijkerman et al., 2011). Sediment deposition in the creeks and mangrove roots growing into the creeks eventually close off these creeks, reducing the hydrological connectivity between the front and the back of the forest even further. Reduced water circulation in Lac combined with high evaporation rates and a low influx of freshwater creates hypersaline conditions in the backwater of Lac called Awa di Lodo (van Moorsel & Meijer, 1993; van Winsen, 2013; Wösten, 2013). Hypersaline conditions, long inundation periods and excess sedimentation in Awa di Lodo have resulted in a die-back of the mangrove forest. This die-back results in the loss of ecologically valuable area and reverses the mangrove's function as carbon sink (Senger et al., 2021). Previous studies into possible solutions to this problem have shown that increasing the inflow of freshwater runoff by the removal of a dam in the catchment would only have limited effects on the hypersaline conditions in the backwater (Vreugdenhil, 2013). Removal of a dam could even create a large inflow of sediments from the dam basin into the backwater of Lac (Lott, 2001).

Van Winsen (2013) shows that tidal fluctuations have a high correlation with salinity levels in Awa di Lodo. Multiple studies agree that the most effective measure to decrease salt stress in Awa di Lodo is to increase the tidal water exchange (Debrot et al., 2010; van Winsen, 2013; Vreugdenhil, 2013; Wösten, 2013). Following these studies, the Mangrove Maniacs are now trying to improve the water circulation in the back of the forest by removing organic debris, cutting roots from the existing creeks and by digging new channels in an attempt to increase tidal exchange (Debrot et al., 2010). However, the effects of increased water circulation through these channels are mostly uncertain and cannot be quantified by a simple model (Regensburg, 2013). Other studies show that restoring the tidal exchange contributes to increasing biomass of mangroves (Taylor et al., 2021). It is yet unclear to what extent the existing creeks contribute to the tidal exchange in Lac Bay and to what extent creek restoration can improve the tidal exchange in Lac Bay.

1.2 Research objective

This research aims to obtain insight into the hydrodynamic behaviour of Lac Bay by looking at the contribution of creeks and creek restoration to the tidal water exchange throughout the mangrove forest. This research will provide key insights into the potential benefits of creek restoration to the survival and re-establishment of mangroves in the backwaters of Lac Bay. These insights will also form a starting point for further research into e.g. sediment transport, bed level changes, and the subsequent ecological development of Lac Bay.

1.3 Research questions

To reach the stated research objective the following research question is proposed:

To what extent do existing creeks contribute to the tidal exchange in the mangrove forest of Lac Bay and how does creek restoration affect this tidal exchange?

This main research question forms the basis for this report. The three research questions stated below are proposed to structure this report.

1. What **physical characteristics** affect the tidal dynamics of the Lac Bay mangroves?
    a. What are the characteristics of the mangroves in Lac Bay?
    b. What are the topographic characteristics of Lac Bay?
    c. What is the dominant tidal constituent?
2. What are the **spatial and temporal effects** of the tidal dynamics in the Lac Bay mangroves?
    a. How does the tidal wave propagate through the mangrove forest?
    b. How do different phases of the spring-neap cycle affect the water levels in the forest and the velocities in the creeks?
    c. What is the temporal and spatial variation in velocity and tidal water levels?
    d. What is the relation between water velocity in the creeks and tidal water levels?
    e. To what extent is tidal asymmetry present?
3. To what extent do **creeks** contribute to the **tidal exchange** in the Lac Bay mangroves and can the tidal exchange be increased by creek restoration?
    a. How does the tidal exchange behave if there are no creeks through the mangrove forest?
    b. What is the effect of the width and depth of the existing creeks on the tidal exchange?
    c. What is the effect of extending the existing creek system on the tidal exchange?
    d. What are possible implications of an increased tidal exchange for the development of the Lac Bay mangroves?

1.4 Research methodology

Answering the main research question will be done by following a systematic approach guided by the research questions (Figure 2). First, in chapter 2, a literature research will be done which will describe the study area. Chapter 3 describes the collection and processing of field data. This will include the deployment of instruments and data collection techniques. Then, in chapter 4, important geographical and hydrodynamic characteristics of Lac Bay will be described by analysing the field data. Chapters 2 and 4 combined will answer the first two research questions. In chapter 5 will be explained how the numerical model of the study is set up. Lastly, in chapter 6, the numerical model will be used to quantify the contribution of creeks to the tidal exchange in the Lac Bay mangroves and the potential effects of creek restoration, thus answering the third research question.

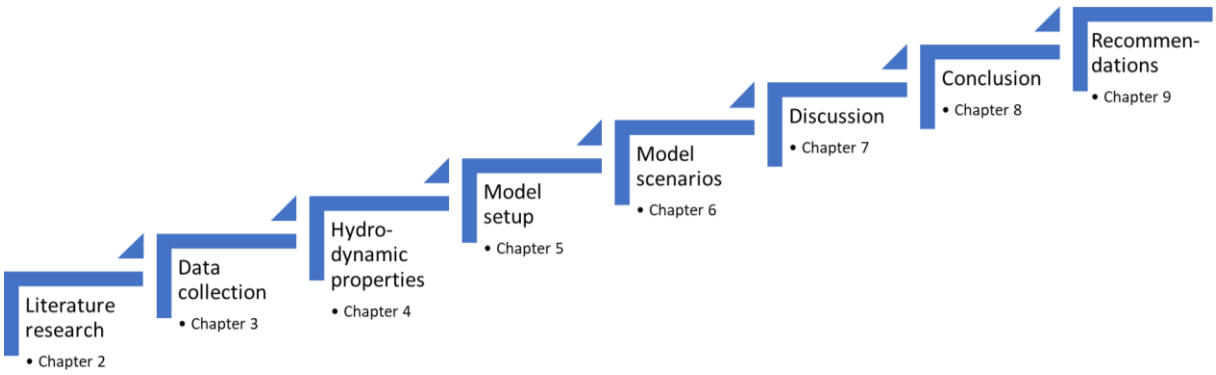

Figure 2: Overview of the order of the report

2. Lac Bay

Before long, the largest clear water lagoon in Caribbean Netherlands was largely unknown. Lac Bay had no meaning for shipping and there was little to no development for recreation (Hummelinck & Roos, 1969). Lac was hard to reach and mainly known for its Conch shell piles, left behind by Venezuelan fishermen because of weight savings (van Moorsel & Meijer, 1993). Later, in 1951, when roads were constructed, Lac became more accessible to the general public (Lott, 2001). Back in the days, Cai, located on the south-eastern side of Lac (Figure 3), was used as a base for fishermen and this has not changed. Multiple families still use Cai as their base for fishing. Nowadays, Cai and Sorobon are visited often by tourists to enjoy the white beaches and practise windsurfing (Wentink & Wulfsen, 2011).

Figure 3: Naming of locations in Lac Bay with the grey areas representing the mangrove population, adjusted from van Moorsel & Meijer (1993)

2.1 Topographic description of Lac Bay

Lac Bay is a lagoon protected from incoming waves by a coral reef at the seaside. The reef breaks the waves resulting in calm water conditions in the bay while also being a nursery for fish (Debrot et al., 2010). Between the coral reef and Cai, there is a small, deep opening, Boca di Lac. Inside Lac, there are vast seagrass fields which support a diversity of fish, invertebrates and turtles. Figure 4 shows that throughout the year there is an easterly wind. During the rainy season, which lasts from October to December, the average wind speeds are higher (8 m/s) than during the dry season (5 m/s).

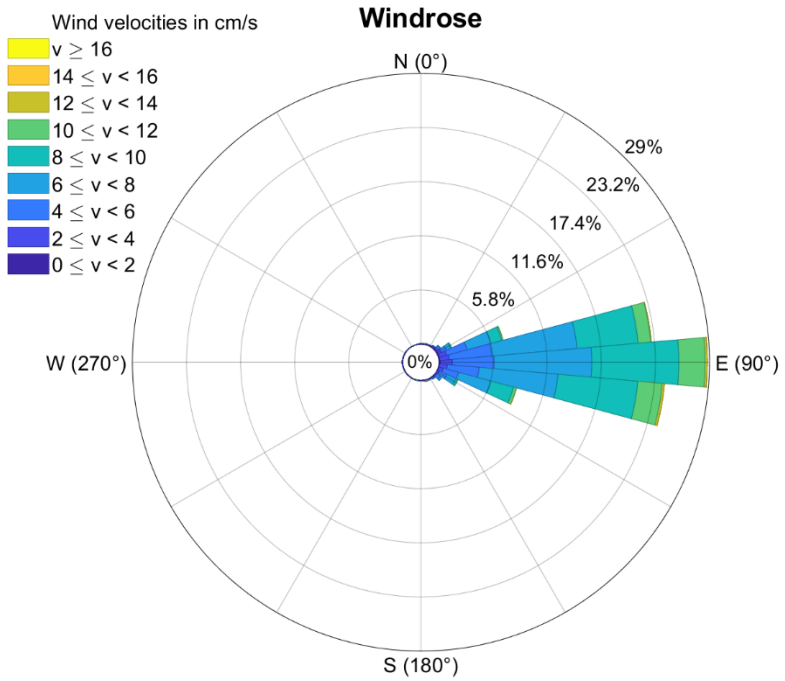

Figure 4: Windrose of Bonaire measured from November 2016 till April 2022 (Data from KNMI (2022)*)*

Located in the mangrove forest (Figure 3), a total of 5 islands are found in Lac: Isla di Pedro, Isla Rancho, Isla Fogon, Isla di Chico and Isla di Yuwana. The first four form a barrier for the tide which is not able to propagate further into Lac because of the landmasses. Based on figures from Hummelinck & Roos (1969), these four islands formed the shoreline in the early 20th century. When a tidal wave reached the islands, the water would flow through creeks via Kreek di Pedro and Kreek di Coco to Awa di Lodo. Gaps in between Isla Fogon & Isla Rancho and Isla Fogon & Isla di Chico had this function as well, but over time these gaps are silted up and overgrown by the expanding mangrove forest. Remnants of creeks in between those islands can still be seen in aerial photographs.

Puitu is prone to the expansion of mangrove trees as well. Puitu once had an open connection to the open water of Lac and was used by ships to get salt from the Salinas (Hummelinck & Roos, 1969). Now the entrance is overgrown and ships cannot reach Puitu anymore. Boca Fogon and Boca di Coco will suffer the same fate over time as they are slowly getting enclosed by mangrove trees.

Figure 3 shows that behind the islands a large area is covered by mangroves and there are two 'muddy' ('lodo' in Papiamentu) water areas: Awa Lodo di San José and Awa Lodo di Bakuna. Due to more die-offs of mangroves in that area, these are now often considered as one larger area: Awa di Lodo or the backwater. Awa di Lodo characterises itself by shallow, hypersaline water with dead mangrove trees (Figure 5), and as an area that has poor connection with the open water of Lac Bay. The sediment that erodes from the catchment of Lac Bay mostly ends up in Awa di Lodo by wind and rain. Despite the harsh conditions, Awa di Lodo is home to several fish species and submerged vegetation. It attracts several bird species like herons, flamingos and ducks (Lott, 2001). Conversely, Awa Yuwana and to a lesser extent Awa Wanapa are connected by Kreek di Pedro to the open water of Lac and have therefore more tidal influence than Awa di Lodo.

Figure 5: Healthy mangrove trees in the forest fringe (left) and dead mangrove trees on the northern side of Lac Bay (right)

On the west side of Lac Bay, from Punta Kalbas to Mangel Altu, there used to be a fine, white sandy shore. In the second part of last century, mangroves colonized this shore (Lott, 2001). Now few of the highest mangroves of Lac can be found at that site. In March 2022 some of these mangroves have been cut down to accommodate the removal of excess sargassum from Lac.

2.2 Mangrove population

Mangrove trees can survive harsh conditions where most other plants cannot survive. Mangroves grow in coastal areas where the water is salty, the air is warm and the soil has low-oxygen concentrations (Smithsonian, 2018). Having an above-ground root system ensures that mangroves can take the oxygen they need out of the air by lenticels on the mangroves' root surface (Duke, 2017). Above-ground root systems in mangroves exist in multiple forms. Stilt roots, like those of the *Rhizophora* species, grow from the trunk or branch towards the water into the soil and are mainly found in areas where the tide at least daily floods the area. Pneumatophores (or cone roots or taproots), like the *Avicennia* species has, are pencil-like roots that stand up vertically. Pneumatophore roots are growing upwards from underground lateral roots and are mainly found further inland than the *Rhizophora* species because the cone roots cannot handle longer inundation periods (Smithsonian, 2018). To be able to withstand the salt water, mangrove trees use two different tactics. Species like the *Avicennia* get rid of excess salt by excreting it through their leaves. Other species, like the *Rhizophora*, have a barrier in their roots that exclude the salt from the seawater so it does not enter its vascular system (Duke, 2017; Smithsonian, 2018).

Figure 6: The stilt roots of the Rhizophora mangle (red mangrove) in Kreek di Pedro (left) and the pneumatophore roots of the Avicennia germinans (black mangrove) in Awa di Lodo (right)

Lac is host to three mangrove species and one mangrove associate (Augustinus, 2005; Davaasuren & Meesters, 2012; Lott, 2001; MacRae & de Meyer, 2006; van Moorsel & Meijer, 1993). *Rhizophora mangle* (red mangrove) is the dominant species at Lac's shoreline while the *Avicennia germinans* (black mangrove) is the dominant species in the interior area (Figure 6). *Conocarpus erectus* (buttonwood) is a mangrove associate and grows in drier areas often in combination with the red or black mangrove. Mixtures of *Avicennia germinans* and *Laguncularia racemosa* (white mangrove) are found in muddy and higher laying saline soils (Davaasuren & Meesters, 2012). The difference in preference of location concerning inundation and salinity regimens causes these trees to occupy different zones of the forest (Alongi, 2009). The *Rhizophora* species is much better resistant against longer inundation periods and greater water level fluctuations than the other species (Lodder, 2013). At higher elevations and higher salinity concentrations, the *Avicennia* and *Laguncularia* species do better than *Rhizophora.* The *Conocarpus* species can be found at the edges of the mangrove forests where the mangrove species have a hard time surviving. This zonation is a result of succession, geomorphology, physiological ecology and population dynamics (Snedaker, 1982). In Lac, there is still a lot of activity happening with growth towards the open water and die-back in Awa di Lodo resulting in a dynamic zonation.

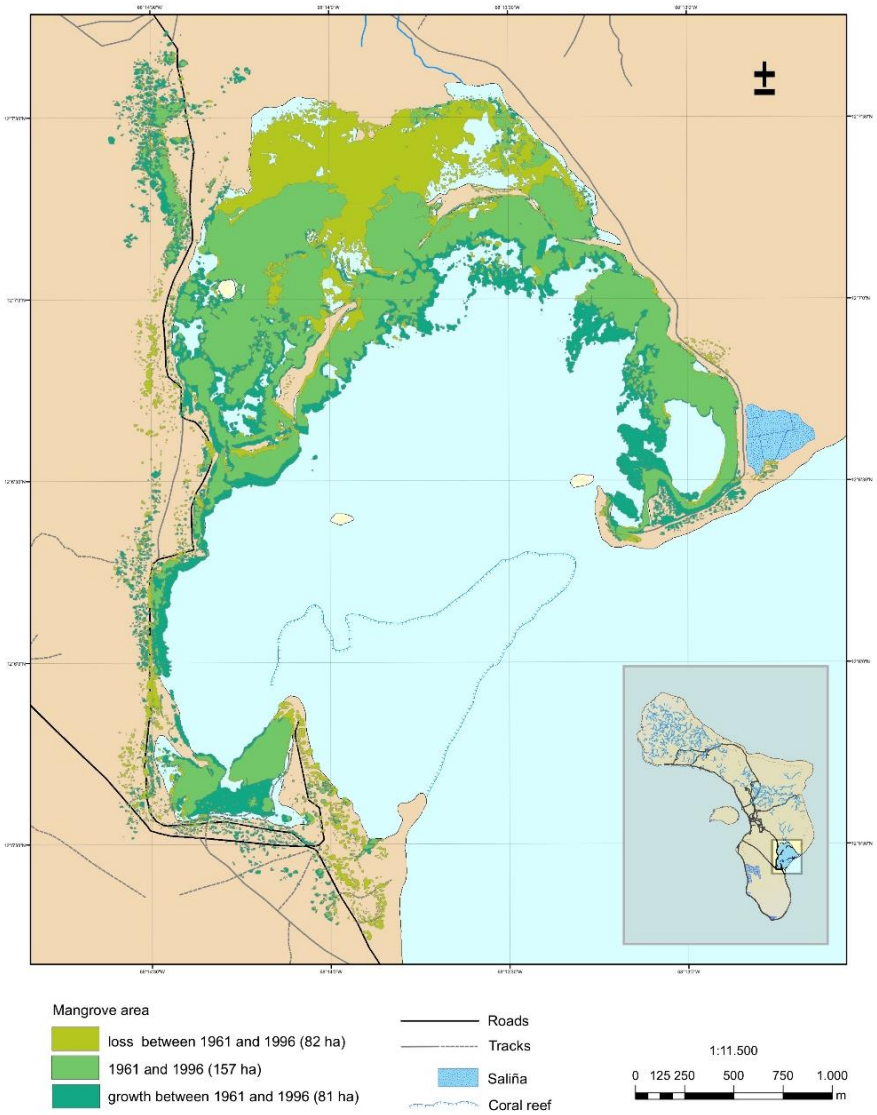

Figure 7: Map of change in mangrove vegetation cover in Lac Bay between 1961 and 1996 (Erdmann & Scheffers, 2006)

In the same period, mangrove growth was observed in the direction of the lagoon and an area of 81 ha was added to the mangrove forest. Lott (2001) notes that due to the growth towards the bay the overall mangrove population increased. One of the goals set by STINAPA (2014) is to restore hydrological conditions so previously present mangrove trees can restore which would again increase the total mangrove population. This growth will be limited to previously occupied areas by mangroves and there will be no growth further into the open water. To achieve this, one of the methods used is to remove the mangrove propagules from these areas (STINAPA, 2014).

2.3 Precipitation and evaporation

The average annual precipitation in Bonaire is 470 mm of which 55% occurs in the rainy season which lasts from October to December (measured for the period 1971-2004) (Borst & de Haas, 2005). There is a large variation in the average annual precipitation, ranging from 190 mm to 1200 mm. The average annual potential evaporation is 2600 mm.

2.4 Influx in the backwater

The inflow of freshwater in Lac is dependent on groundwater flow and precipitation runoff (Vreugdenhil, 2013). Of the precipitation, 10% runs off via the surface and 5% infiltrates into groundwater, the other 85% evaporates (Grontmij & Sogreah, 1968). Figure 8 displays the catchment of Lac which covers 22.6 km^2. In 1952, in the catchment of Lac, a dam and a road were constructed with two goals: to make Cai more accessible during the rainy season, since the precipitation formed a sheet flow over the area making it hard to enter during and shortly after rainfall (Lott, 2001), and to use the precipitation captured by the dam for agriculture (van Moorsel & Meijer, 1993). These constructions reduced the runoff towards Awa di Lodo from the Bakuna area ($1.5 \bullet 10^6$ m^3/y) and the Lima area (10^6 m^3/y) by 50% (Lott, 2001; van Moorsel & Meijer, 1993). This would result in an annual influx from the catchment of 1.25×10^6 m^3 annually. However, Debrot et al. (2010) mention that the water behind dams in the catchment is mostly lost through evaporation, and groundwater penetration is minimal, so the actual influx could be much lower.

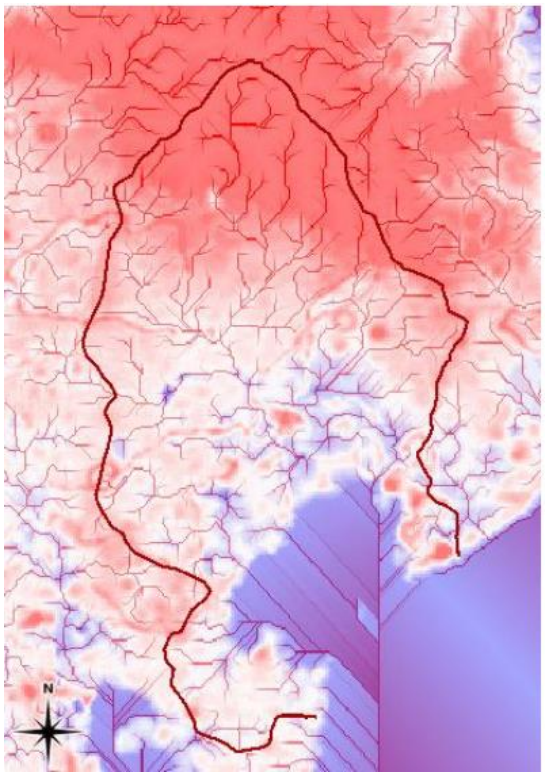

Figure 8: Catchment area of Lac Bay with an indication of the water streams (Wentink & Wulfsen, 2011)

Groundwater flow in the catchment is affected by the many wells in the catchment (Debrot et al., 2012). The response of groundwater to external effects is highly dependent on the location. In the northern part of the catchment, groundwater has a strong response to precipitation but poor hydraulic contact with Lac Bay. In the southern part of the catchment, groundwater has a weak response to precipitation but has a high response to the tides (Rønde, 2013).

Few studies consider the influx through tidal creeks into the backwater of Lac Bay. What is known is that the salinity levels of the backwater have a high correlation with the tidal fluctuation with the eastern creek having a greater influence than the western creek (van Winsen, 2013). The salinity levels in the backwater are much lower near channels compared to the rest of the backwater which indicates that Awa di Lodo has bad mixing. Lott (2001) observed that there is also tidal overwash across the central island of Isla di Chico towards the backwater where bay water mixes with the water from Awa di Lodo. To remove mangrove stress factors in the backwater like high salinity, anaerobic conditions, and high water temperature the water circulation must be improved (Wösten, 2013). Improvement of water circulation will reduce or remove these stress factors and allow mangrove vegetation to recover. An example of this is the opening of the Kreek di Taco in 2018 which likely reduced the stress factors and avoided the mass fish die-off observed by Lott (2001) that occurred annually (Engel (2022), pers. comm.).

3. Data collection

To answer the formulated research questions, measurements were conducted in Lac Bay, Bonaire. The fieldwork was conducted in cooperation with Rik Gijsman (University of Twente), Sabine Engel (Mangrove Maniacs) and Erik Horstman (University of Twente) from mid-January 2022 to the beginning of March 2022. This section describes the fieldwork methods used. To map bed levels and monitor the hydrodynamics of Lac Bay, monitoring equipment was brought to Bonaire. Table 1 contains a complete overview of the deployed instruments and Figure 9 the spatial distribution.

Table 1: Information on the deployed instruments during the field study

Equipment	Is measuring …	Sampling frequency [Hz]	Location
HOBO U20L-04 Water Level Data Logger (Onset, 2022)	Water pressure (Water depth) at the deployment location Atmospheric pressure at the deployment location	1/300 (continuous)	Awa di Lodo (BW) Centre creek (CC) Awa di Lodo (BW)
TCM-4, Shallow Water Tilt Current Meter (Lowell Instruments LLC, 2022)	Flow speeds and flow directions at the deployment location	1/120 (average of a 30-second burst at 8 Hz)	West creek (WC) West fringe (WF) Centre fringe (CF) Centre creek (CC) East fringe (EF) East creek (EC) Near Cai
RBRsolo³ D (rbr-global, 2022a)	Water pressure (Waves and water depth) at the deployment location	2 (continuous)	West fringe (WF) East fringe (EF) Sea
RBRvirtuoso³ D|wave16 (rbr-global, 2022b)	Water pressure (Waves and water depth) at the deployment location	1/300 (average of a 128-second burst at 16 Hz)	Centre fringe (CF) Near Cai
StreamPro ADCP (Teledyne Marine, 2022)	Water depth and velocity profile connected to the boat	1	Throughout the Bay and the creeks
GPS eTrex® 10 (Garmin, 2022)	x- and y-coordinates	Manual activation	-
Real-Time Kinematic GPS (Leica Geosystems, 2022)	x-, y- and z-coordinates	Manual activation	Monitoring stations, Awa di Lodo, islands

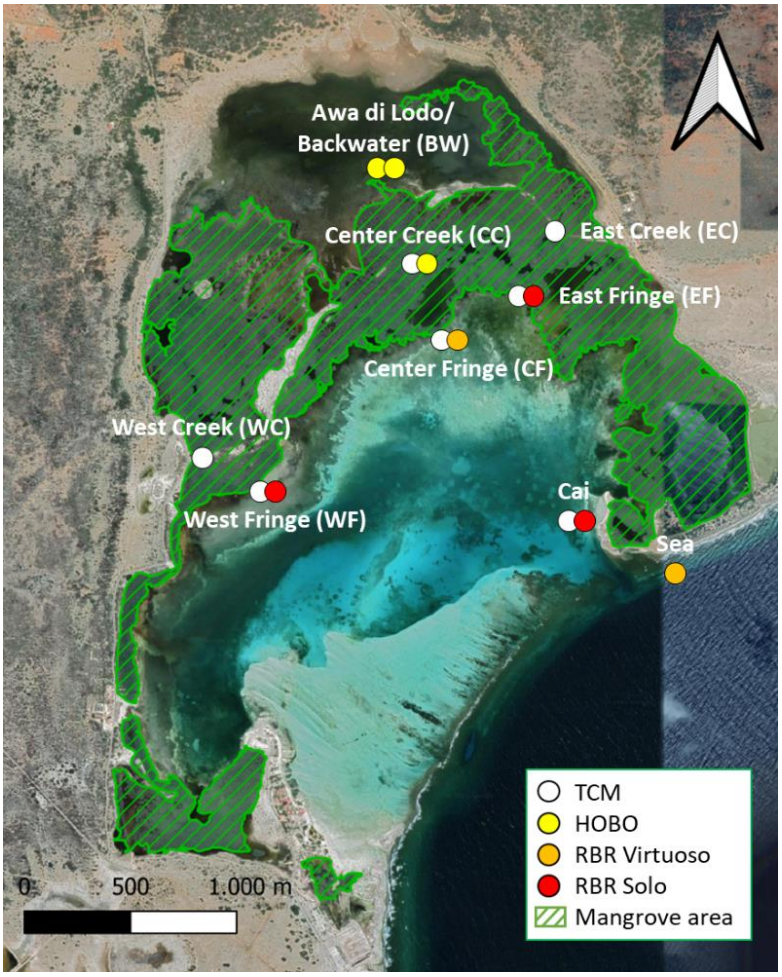

Figure 9: Placement of instruments over Lac Bay, the naming of the locations and the marked mangrove area based on own observations

3.1 Bathymetry and topography

Real-Time Kinematic (RTK) GPS measurements were conducted to obtain bed level data with a vertical accuracy of 15 mm at the monitoring stations and in Awa di Lodo. In the mangrove forest, the instrument could not connect to satellites because of the vegetation that blocks the satellite connection and was unable to give a location. The elevated islands in Lac (Figure 3) are large areas where only low vegetation or no vegetation grows. The ground level of the islands in the mangrove forest is mapped with approximately 10 m in between the data locations in the horizontal direction. In Awa di Lodo, elevation data were collected along two transects to create a representative bed level profile of that area. The spatial boundary conditions on the landside (for which the road surrounding Lac Bay is taken) were also measured with the RTK GPS for a representative height of the boundary. The boundary condition is mostly determined with a handheld GPS. In total, more than 1000 data points were taken.

Figure 10: Gathering water depth data with the ADCP in the creeks of Lac Bay

To map the topography of the mangrove forest and the shallow area in front of the forest fringe, the ADCP in combination with the handheld GPS was used. By boating through the creeks the location and depth of the creeks were determined (Figure 10). Three cross-sections of the west creek and one in the east creek are made using the ADCP. A handmade cross-section from the edge of the creek deeper into the forest is made to get a representation of the bed level surrounding the creeks. In front of the mangrove forest, in the open water of Lac, several surveys both parallel and perpendicular relative to the mangrove fringe were conducted. This strategy is used to create a bathymetry by interpolating between these measured depths. Since the water depth obtained with the ADCP deviates from the actual water depth, water depth data were measured manually next to the ADCP to adjust the ADCP data. Also, 7 cm is added to the water depth data of the ADCP to compensate for the sensor being 7 cm under the water surface. The inaccuracy varies per water depth, the actual water depth measured manually was usually greater than the ADCP-measured water depth. No clear pattern is found in this inaccuracy. To prevent making inaccurate adjustments, no compensation is done for this inaccuracy which results in the actual bed level being an order of centimetres deeper than the bed level in the data. During the monitoring sessions with the ADCP, several bed level RTK data points were taken to get the actual water level by adding the bed level to the water depth:

$$h = h_d + h_{bed} \tag{1}$$

h is the water level in meters above the local vertical datum (LVD), h_d is the water depth in meters and h_{bed} is the bed level in meters above the LVD (m+LVD). h_{bed} is measured by the RTK-GPS. Monitoring locations where the frames were put also have RTK data of the bed level, which is used to get the water levels at those locations.

3.2 Water levels

Water levels were determined from absolute pressure data monitored by 3 HOBO sensors and 5 RBR sensors. The HOBO sensors were placed in the back of the forest and in the middle creek, to study the difference in water level between these areas (Figure 9). The HOBO sensor that was placed in the middle creek was not placed further towards the open water of Lac to prevent the influence of waves in the pressure measurements. It was fixed to a metal frame so it would not move horizontally or vertically over time while staying below the water level. The HOBO in the backwater was placed in a

tube and hung below the bed level to still measure the water pressure during low water levels. Additionally, the atmospheric pressure is measured by a second HOBO sensor in the backwater is hung above the water to ensure it measured the atmospheric pressure only. The atmospheric pressure is used to correct the pressure signals obtained by the other instruments (which monitor the combined changes in atmospheric pressure and water pressure).

The RBR pressure sensors measure waves and tides. Due to the wave damping characteristics of the mangroves, they are not located inside the forest. This is not important for this research, but it is the motivation behind the positioning of those instruments. The RBR sensor located at Sea, just outside Lac, captures a tidal signal that is not yet altered by the bay and shows the tide that enters Lac. The RBRs near Cai and alongside the fringe monitor the water levels and tidal signal that are altered by Lac.

3.3 Flow velocities

The current velocities at 7 different locations were monitored by Tilt Current Meters (TCM). Figure 11 displays the setup of the TCMs in Lac Bay. The TCMs are connected to pavers from which they stand upright in the water when fully inundated.

Figure 11: A Tilt Current Meter (TCM) attached to a paver near Cai

Since the pavers lay on the bottom, the lower part of the water column is measured. When a TCM is tilted by the flow of water to which it is subjected, it converts this tilt into the flow speed and direction of that water. Since the TCMs capture the water velocity from 5 to 30 cm above the bed, the depth-averaged velocity at that location could be different due to the depth flow profile. Nevertheless, because of the relatively shallow waters, the data gives information on the speed and the direction of the flow. Placing three TCMs in the three main creeks is done to obtain a better understanding of the main flows through the forest since creeks are the important transporters of water in and out of the forest. Three TCMs are placed near the forest fringe to get a grip on the movement of the tide through Lac Bay. The last TCM is placed near Cai. Most of the water that enters Lac Bay by flowing over the coral reef leaves through the channel near Cai (van Moorsel & Meijer, 1993). Data about the speed and direction at Cai over time is therefore valuable since it represents a large water flow into and out of the bay. No TCMs are placed inside the mangrove forest, aside from in the creeks, because a minimum water depth of 0.3 meters is required and the presence of the roots would block the TCMs movement.

3.4 Vegetation characteristics

Mangrove trees influence the dynamics of the tides. The circumference, height and number of the roots of the trees are of importance because those determine the drag exerted on the sheet flow through the forest, which affects the tidal exchange. In this research, only the root characteristics are important since the roots are responsible for the flow resistance. To get information on the characteristics of the mangrove tree roots, 1-by-1 meter plots were set out. In a plot, the number of roots was counted and their characteristics (height, circumference) per species were measured. Differences between the species are not relevant for this research since the values for the number of roots, height and circumference are averaged over all measurement plots. To give insight into the spatial distribution of the mangrove species, Table 2 mentions if *Rhizophora* and *Avicennia* are present in the plots. Figure 12 shows the location of the 14 plots that were set out over Lac.

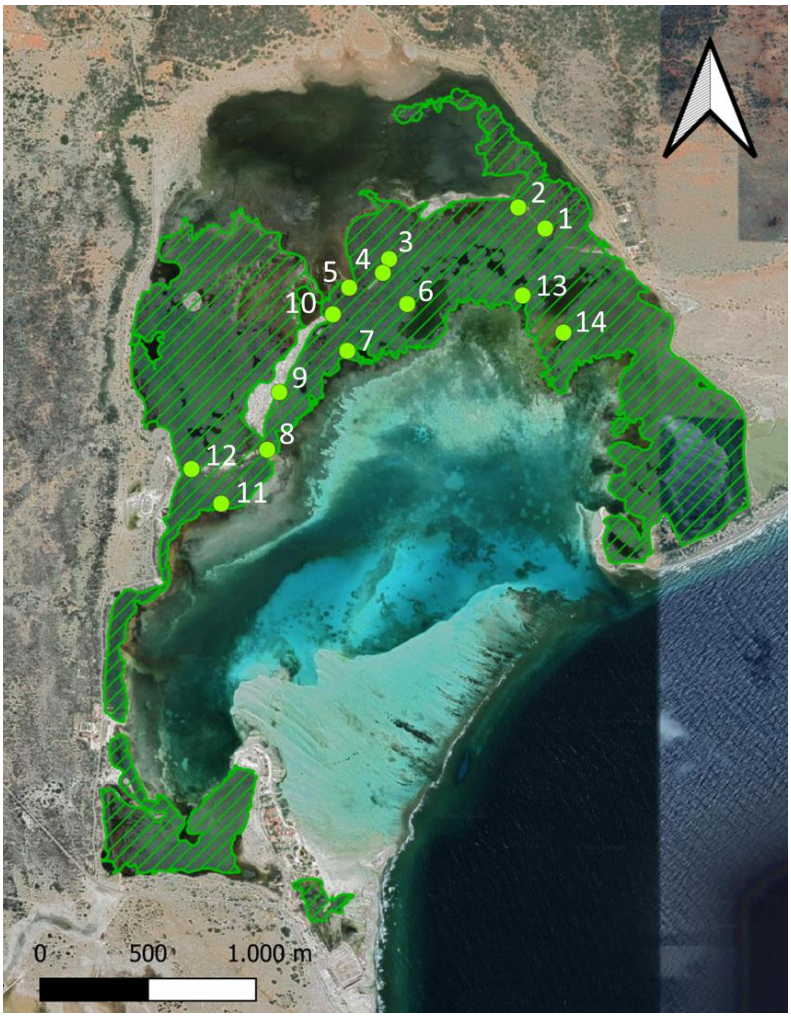

Figure 12: Locations of the vegetation plots

Table 2: Data on the mangrove root characteristics for the 14 1-by-1 plots

Plot nr	Presence of *Rhizophora*?	Presence of *Avicennia*?	Root density [/m2]	Root height [m]	Root diameter [m]
1	Yes	Yes	86	0.159	0.006
2	No	Yes	525	0.144	0.008
3	Yes	No	19	0.606	0.030
4	Yes	Yes	134	0.177	0.004
5	No	Yes	168	0.080	0.003

6	Yes	No	51	0.637	0.021
7	Yes	No	77	0.573	0.032
8	Yes	No	63	1.039	0.010
9	No	Yes	590	0.129	0.011
10	Yes	No	422	0.196	0.006
11	Yes	No	90	0.519	0.024
12	Yes	No	119	1.320	0.031
13	Yes	No	43	0.560	0.022
14	Yes	No	55	0.520	0.021

4. Hydrodynamic properties of Lac Bay

Awa di Lodo has a poor hydraulic connection to the open water of Lac Bay. It is mainly connected by two creeks, Kreek di Pedro and Kreek di Taco (Figure 3), that transport the water from and towards Awa di Lodo. During high tide, some water flows into Awa di Lodo through sheet flow across the forest. Most of the flow during ebb flows back into the open water of Lac Bay via the creeks. Ebb and flood are defined based on the water levels at Cai. Flood is defined as the period when the water level rises, from low water to high water. Ebb is defined as the period when the water level declines, from high water to low water. Fluctuating water levels cause water flows through Lac Bay. In general, the incoming flow is flood-flow and the flow leaving the area is ebb-flow. This analogy will be used unless stated otherwise.

4.1 Smoothening of field data

Instruments deployed in the field monitor a certain physical property and convert that into data, including noise. To smoothen the data and reduce the noise, a median filter is used. Noise is filtered out and the 'true' signal remains. In Lac Bay, mainly diurnal tides are observed, but during neap tide conditions, other tidal signals with smaller periods become apparent.

The TCMs and RBR virtuosos were monitoring in 5-minute bursts. The median of these bursts for a period of 5 minutes is taken and this median burst data (once every 5 minutes) is used for the smoothening. For the RBR solo data, which is monitored at a constant frequency of 2 Hz, the median of each successive 5 minutes is taken to create a dataset with a 5 minutes interval. The HOBO instruments' sampling frequency was once every 5 minutes, so no extra step had to be taken.

The median values for every 5 minutes are used for the smoothening. To capture the tidal signal, the median smoothening is done over half an hour of data (15 minutes before and 15 minutes after a certain moment in time). Since all data is converted to data with a 5-minute interval, the number of data points used by the median smoothening is 7.

4.2 Topography, bathymetry and hypsometry

No elevation map of the mangrove forest, its islands and Awa di Lodo is available. Therefore, RTK, GPS and ADCP data from the field campaign is combined with previously measured bathymetry data (Engel, 2017) to form a topographic map of the entire area of Lac. No continuous elevation measurements of the creeks are available. Hence, a cross-sectional profile of a creek (Figure 13) including the hand-measured bed level elevation next to the creek is implemented at the location of the creeks to form the bathymetry of the creeks and their banks. To create a representative profile of a creek the three cross-sections of the west creek are interpolated (Figure 13).

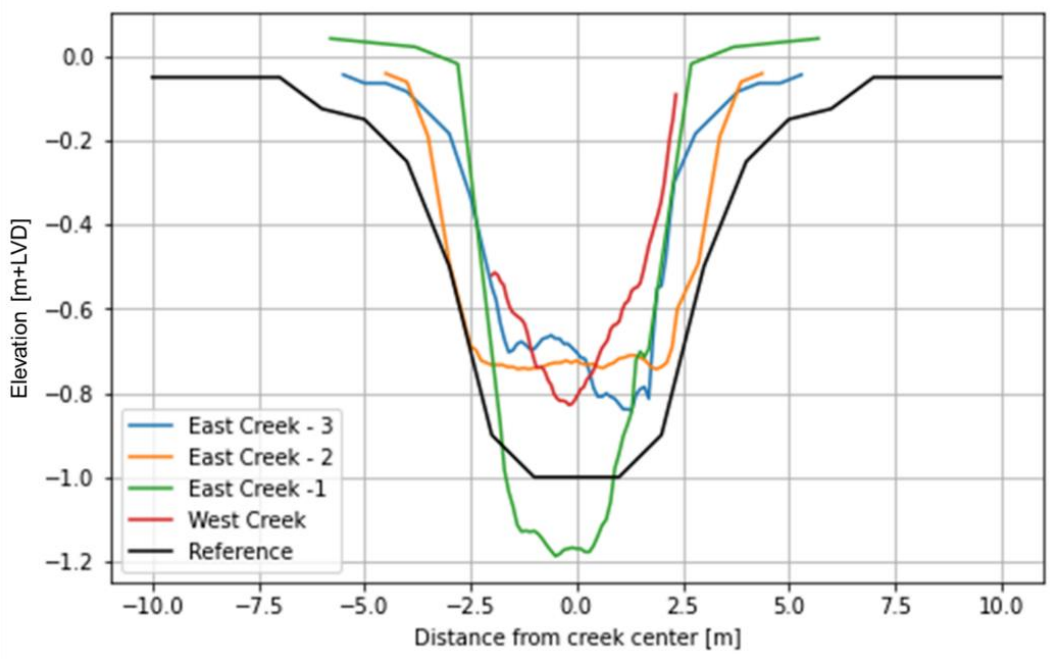

Figure 13: Interpolated creek profile from ADCP field measurements

The depth of the creek is based on the ADCP data at that location and it goes up to -0.05m+LVD. Half the cross-section of a creek, so only from the bottom part of the creek to one of the sides, is used to simulate the ascending bed level of the lagoons and the fringe. The islands of Lac are implemented in a similar way, only with a profile sloping down to 0.15m+LVD. In Awa di Lodo, two cross-sections are made using the RTK-GPS and these are used as representative cross-sections for the entire area. These cross-sections are copied and pasted across the backwater to represent Awa di Lodo. A road surrounding Lac is taken as boundary. Based on several RTK points, the height of this road is set at a height of 1 meter. Triangular interpolation by Delft3D (Deltares, 2022b) is used to create a topography of Lac based on the collected elevation data.

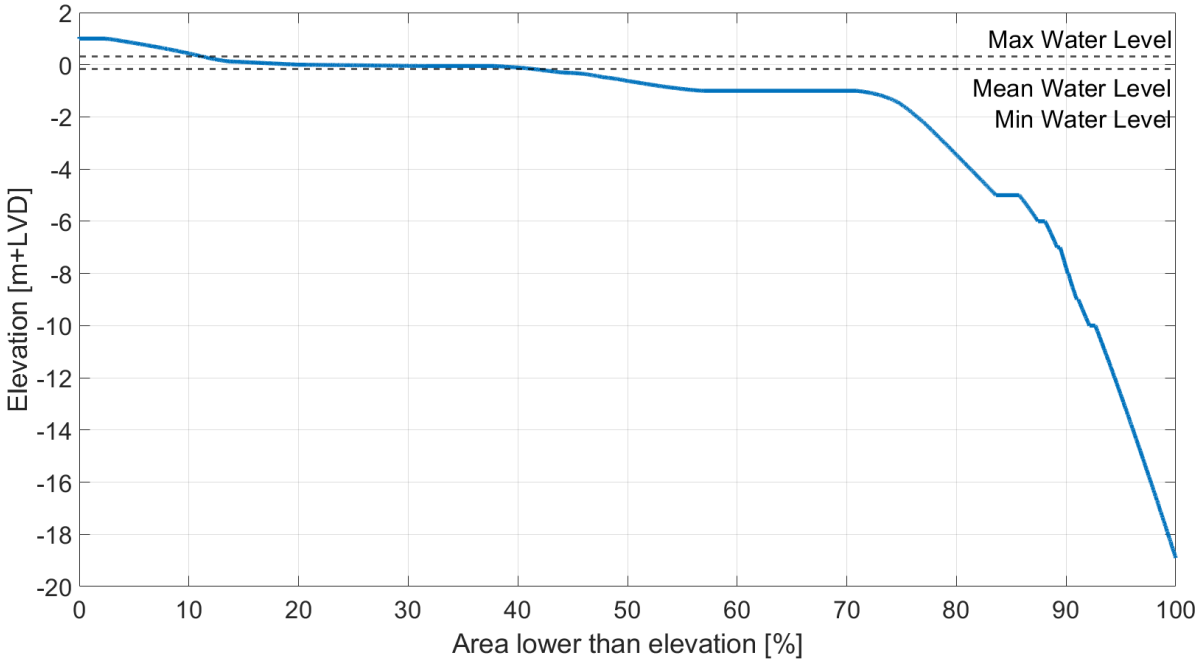

Figure 14: Full hypsometry of Lac Bay

To form a hypsometry of the area, the topography is projected on a 5-by-5 meter grid. As creeks are about as wide as one grid cell, creeks are not represented very well in the hypsometry. The hypsometry in Figure 14 shows that a quarter of the area of Lac Bay is below -2m+LVD. Large part of the area is always submerged as that is the part of the open water of Lac and the sea (Figure 16). Zooming in on the higher elevations of the hypsometry in Figure 15 shows that about 30% of the Bay area is intertidal. At -1m+LVD there is a flat section in the hypsometric curve due to larger steps in the bed level data from Engel (2017) which is used for a large part of the open water of Lac (Figure 16). A large part of the mangrove forest has elevations between the mean and minimum water level and will therefore be submerged most of the time. The bed level of Awa di Lodo is for a large part below the -0.2m+LVD and will therefore always be submerged. Also, a large part of Awa di Lodo is lower than its surroundings and the water has no way to leave the area via for example creeks. Water can and will be lost via evaporation, leading to hypersaline water. The percentage area that is above the mean water level contains the areas near Cai and Sorobon, the islands of Lac and the northern part of the Bay. These areas are less interesting for this study as there is no tidal influence and as a result of that, no mangrove trees. The area near the boundaries is overrepresented by approximately 2% of the total area in the hypsometric curve as it counts the number of grid cells which can be found in greater numbers near the model boundaries.

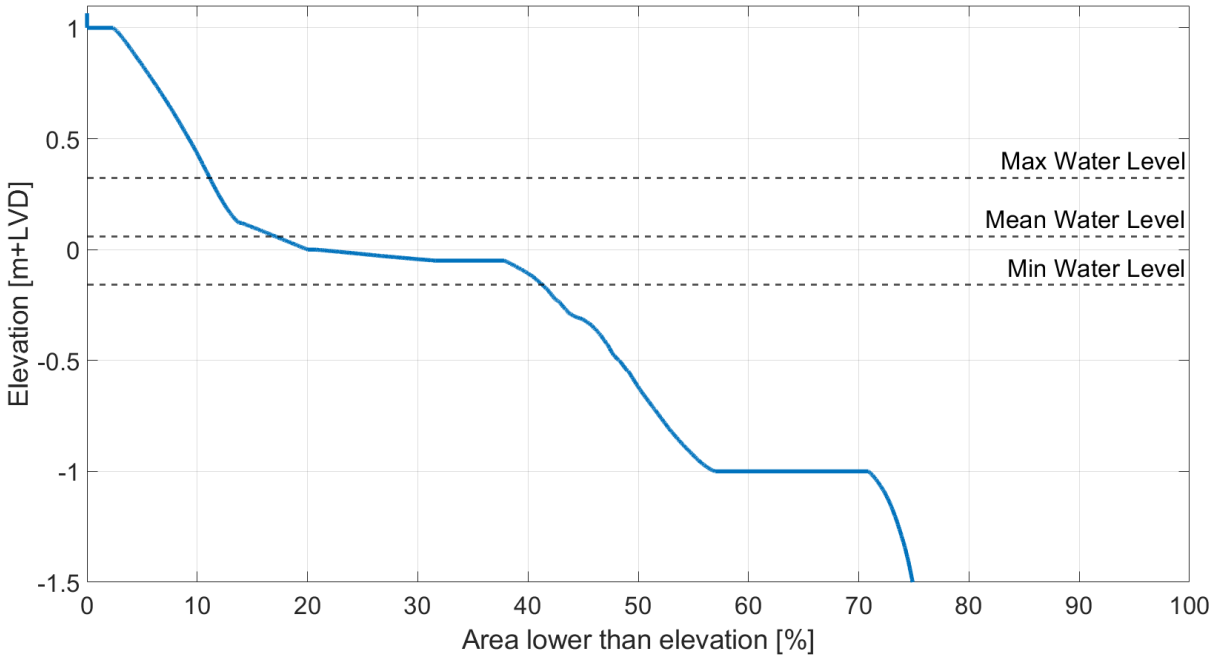

Figure 15: Zoomed-in hypsometry of Lac Bay

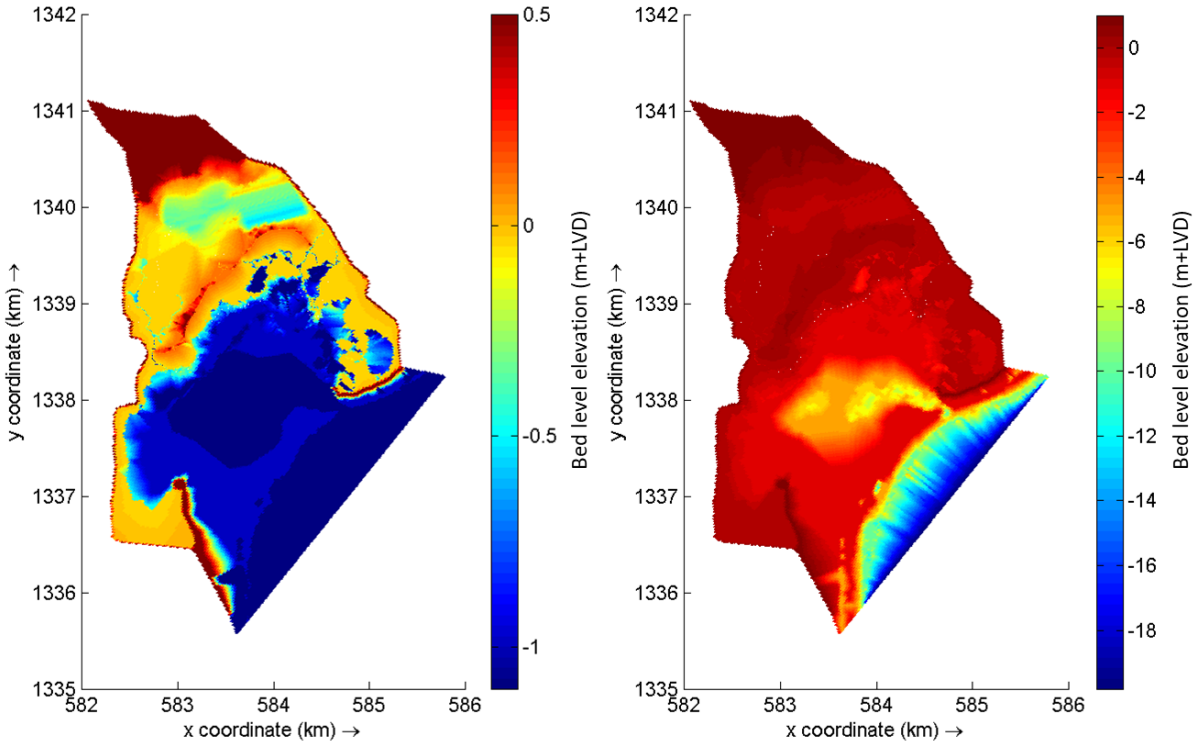

Figure 16: Bathymetry of Lac Bay ranging from -1.1m to 0.5m+LVD (left) and -20m to 1m+LVD (right)

4.3 Tidal constituents

The tides are the main driver of water flows through Lac Bay. Characteristics of the tidal wave are important to understand because it is closely linked to the water levels and direction and speed of water flows in Lac. With the use of the program 't_tide.m', a harmonic analysis is performed on the water level data. This program extracts the tidal constituents from the water level data and can reconstruct them using these tidal constituents. The tidal signal gets altered by the bay and therefore the harmonic analysis is not always able to extract tidal constituents from the data in Lac. Also, shorter measurement periods have a hard time providing a full harmonic analysis. The data from the full measurement period is used at the measurement locations near Cai and outside of Lac since those locations have almost continuous time series.

Earlier research showed that further into the mangrove forest the tidal signal gets altered such that harmonic analysis is hard to perform on water level data from inside the forest (van Zee, 2022). The highest variance explained by the harmonic analysis is just outside the bay (88.1%) followed by the location near Cai (82.1%). For both these locations, a signal-to-noise ratio (snr) of at least 50 is used for a tidal constituent to be considered significant in the harmonic analysis. To even get a signal, the snr is lowered to a minimum of 5 to be able to recreate the tides for the other four locations. Table 3 shows the variance explained by the harmonic analysis of the tidal signal at each of the measurement locations, as well as the tidal constituents and their contributions.

The general pattern is that if a monitoring station is located further from the sea, the tidal signal is more distorted. Table 3 shows the extent of the distortion of the tidal signal. A lower variance explained is a greater distortion of the tidal signal. The variance explained from the centre creek monitoring station is lower than the variance explained of the fringe monitoring stations which are again lower compared to the monitoring stations at Cai and at sea.

Looking at just the stations near Cai and in the sea, the lunisolar diurnal tidal constituent (K1), with a period of 23.93 hours, is the dominant tidal constituent. The K1 tidal constituent is followed by the principal lunar diurnal tidal constituent (O1) and the principal lunar semi-diurnal tidal constituent (M2), with periods of 25.82 hours and 12.42 hours respectively. Earlier research by van Zee (2022), based on previously collected data by Lodder (2013), also shows the prominent presence of the K1 and O1 tidal constituents. Data obtained from this field study shows that the M2 tidal constituent is also an important component.

Table 3: Dominant tidal constituents per measurement location

Location	Instrument	Variance explained (%)	Minimal snr value	Tidal constituents	Corresponding snr values
Sea	RBR solo	88.1	50	MM, MSF, O1, P1, K1, M2	67, 180, 350, 75, 690, 120
Cai	RBR virtuoso	82.1	50	O1, K1, N2, M2	150, 360, 53, 140
West fringe (WF)	RBR solo	43.6	5	MSF, O1, K1, L2	5.6, 9.7, 11, 5.4
Centre fringe (CF)	RBR virtuoso	69.8	5	O1, P1, K1, N2, M2, M4	33, 9.1, 83, 9.4, 56, 5.2
East fringe (EF)	RBR solo	65.5	5	MM, MSF, O1, P1, K1, MU2, M2, L2, S2, M8	59000, 19, 9.6, 6.7, 61, 14, 5.9, 5.9, 26, 9.6
Centre creek (CC)	HOBO	33.8	5	O1, K1, L2	8.5, 7.9, 5.5

4.4 Propagation of the tidal wave through Lac

A tidal wave entering a shallow area will be slowed down. When a tidal wave reaches a mangrove forest it experiences a large increase in flow resistance because of the even shallower water and the resistance imposed by the trees. To quantify the delay of the tide imposed by the bathymetry and vegetation of Lac Bay, the moment of high water is taken for each tidal cycle per measurement location. Figure 17 shows that between WF and BW there is a delay in high water of several hours. Cai is taken as the reference location to compute the high water delay of all other stations since it is the location where the tidal wave enters Cai and to be able to compare with earlier research. Linking the time differences between the moment of high tide to the location is done so the propagation of the tidal wave through Lac Bay can be visualized.

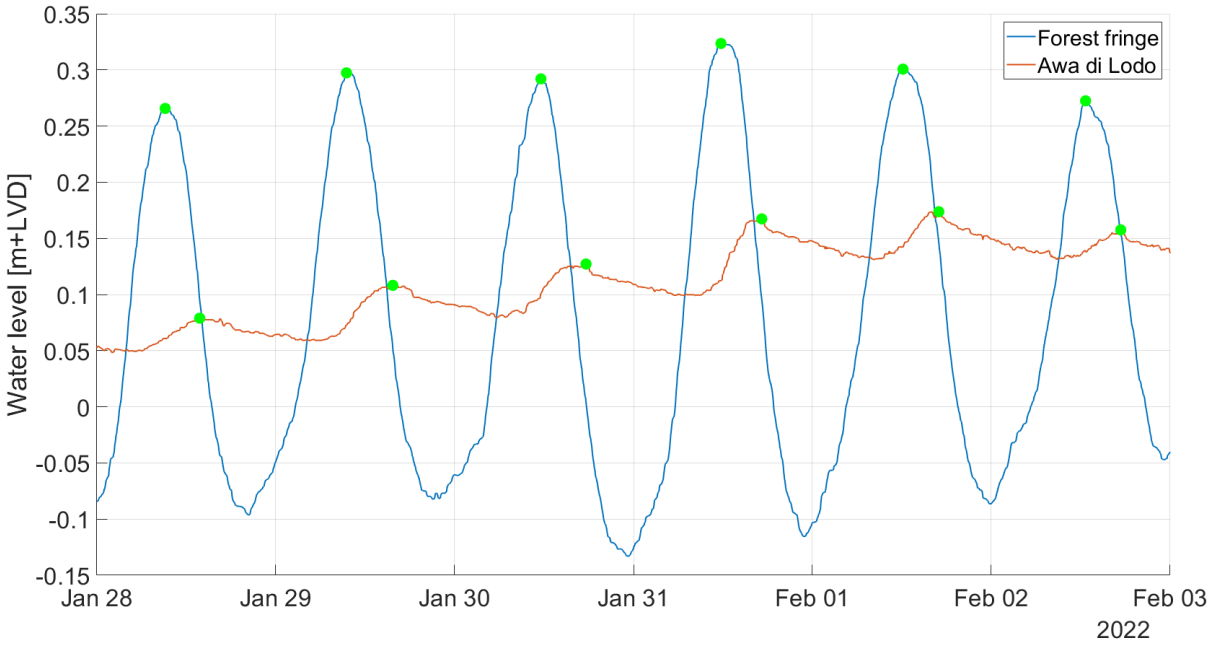

Figure 17: Differences in moment of high tide (green dots) between the forest fringe (WF) and Awa di Lodo (BW)

Based on the shallow water equations, an estimation can be made of the time the tidal wave travels through Lac Bay:

$$c = \sqrt{gh} \tag{2}$$

Herein, c is the propagation speed of the tidal wave in ms^{-1}, g the gravitational acceleration in m/s^2 and h the water depth. At Sea, a negative delay is expected because the tidal wave arrives earlier. Assuming an average depth of 8 m, the tidal wave should arrive approximately 1 minute earlier at Sea than at Cai. Based on a distance of approximately 1.2 km between Cai and the forest fringe with a water depth ranging from 1 to 5 meters, the travel time of the tidal wave should be approximately 5 minutes. The additional delay to CC, where 400 m distance and a 1 m depth of the forest are assumed, is 2 minutes. Making the total delay from Cai to CC between 5 and 8.5 minutes. Following the west creek from the fringe to Awa di Lodo, the tidal wave covers a distance of approximately 2 km where the creek depth is assumed to be 1 m. Adding 800 m, the distance from the end of the creek to the measurement station BW, with an average depth of 0.5 m gives the entire path from Cai to the BW. The total travel time from Cai to BW according to the shallow water equations is approximately 30 minutes.

Table 4 and Figure 18 show the observed delay in time of high water with respect to Cai per location. The location at sea sees a negative delay thus the tidal wave reaches that location about 9 minutes earlier. Note that this is much more than the 1-minute delay that the shallow water equation predicts. Inside the open water part of Lac (at WF, CF and EF) the delay compared to Cai is very small. Since these differences are small and could be based on the variance of the data it is assumed that the entire open water level raises and drops uniformly. At CC the delay values are more in line with the shallow water equation predictions, possibly influenced by the mangrove forest. At BW the delay is up to several hours, much more than expected based on the calculations. This shows that there is more friction in this system than expected by the propagation of a tidal wave through shallow water. Van Zee (2022) showed that the tidal wave travels around the islands of Lac Bay and that the delay in high water from Cai to BW is in the same order of magnitude (delay of 3h 45min).

Table 4: Median and mean delay of the tidal wave with respect to Cai including the standard deviation

	BW (hh:mm)	CC (hh:mm)	WF (hh:mm)	CF (hh:mm)	EF (hh:mm)	Cai (hh:mm)	Sea (hh:mm)
Median	04:03	00:08	00:03	00:06	00:01	-	-00:09
Mean	04:23	00:12	00:01	00:08	00:05	-	-00:08
Standard deviation	02:00	00:20	00:27	00:17	00:18	-	00:33

The range in delay of the tidal waves is up to several hours which is large compared to the average delays found. This can have two reasons: natural variability in the interactions of Lac Bay or there is a difference in delay in the spring-neap cycle. Between the spring-neap cycles, there is some difference in tidal delay between Cai and BW. For the first and second spring-neap cycles, the median delay is approximately 4h 50min and for the third spring-neap cycle the delay is 3h 23min. So, there is variation between the different spring-neap cycles but it is unclear if this difference is physically based.

Figure 19 shows the spatial spread of the delays. The location at sea sees a negative delay thus the tidal wave reaches that location about 9 minutes earlier. Note that this is much more than the 1-minute delay that the shallow water equation predicts. Inside the open water part of Lac (at WF, CF and EF) the delay compared to Cai is very small. Since these differences are small and could be based on the variance of the data it is assumed that the entire open water level raises and drops uniformly. At CC the delay values are more in line with the shallow water equation predictions, possibly influenced by the mangrove forest. At BW the delay is up to several hours, much more than expected based on the calculations. This shows that there is more friction in this system than expected by the propagation of a tidal wave through shallow water. Van Zee (2022) showed that the tidal wave travels around the islands of Lac Bay and that the delay in high water from Cai to BW is in the same order of magnitude (delay of 3h 45min). Table 4 displays the standard deviation of these delays. Interesting to note is that only the delay of the backwater is larger than the standard deviations. However, due to the natural variance in the data, this does not have to mean the data is not significant.

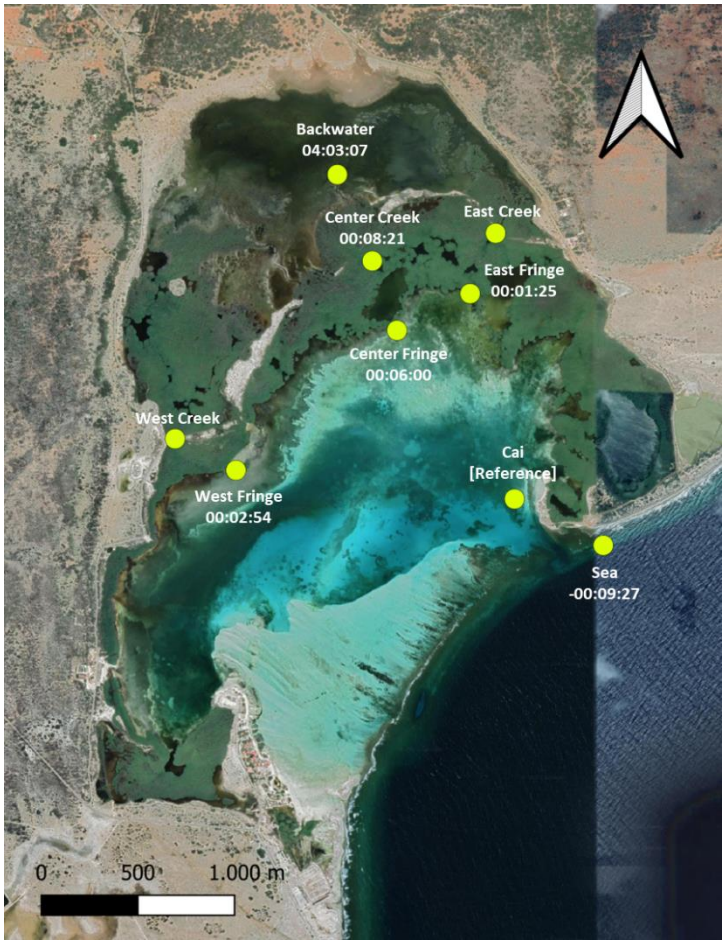

Figure 18: Spatial representation of the median delays of the tidal wave with respect to Cai

During the field monitoring another water flow into Awa di Lodo besides the (former) creeks was observed. During high tide, a water flow arose over the central part of Isla di Chico adding salt water from the front into the backwater. Lott (2001) observed the same water flow during her field study.

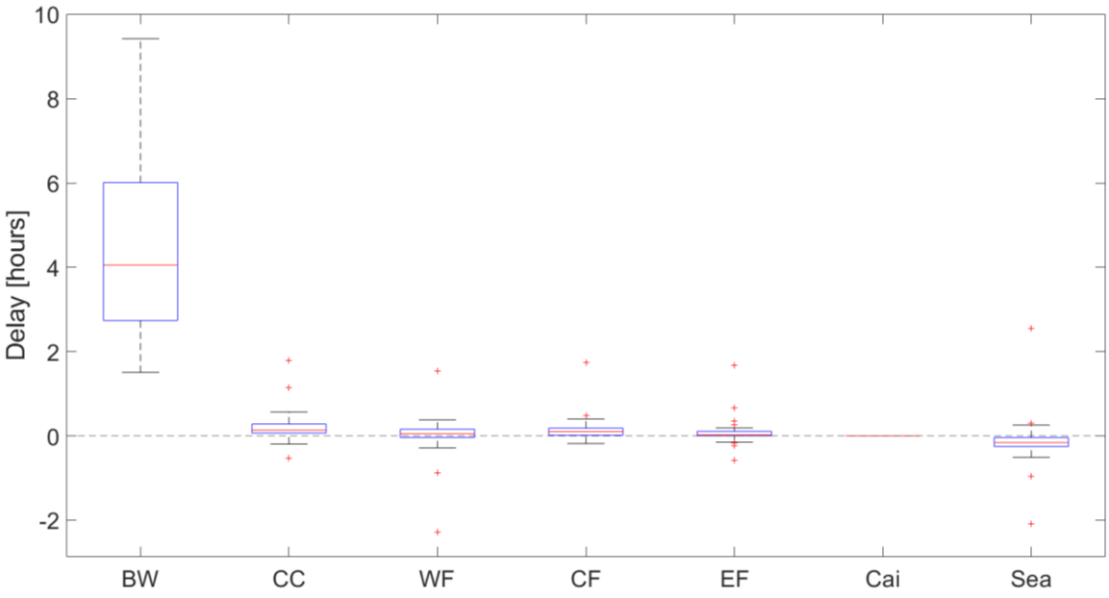

Figure 19: Boxplot of the tidal wave delay data per location with respect to Cai

4.5 Converting pressure data into water levels

Converting the pressure from the HOBO and RBR pressure sensors into water depth data is done using equations 3-5. To be able to compute tidal water level differences across Lac, the RTK data of the bed levels that are monitored next to the frames were used. By adding the water depth to the bed level, a water level with respect to a LVD set by the RTK-GPS can be determined (equation 1). This LVD is based on the coordinate system of Curacao, EPSG:3807. Figure 20 gives an overview of the calculated heights and depths for the water level and instruments.

$$P = \rho g h_d \tag{3}$$

$$h_i = \frac{[P_i - P_{atm}]}{\rho g} \tag{4}$$

$$h_d = h_i + hab_i \tag{5}$$

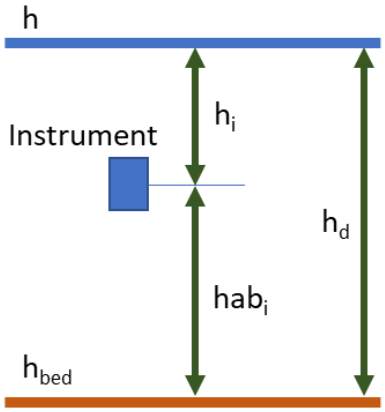

P = Pressure (kPa) – measured value at instrument
ρ = Density of water (kg/m^3) – sea water has a value of 1025 kg/m^3
g = Gravitational acceleration (m/s^2)
h_i = water depth at instrument (m)
P_i = pressure at instrument (kPa)
P_{atm} = atmospheric pressure (kPa) – measured value at HOBO in the air (assumed that it is uniform over Lac)
hab_i = Measured height above bed of instrument (m)

Figure 20: Overview of heights and depth used to calculate water level

Deviation between the water levels in the fringe exists in the data due to uncertainties. There is the uncertainty of 1.5 cm in the RTK data, uncertainty in our manual measurements, and there has been some movement of the frames in the field. This creates a total uncertainty in the order of magnitude of about 10 cm. Based on the propagation of the tidal wave, there should be minimal deviations in water levels between the fringe frames since the entire open water level in the bay fluctuates more or less as one. To compensate for this, all fringe water level data is corrected by the west fringe frame. This frame has seen little to no movement, thus producing the most reliable water level data. The correction is done for all three spring-neap cycles (Table 5).

Table 5: Water level corrections for CF and EF, based on the water levels of WF for all three spring-neap cycles

	1st spring-neap cycle	2nd spring-neap cycle	3rd spring-neap cycle
Centre Fringe	-2.7 cm	+5.0 cm	+4.1 cm
East Fringe	+3.0 cm	+10.0 cm	+5.7 cm

4.6 The bathtub effect

To understand the water level difference between the forest fringe and Awa di Lodo, the absolute water levels must first be understood. Awa di Lodo is a sort of bathtub that slowly fills itself during high spring tides. During the consecutive low tide, the water starts to drain from Awa di Lodo again. But when there are consecutive high water levels at the forest fringe during spring tides, the water in Awa di Lodo does not have the time to all flow back to the lagoon. When the water level difference is not

great enough anymore to keep adding water to the backwater, it starts draining again. If the water in the lagoon stays low for a longer period, for instance during neap tides, the water level in the backwater does not decline further because of flows through the creeks (bed levels are too high), but because of evaporation in the area. Lott (2001) describes this effect and links it to high salinity values during periods when the tidal activity is much lower and thus having a much smaller refreshment rate of Awa di Lodo.

Filling of the bathtub is what is observed during the first spring-neap cycle (first period) when the water level in Awa di Lodo increases to 0.17m+LVD during spring tides (Figure 21). In the second spring-neap cycle (second period), the water level in Awa di Lodo does not increase like in the first period indicating that the water level of the spring high tide is important in increasing the water level in Awa di Lodo. In the third spring-neap cycle (third period), the water level in Awa di Lodo only systematically rises to 0.11m+LVD during spring tide.

During the measurement campaign, no trend is found in lowering of the water level by for example evaporation. In the dry season, when the influx of fresh water is low while the evaporation rates remain high, the water level in Awa di Lodo is more likely to drop resulting in a more extreme situation than normally during the year (Lott, 2001).

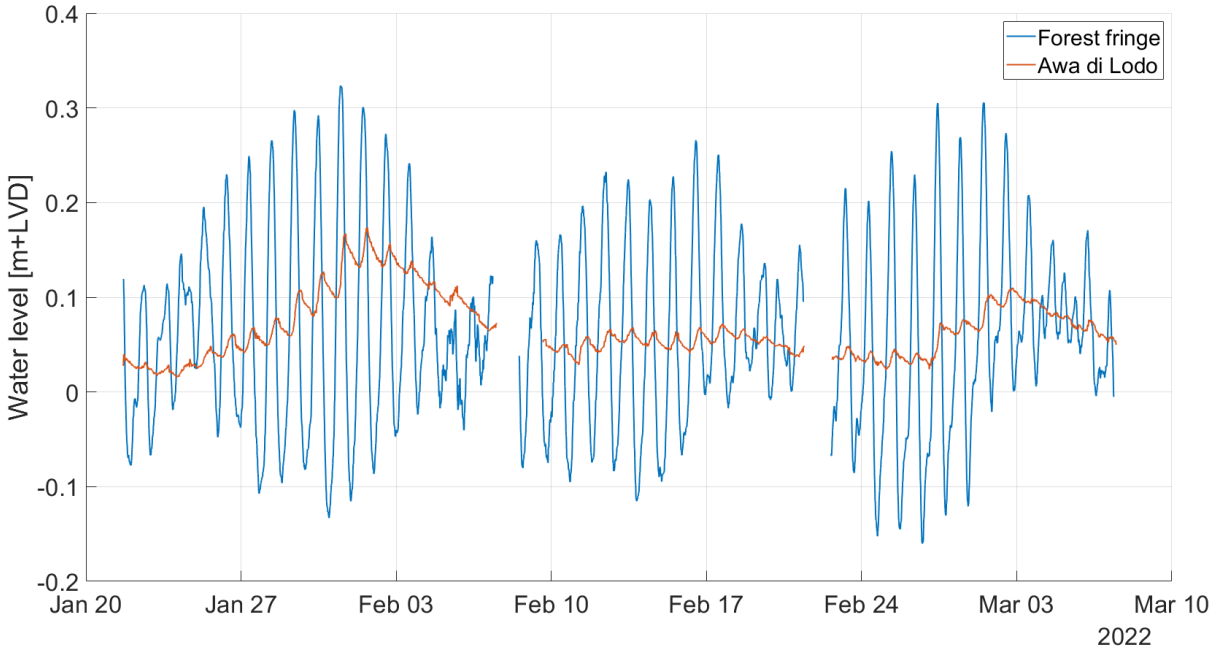

Figure 21: Water levels of the forest fringe (WF) and Awa di Lodo (BW) during the field study (21 January – 7 March)

Figure 22 shows the working of the bathtub effect in Awa di Lodo. In the rising part of the first period, the maximum water level at Cai increases from 0.06 to 0.23m+LVD and Awa di Lodo follows, increasing the water level from 0.03m to 0.08m+LVD. During spring tide the maximum water level at Cai does not increase anymore but the water level in Awa di Lodo is increasing from 0.11m to 0.17m+LVD. During the falling part of the spring-neap cycle, the maximum water level at Cai is decreasing much faster (from 0.24 to 0.06m+LVD) than the maximum water level at Awa di Lodo (from 0.17m to 0.11m+LVD), leaving Awa di Lodo as a sort of bathtub that slowly drains. This effect is also called hysteresis, where for two states (spring and neap tide) the relation between two parameters follows different paths. In the second period there is some fluctuation in the maximum water depth at Cai per tidal cycle, but little to no effect on the maximum water level at Awa di Lodo which is stable at approximately 0.06m+LVD. The third period sees a similar but less strong hysteresis effect with the maximum water

level in Awa di Lodo during that spring-neap cycle reaching 0.11m+LVD. This probably has to do with having lower minimum water levels during spring tide compared to the first period. Also, the effect is not fully captured in Figure 22 because of not having measured the full neap tide at the start of the third period and therefore missing some data points.

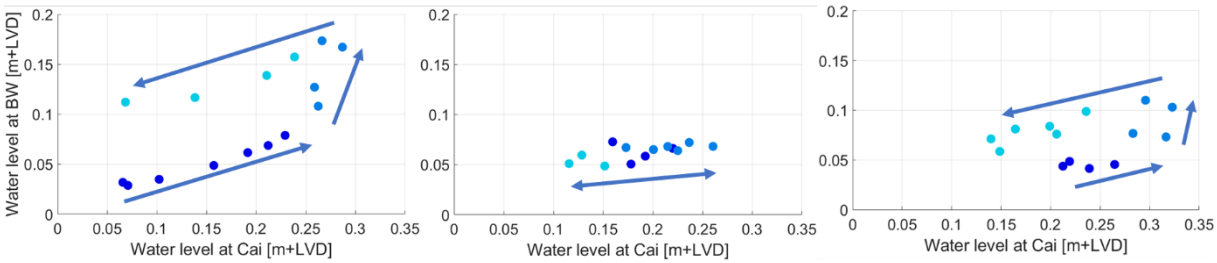

Figure 22: Maximum water level of Awa di Lodo plotted against the maximum water depth at Cai per tidal cycle for period 1 (left), period 2 (middle) and period 3 (right) with dots indicating periods in the spring-neap cycle (dark blue – start of the cycle; standard blue –spring tide; light blue – end of the cycle)

4.7 Temporal and spatial variability in velocities

Water flows throughout Lac change in speed and direction during a tidal cycle. This section introduces 'velocity roses', a 360 degrees representation of the water flow speed and direction. Speed and direction data monitored by the TCMs are used to create the velocity roses which give insight into the occurrence of flow directions and the distribution of corresponding flow speeds.

Figure 23 shows that Cai has a dominant flow out of Lac. Important to note is that the velocity rose is based on the TCM which only covers the bottom 30 cm while the entire water depth at that location is around 4 meters. This means, at Cai even more than at other locations, that the direction of the flow does not have to be in that direction since the top flow can flow in other directions. Data shows that during spring tide the flow is not always in the SE direction, sometimes it reverses resulting in very low flow speeds in the NW direction, into Lac. This would be in line with earlier research by van Moorsel & Meijer (1993) that most of the water enters Lac Bay across the coral reef but is leaving the area again at Cai.

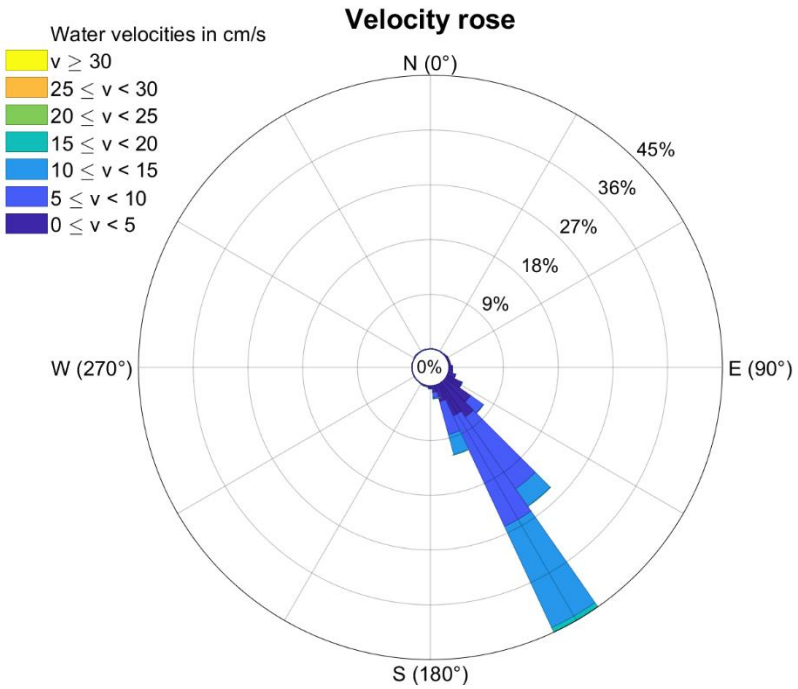

Figure 23: Velocity rose of Cai

That the direction of the flow data is not always in line with the direction of the creek indicates that the western creek (WC) is influenced by sheet flow entering the channel. Since the Isla di Pedro is obstructing the water flow towards the open water, all flow is concentrated towards the location at WC, resulting in a flow direction that is not necessarily aligned with the creek. The velocity rose of WC in Figure 24 shows that this pattern mainly appears for southwards velocities.

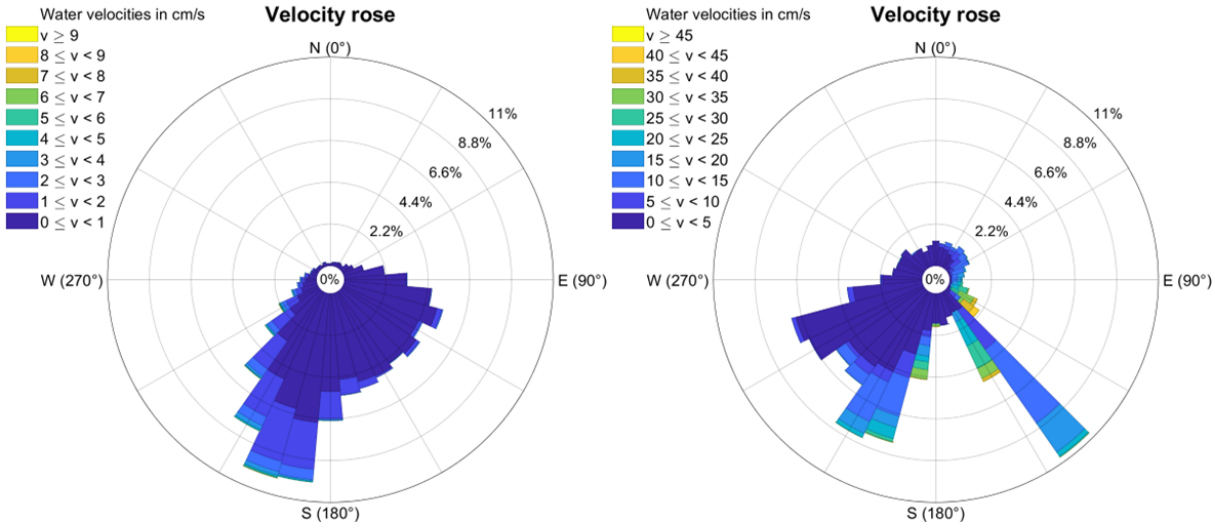

Figure 24: Velocity roses of WF (left) and Kreek di Taco (WC)(right)

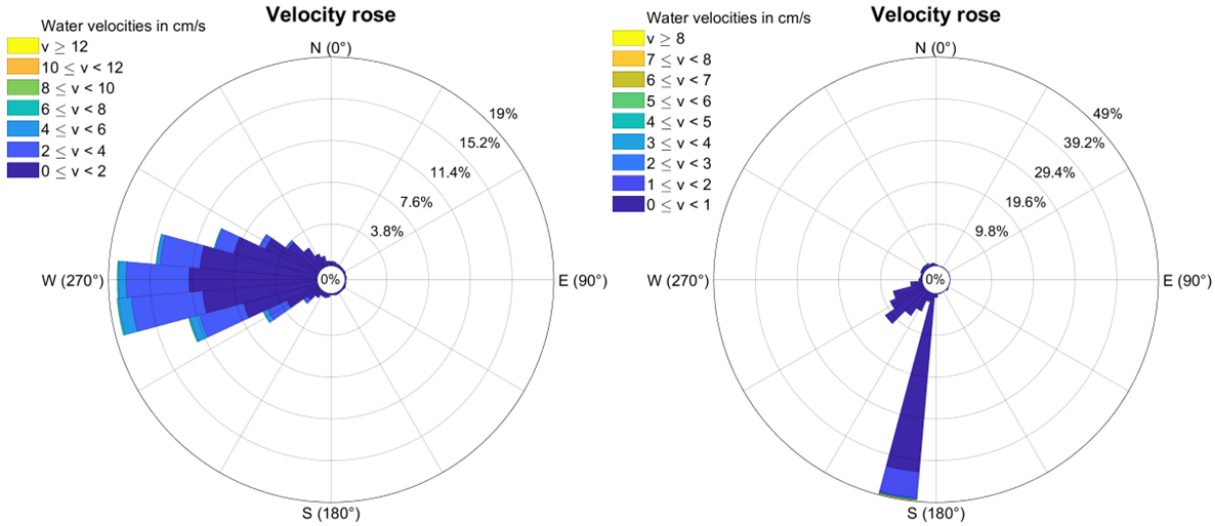

Figure 25: Velocity roses of CF (left) and CC (right)

Flow patterns at the eastern creek (EC) (Figure 26) show a clear signal that the water flow is spread over two dominant directions, west and east, in line with the direction of the creek. Most of the time the flow is out of the forest (ebb flow), but there is a small percentage of time where there is flow into the forest (flood flow) when it reaches high flow speeds. Figure 24 shows that WC also sees high flow velocities flowing in the direction of the open water of Lac, out of the forest. This velocity rose is more spread over multiple directions than at EC but still shows the dominant flows in the direction of the creek. The centre creek (CC), displayed in Figure 25 only has velocity data of the first period. In that period it is visible that there is a flow direction towards the open water from Lac.

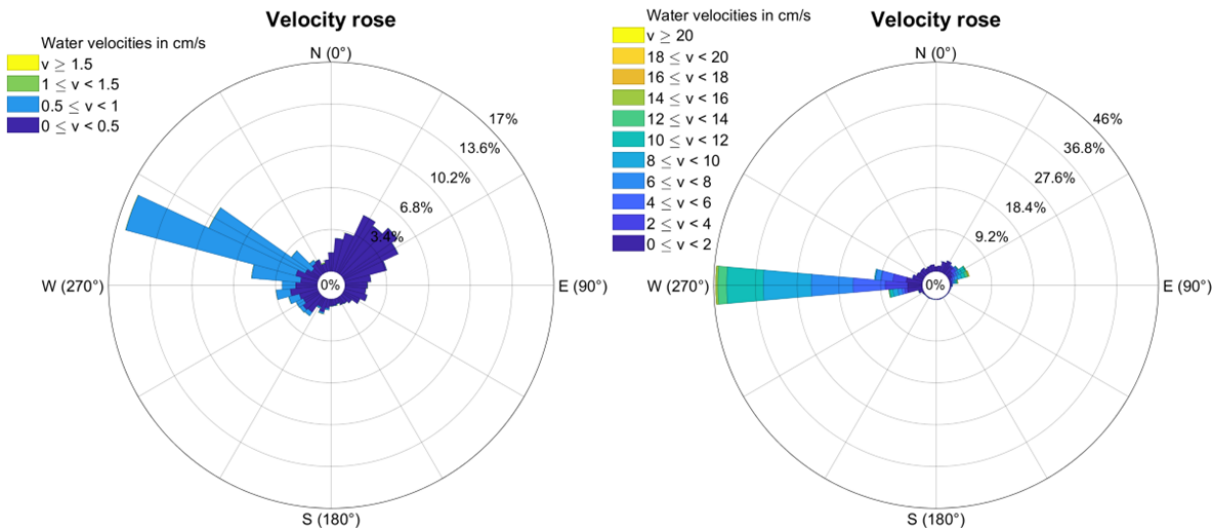

Figure 26: Velocity roses of EF (left) and Kreek di Taco (EC) (right)

The speed and direction of the flow near the forest fringe (left velocity roses in Figure 24, Figure 25 and Figure 26) seem to be based on other forces than the tide. Based on earlier research, it is expected that the water flow makes a clockwise rotation through Lac. However, the fringe stations do not follow this pattern. WF has mostly flows southwards, CF has a westward flow and EF has flows towards NW and NE. The latter one has low flow speeds (<1.5 cm/s). It seems that EF is driven by a local flow pattern near the forest fringe and does not follow a dominant flow pattern through Lac, if there is any. An argument can also be made that the fringe stations are influenced by the wind. CF is directed in the dominant wind direction. WF is probably influenced by the nearby creek and by a nearby mangrove island. The island directs the flow and wind north of the island rotating southwards on the downwind side of the island where WF is located, resulting in flow directions southwards. EF was placed in a more sheltered area than the other fringe stations in deeper water (approximately 1.5 m) which resulted in less influence from the wind and more influence from the local flow patterns induced by the nearby creek entrance. All these complex, local flow patterns make it not possible to make a statement about the flow in the open water of Lac. Earlier studies by Wagenaar Hummelinck & Roos (1969) and Van Moorsel & Meijer (1993) on the flow of the open water of Lac cannot be compared to this study because of the complex, local flow patterns and because their focus was more on the deeper parts of Lac Bay.

4.8 The relation between velocity and water level

Water velocities in a mangrove forest are driven by the tide. At the front of the forest, the water rises while in the back it reacts later, creating a difference in water level between those areas. Naturally, water starts flowing towards the back of the forest to even the water level out, creating flows through the forest with certain velocities. The same theory can be applied during ebb tide, this time with the water level in the back being higher creating a flow out of the mangrove forest. Figure 27 shows that during ebb the water flows out of Awa di Lodo because of the declining water level while during flood the water level increases.

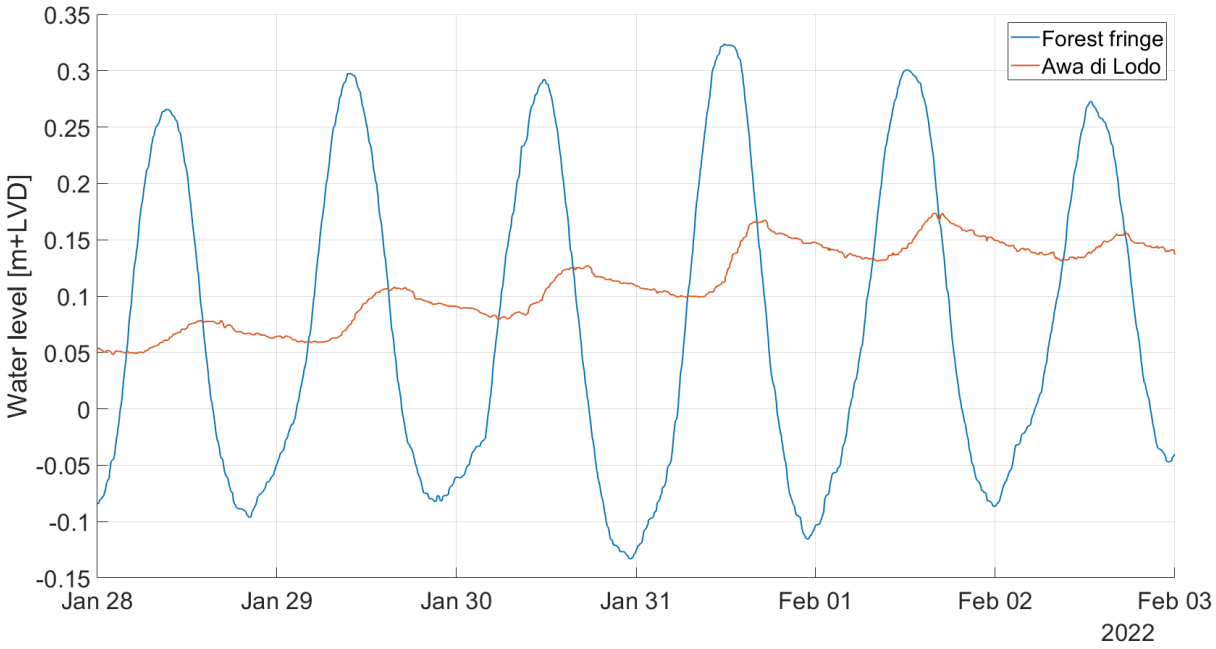

Figure 27: Water levels of the forest fringe (WF) and Awa di Lodo (BW) for the period 28 January – 3 February

Ebb and flood direction of the flow in the creeks

Separating flow into an ebb and a flood direction is useful for the distinction between the duration of ebb and/or flood flow and for the comparison between e.g. maximum flood velocities. To separate ebb and flood flow directions, the velocity data are separated in periods when the velocity is directed inland (flood) and when the velocity is directed seaward (ebb). At EC, the velocity data is split over 150-330 degrees based on observations and boat routes through the creek. Thus the flow direction is based if it flows in line with the creek. Based on the same principle WC should be split over 75-255 degrees, with the ebb direction being inside the interval and the flood direction being outside the interval. However, based on the time series of flow direction, the direction of ebb and flood changes per period for that location. Personal observations support the theory that there is a changing flow in and out the mangrove forest in line with the pattern of the tides which makes this approach viable.

Table 6: Interval of the ebb and flood direction in the creeks

	Interval ebb direction (degrees)	Interval flood direction (degrees)
EC	150 – 330	0 – 150 ; 330 – 360
WC period 1	20 – 180	0 – 20 ; 180 – 360
WC period 2	100 – 250	0 – 100 ; 250 – 360
WC period 3	150 – 330	0 – 150 ; 330 – 360

Water level difference and flow velocities

A greater water level difference induces a steeper water level gradient, creating faster flow velocities. Thus it is expected that during spring tide, greater velocities will be seen than during neap tide. Figure 28 and Figure 29 show that with a decrease in water level difference between the forest fringe and Awa di Lodo, the peak velocities in the creeks decrease as well. A positive water level difference means a higher water level in the forest fringe than in Awa di Lodo while a negative water level difference means that the water level in Awa di Lodo is greater than in the forest fringe. It appears that a water level difference of approximately 5-8 cm is needed to reverse the ebb flow at Kreek di Taco (EC).

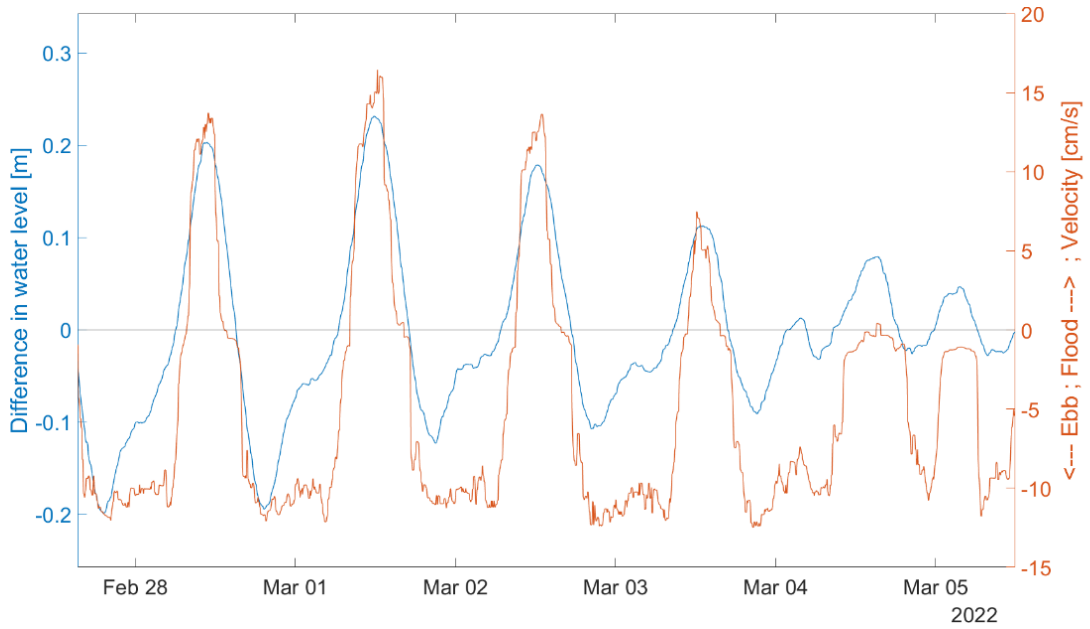

Figure 28: Water level difference between the forest fringe (WF) and Awa di Lodo on the left axis and the velocity in Kreek di Taco (EC) on the right axis

At Kreek di Pedro (WC), the water level difference needed to reverse the ebb flow is between 0 and -10 cm. That the flow direction reverses at smaller water level differences at WC than at EC is caused by WC being closer to the open water, so there is a delay in the flow-reversal moment. This delay also creates periods where in one creek the flow is in the ebb direction and in the other creek it is in the flood direction and vice versa. The flow direction at WC reverses from ebb to flood approximately 3-4 hours earlier than the flow direction changes from ebb to flood at EC. The flow direction at WC reverses from flood to ebb approximately 0.5-2 hours earlier than it changes from flood to ebb at EC. At EC the water needs time to reach that location, delaying the flow reversal and resulting in larger water level differences needed to reverse the flow direction. WC needing a negative water level difference for the flow to reverse is not logical looking purely at ebb-flood directions.

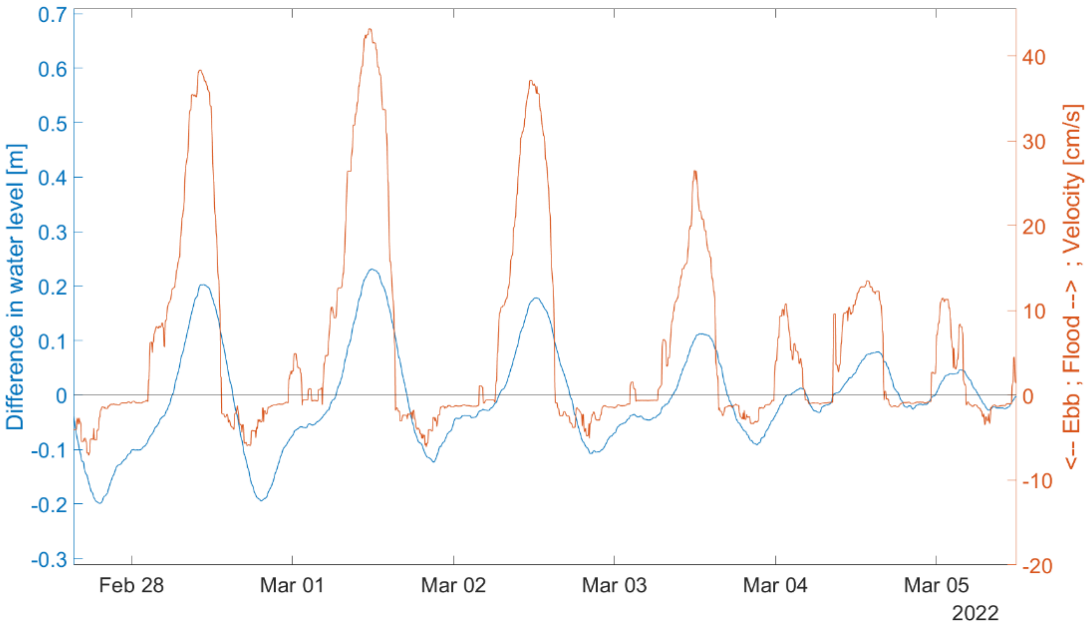

Figure 29: Water level difference between the forest fringe (WF) and Awa di Lodo on the left axis and the velocity in Kreek di Pedro (WC) on the right axis

Comparison of flow velocities between the different spring-neap cycles

Taking a broader look at the water velocity time series of EC shows that there is variation in maxima between the spring-neap cycles (Figure 30). This again emphasizes the importance to do measurements lasting at least one spring-neap cycle to state conclusions on the tidal dynamics of Lac. By looking at Figure 30 there can even be argued that multiple spring-neap cycles are needed to analyse the characteristics of Lac Bay due to the significant variation in water levels and concurrent velocities. Not only because the velocities differ, but also because the tidal range differs per period. Greater tidal ranges are observed during spring tide, while during neap tide the tidal range is usually below 15 cm. In the first and third periods, the tidal ranges during flood are both 46 cm. The second period has a maximum tidal range during spring tide of 34 cm.

In the first period, the water level difference decreases towards the end because it approaches neap tide. During spring tide in the first period, the minimum water level difference becomes greater while the maximum level difference decreases. This is due to the water level in Awa di Lodo rising during the first period (Figure 21 and Figure 22). This causes the flood speeds to decrease but there is a larger gradient during ebb from Awa di Lodo towards the open water resulting in faster ebb flow speeds. In the second period, the ebb speeds seem to be stable while the flood velocity varies with small water level differences. During neap tide, the water level difference sometimes is too low to reverse the direction of the flow resulting in only flow out of the mangrove forest. The duration of the ebb speeds is also longer but this is expected due to the ebb-dominant character of creeks (Horstman et al., 2021). The third period follows a similar pattern as the first period with respect to peak flood speeds, namely larger peak flood speeds during spring tide and slower peak flood speeds during neap tide. The peak ebb speeds do not see much fluctuation over the third period, with only a small increase during spring tide.

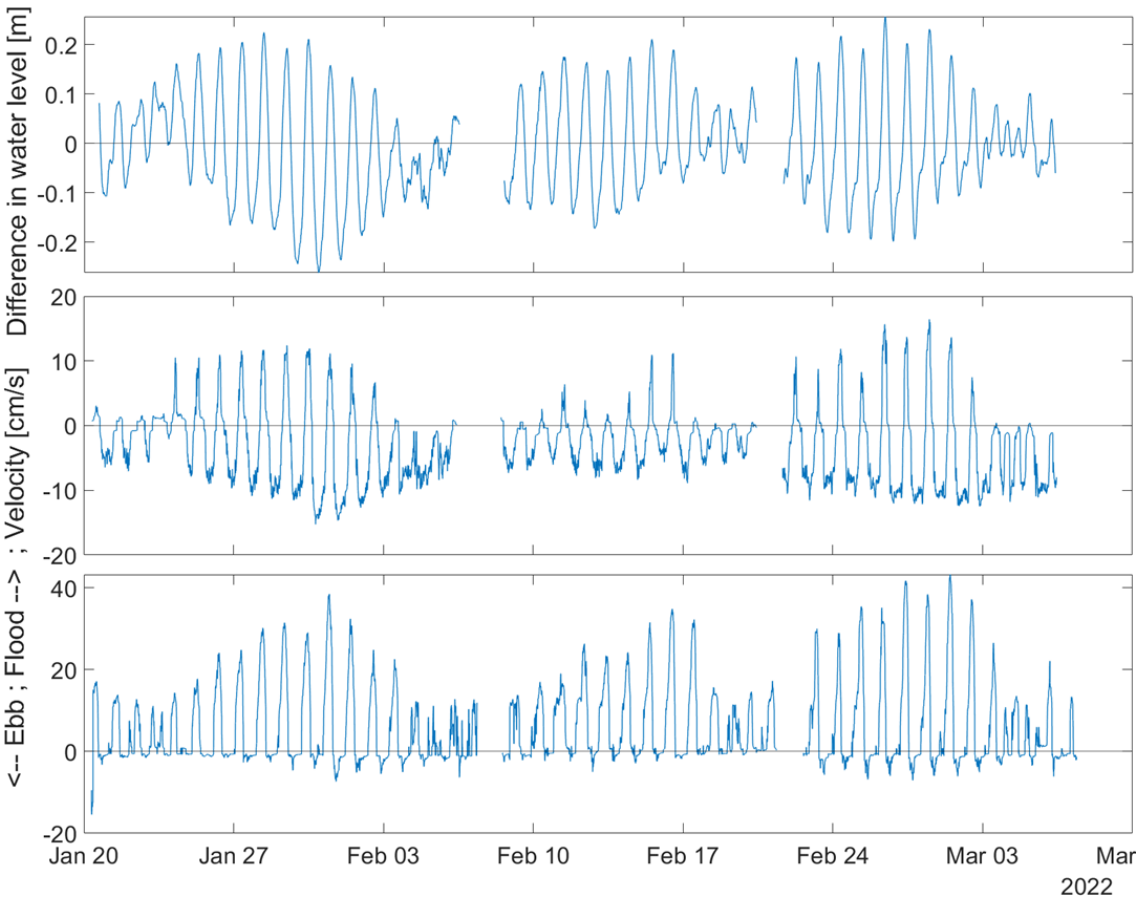

Figure 30: Water level difference between the forest fringe (WF) and Awa di Lodo (BW) (upper figure), the flow velocities in Kreek di Taco (EC) (middle figure) and the flow velocities in Kreek di Pedro (WC) (lower figure)

The ebb-flood velocities in Kreek di Pedro differ in magnitude from the velocities in Kreek di Taco (Figure 30). Note the different scales on the y-axis of Figure 30. Similar to EC, the duration of the water flow in the ebb direction is longer than in the flood direction. At WC the peak ebb velocities are much smaller compared to the peak flood velocities. In the first period, the peak velocities for both ebb and flood are increasing towards spring tide and decrease near neap tide. This pattern prevails in the other periods as well. The ebb-flood velocities for WC show that there is mainly a flow directed into the mangrove forest and less water is flowing out.

Based on Figure 30 there seems to be a clockwise pattern in the tidal flow through the forest. There is much more water flowing in at WC while there is more water flowing out at EC. These creeks are connected by Awa di Lodo where water throughflow could happen. This flow cannot be driven by the wind since the dominant wind direction is coming from the east, while this current is flowing towards the east in Awa di Lodo. Since the direction of the ebb and flood currents is changing per period and is not often in line with the direction of the creek, (Table 6) the clockwise flow pattern might not be as prominent as the results make it look.

Tidal stage-flow speed curves

Tidal stage-flow speed curves help visualize the relationship between the water level and the velocity variations. In Figure 31 and Figure 32 the water level is plotted against the water velocity for each of the three periods during spring tide. An increase in water level causes an increase in flood velocities. The magnitude of the ebb velocities is linked to the channel dimensions and is less dependent on the water level compared to the flood velocities.

Differences between the spring-neap cycles of the tidal stage-flow speed curves are mainly found between the second period and the other two. Due to a smaller tidal range in the second tidal cycle, the velocities induced by the tide are also lower. These lower velocities result in a smaller velocity range of the tidal stage-flow speed curves.

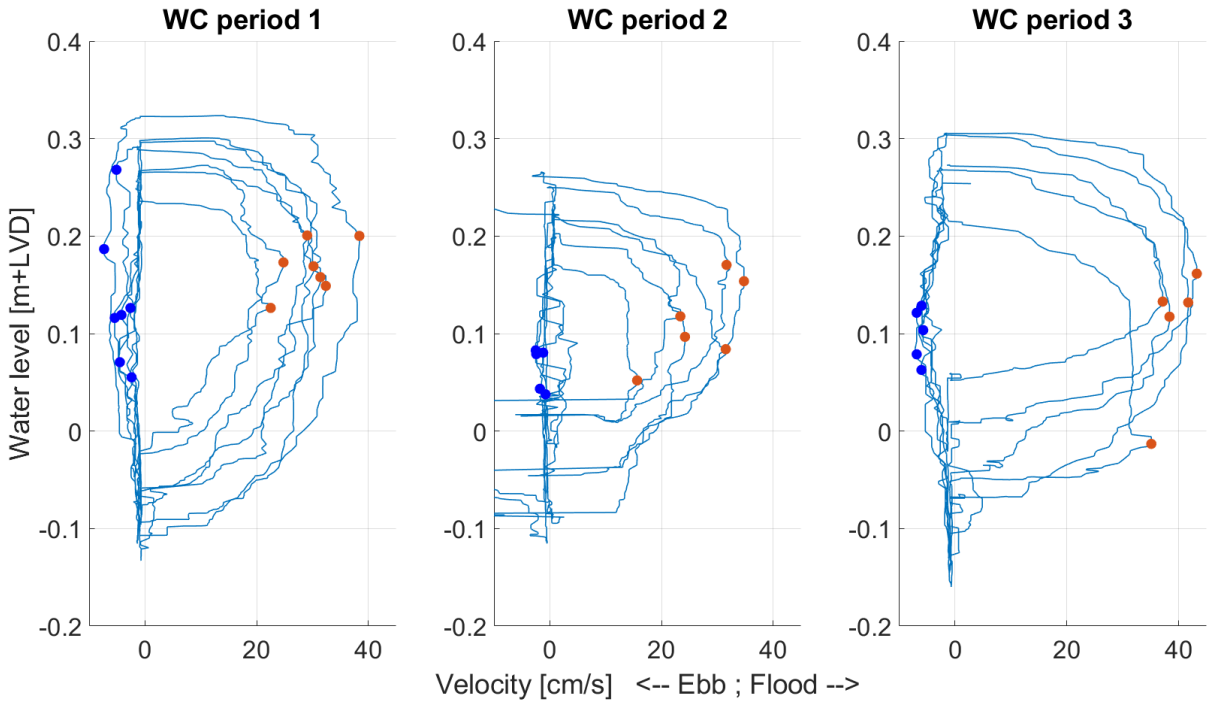

Figure 31: Tidal stage-flow speed curves of WC during spring tide for all three spring-neap cycles with the blue dots being the maximum ebb velocities and the red dots the maximum flood velocities of a tidal cycle

Figure 31 shows that the maximum flood velocities at WC are generally in a range of 20 and 44 cm/s with their corresponding water levels being between 0.05 and 0.20m+LVD (with two outliers). The maximum ebb velocities at WC are generally between 1 and 8 cm/s with their corresponding water levels being between 0.04 and 0.27m+LVD.

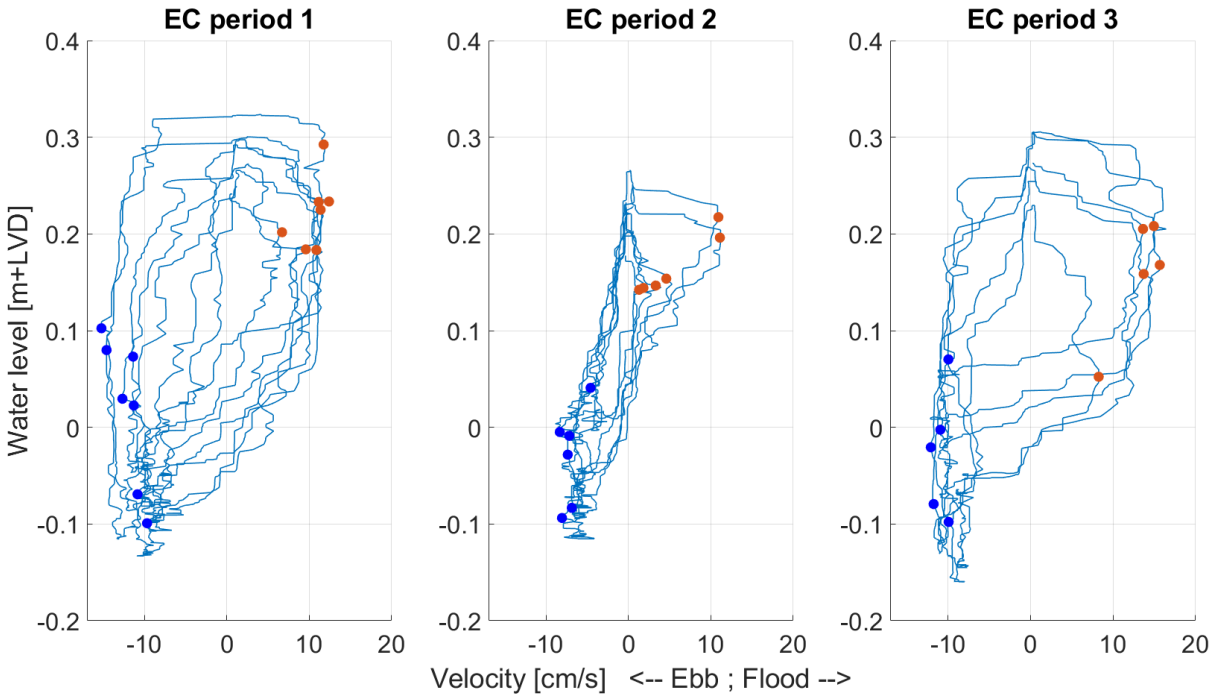

Figure 32: Tidal stage-flow speed curves of EC during spring tide for all three spring-neap cycles with the blue dots being the maximum ebb velocities and the red dots the maximum flood velocities of a tidal cycle

Figure 32 shows that the maximum flood velocities of EC range from 1 to 16 cm/s with their corresponding water levels being between 0.05 and 0.30m+LVD. Maximum ebb velocities for EC are generally between 4.5 cm/s and 16 cm/s with their corresponding water levels between -0.10 and 0.11m+LVD.

At WC most of the maximum ebb velocities are reached near 0.1m+LVD. This indicates that at that water level there is a transition of most of the water volume transported from sheet and creek flow to mainly creek flow resulting in an acceleration of the flow in the creek. Most ebb flow speeds, for both creeks, are concentrated around 2 cm/s.

4.9 Tidal asymmetry

In mangrove creeks, the maximum ebb current velocity is usually larger than the maximum flood current velocity (Mazda et al., 1995). This difference in ebb and flood velocity can be referred to as tidal asymmetry. Tidal asymmetry can result in self-scouring of the tidal creeks, keeping the creeks open over time (Wolanski et al., 1990). Mangrove forests induce tidal asymmetry by causing a phase shift in the velocity in the mangrove forest compared to the creek, shifting the peak velocity in the creek to the ebb flow (Mazda et al., 1995). Very dense vegetation induces drag forces slowing the flow in the mangrove forest down so much that the tidal asymmetry decreases. When the drag force is excessive, the reduction of the creek velocity possibly even causes sedimentation in the creeks (Mazda et al., 1995).

For Lac Bay, this study considered the *peak velocity asymmetry*, an uneven peak ebb and flood velocity, and *tidal duration asymmetry,* an unequal duration of the rising and falling tide (Dronkers, 1986; Guo et al., 2019). Flood dominance is when the flood peak velocities are greater than the ebb peak velocities and when the rising tide is shorter than the falling tide. Ebb dominance has greater ebb peak velocities and a fasting falling tide. Flood-directed residual sediment transport is caused by flood dominance, whilst ebb dominance causes the sediment to be flushed out seawards (Guo et al., 2019).

Peak velocity asymmetry

Figure 33 shows the velocities in the west and east creek over time. The ratio between the peak flood ($V_{max,flood}$) and peak ebb velocities ($V_{max,flood}$) gives insight into the peak velocity asymmetry (V_a) of both creeks (equation 6). If the ratio is greater than 1, the creek is ebb dominant and if it is smaller than 1, it is flood dominant. However, sometimes the flow does not reverse, creating a negative peak flood velocity. Peak velocity asymmetry values with a negative peak flood velocity are marked orange instead of red in Figure 34 and Figure 35. In the second period and during neap tide, the peak flood velocities are really small which creates large values for the peak velocity asymmetry.

$$V_a = \left| \frac{-V_{max,ebb}}{V_{max,flood}} \right| \quad (6)$$

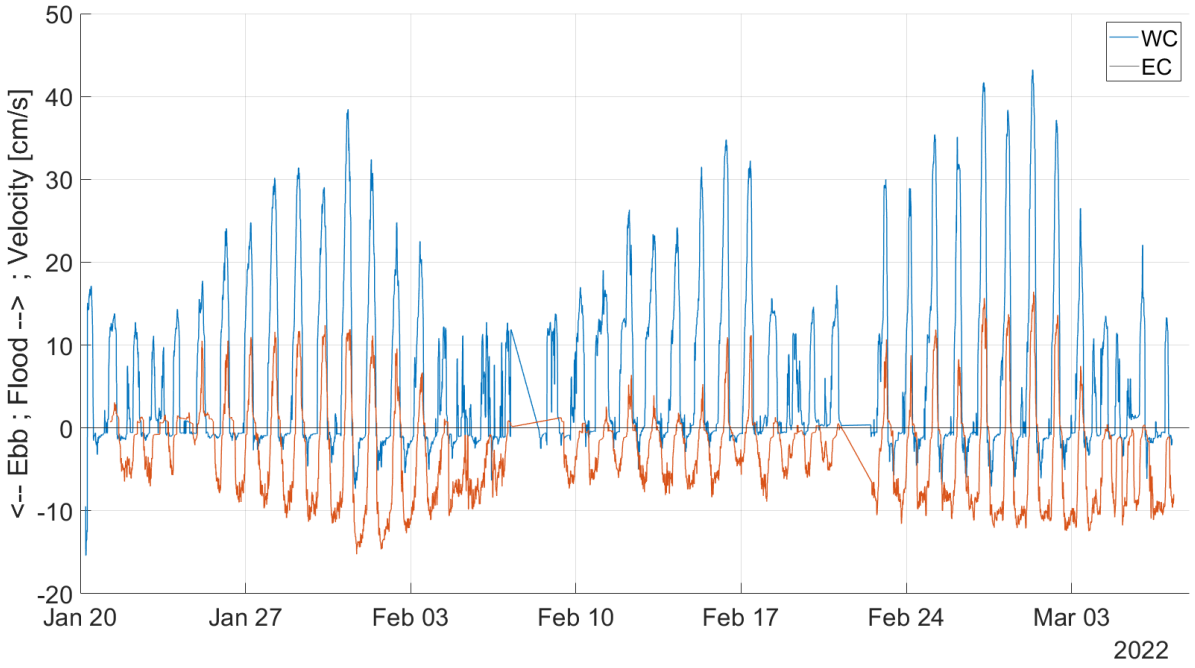

Figure 33: Flow velocities at Kreek di Pedro (WC) and Kreek di Taco (EC)

Since the velocity and the water level difference are in phase, attributing a maximum flow velocity to a certain phase creates inaccurate results. These inaccurate results occur because the maximum velocity has a high chance of being on the edge of ebb/flood periods and could therefore be counted twice. Therefore, the velocity data is shifted 3 hours earlier in time so the velocity caused by a tide is placed into the ebb/flood phase that caused those velocities.

The water level difference between Awa di Lodo and the forest fringe is important for the tidal asymmetry. With a large positive water level difference (higher water in the fringe) the flow is flood dominant which can be seen mostly during spring tide. In Kreek di Taco, the ebb/flood dominance shifts over during a spring-neap cycle. At the falling stage of the first period, the water level in Awa di Lodo has risen while the tidal cycle approaches neap tide, which creates a larger negative difference (high water in Awa di Lodo). This results in the shift of the peak velocity asymmetry from flood to ebb dominant. During the measurement campaign, the direction of the flow for all neap tides in Kreek di Taco does not or barely reverses, creating a strong ebb dominance. Figure 34 shows this by having large positive and negative ratios. The second period is characterised by an ebb dominant pattern with high ratios during neap tide due to the small peak flood velocities. During spring tide in the third period, the ratios mostly remain below 1, thus being flood dominant.

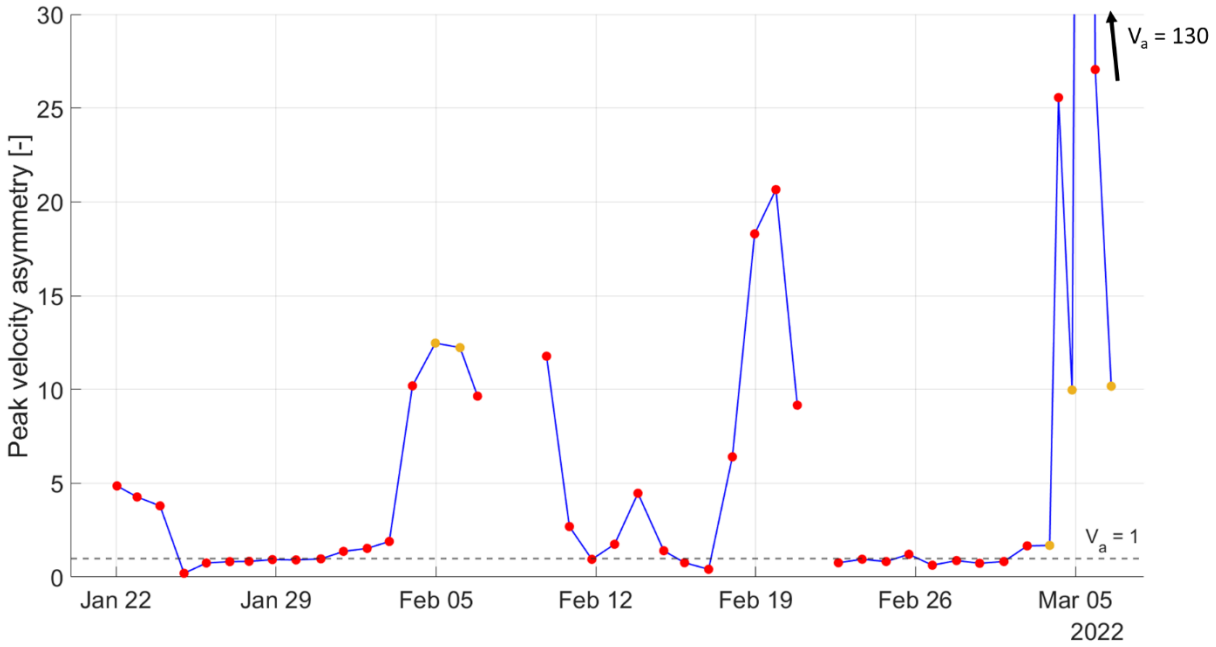

Figure 34: Peak velocity asymmetry of Kreek di Taco (EC)

In Kreek di Pedro there is a strong flood dominated pattern resulting in ratios between 0 and 1 (Figure 35). In the falling stage of the first period the ratio increases due to the increasing peak ebb velocities. Overall the ratio stays firmly below 1 with no clear difference between spring and neap tide.

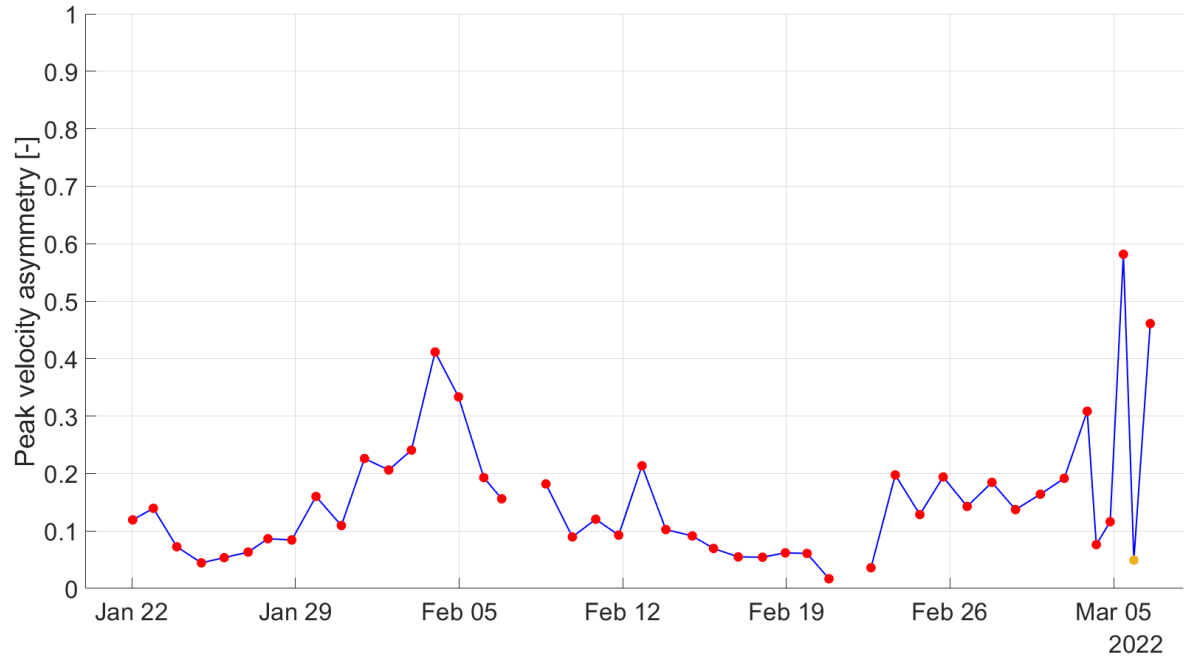

Figure 35: Peak velocity asymmetry at Kreek di Pedro (WC)

Tidal duration asymmetry

Water levels in Awa di Lodo show tidal duration asymmetry in the form of flood dominance as shown in Figure 36. The flood takes 9.5 hours which is much shorter than ebb which lasts for 15 hours. This difference is mainly due to the bathtub effect described in section 4.6. The fact that this tidal asymmetry is present also indicates that the inflow into the backwater is dominated by sheet flow while the outflow is dominated by creek flow.

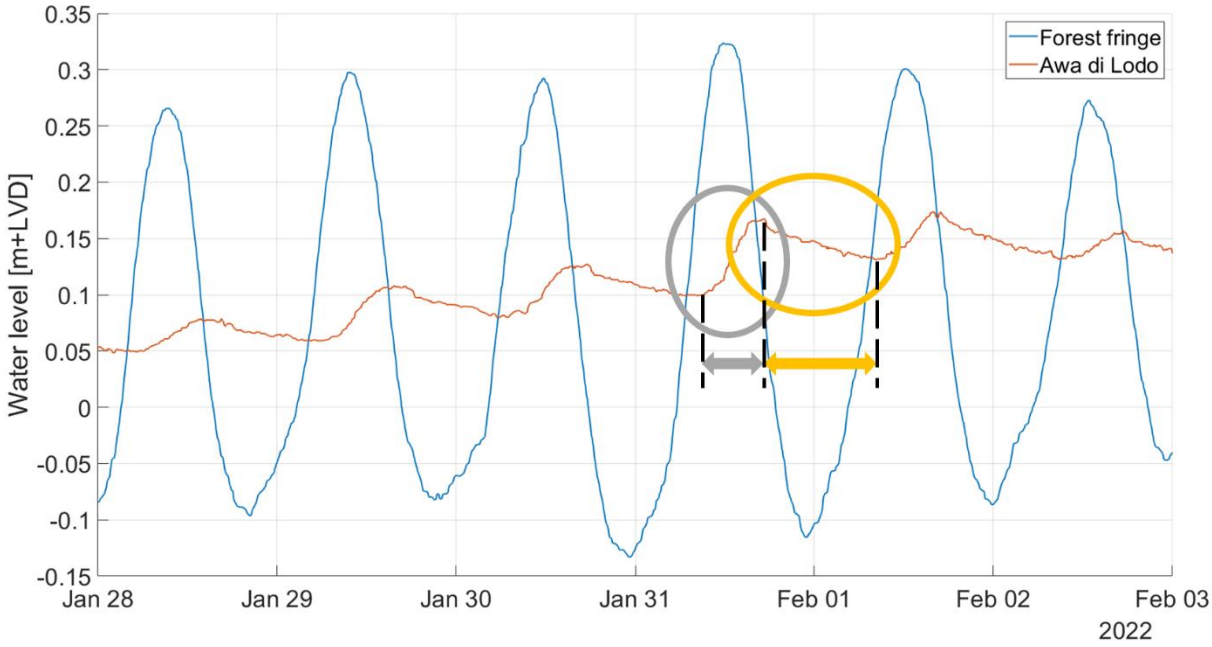

Figure 36: Tidal duration asymmetry as observed in Awa di Lodo (BW) between 31 January and 1 February with the grey circle and arrow depicting the duration of flood and the yellow circle and arrow depicting the duration of ebb

5. Delft3D model set-up

The numerical modelling package of Delft3D that models flow is combined with a vegetation model for the assessment of Lac Bay. The bathymetry as described in section 4.2 was used in this model. All landward boundaries are defined by the road around Lac. The seaward boundary is based on extending the road boundary towards the sea and connecting those locations with a straight line (Figure 37).

Figure 37: Model domain of Lac Bay with the landward boundary in yellow and the seaward boundary in blue

5.1 Boundary conditions

A tidal wave is imposed on the seaward boundary based on the water level measurements from the field study. The sea measurement station was selected for this purpose since it is located near the seaward boundary of the model. Since there is no RTK data of the RBR Virtuoso placed at sea, a manual correction is made. Data of the west fringe (WF) (as the most stable measurement location) and data of the measurement station at sea are almost identical (Figure 38). The overlapping period is from 28-01-2022 9:30 till 2022-02-06 18:00. To compensate for not having a water level, the water depth data of the measurement station at sea is converted to water level data by manually subtracting 6.59m from the water depth data so the data overlaps with that of WF (Figure 38). The sea measurement station is put into place later than the fringe stations. To create a longer-ranging time span for the tidal wave at the seaward boundary, the water levels from WF are added to the data of that of the sea measurement data. This can be done because data of WF and sea are almost alike.

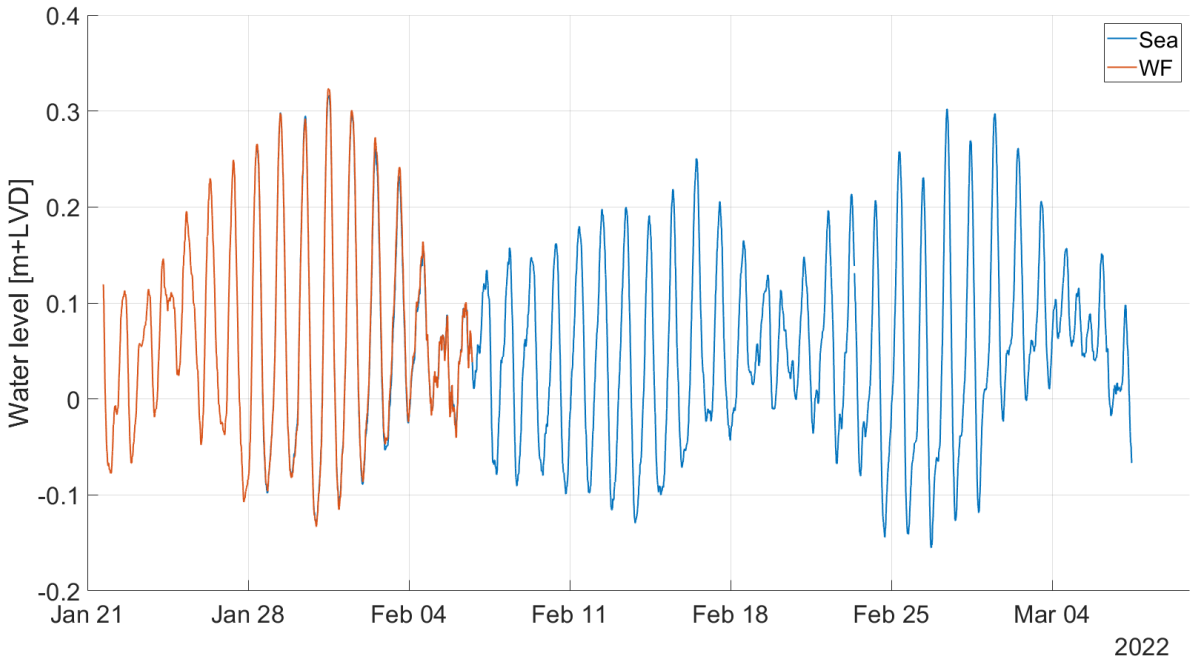

Figure 38: Comparing the water level data of the measurement stations Sea and WF

5.2 Grid

Creating a grid is needed for Delft3D so numerical calculations can be done. Multiple steps are taken to get to the final model grid. It is important to create an accurate representation of the bathymetry in the model since the tidal patterns are mostly based on the characteristic topography of the area (Horstman et al., 2015). Hence, a trade-off is made between computational time and accuracy of the representation of the bathymetry.

Initially, a base grid of 20-by-20 meters was made for the open water parts of Lac. At locations where more complex interactions are present, a finer grid is needed to be able to represent the interactions in creeks and in the mangrove forest. Therefore, the grid was refined in the mangrove area to 10-by-10 meters. Even more complex interactions can be found at the creeks which are between 4 and 6 meters wide. Without refining the grid, creeks would not be represented because the creek bathymetry would be averaged over the grid cells. Along the creeks, the grid cells are refined to a 5-by-5 meter grid cells. To be able to match the dimensions of the creeks, the areas close to the creeks are refined further to 2.5-by-2.5 meters.

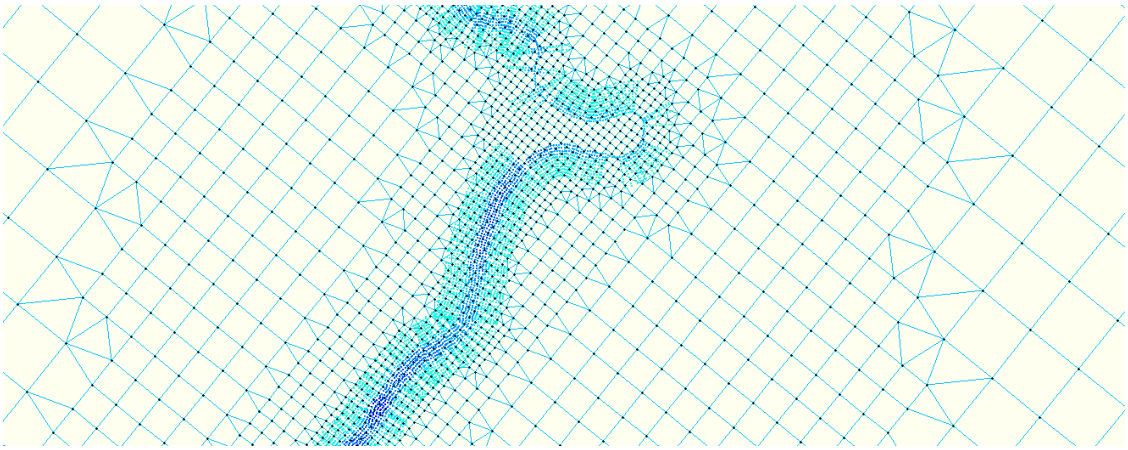

Figure 39: Grid of the Delft3D model going from 20-by-20 meters on the left and right side, to 2.5-by-2.5 meter inside the creeks

Including a finer grid structure in and near the creeks allows water to flow through easier since these cells have a low hydraulic resistance due to their increased depth. With larger grid cells, these height differences are much smaller due to spatial averaging of the bed levels, resulting in a wider but less deep 'creek' which has more resistance due to bottom friction. The grid is not refined any further than 2.5-by-2.5 metres because the computational time needed would be too long to work well with the model.

Figure 40 shows the effect of the grid refinements on the simulated water levels in Awa di Lodo. Since water can enter and leave the area better through the creeks for greater grid resolutions, the tidal exchange and thus the tidal range increases substantially in Awa di Lodo.

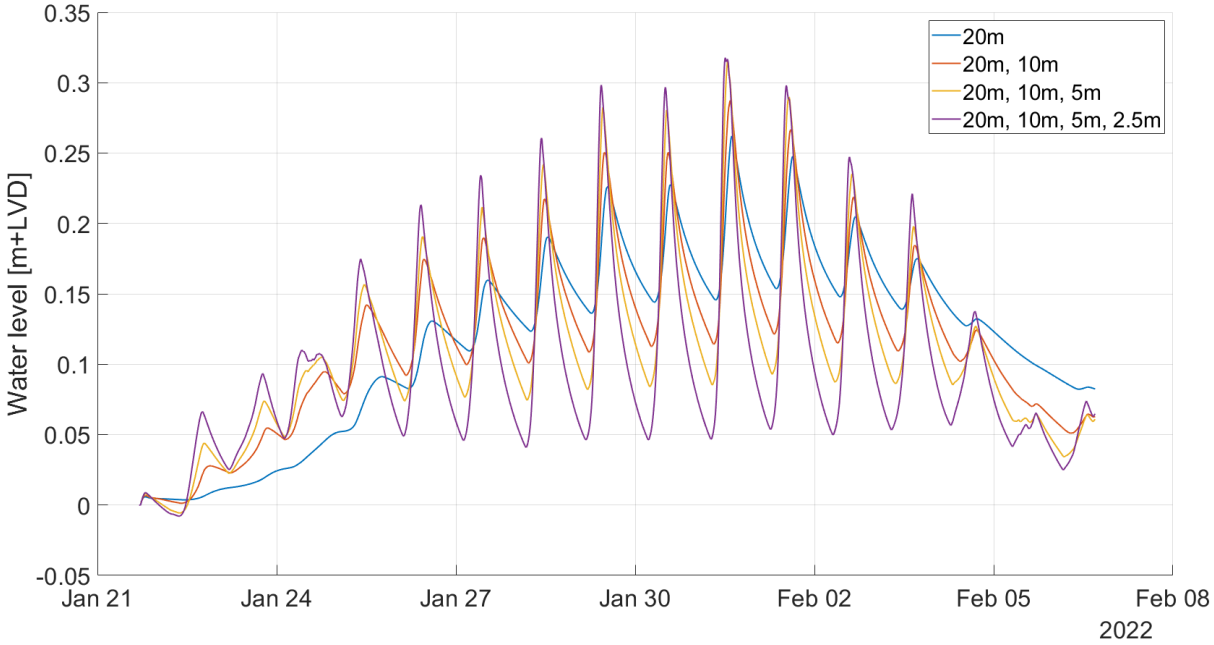

Figure 40: Water level in Awa di Lodo per grid refinement in model runs without vegetation and a Manning bottom roughness value of 0.023

5.3 Runtime

When the model starts, the water has a uniform level of 0 m to ensure water was present at the start of the simulation. A spin-up time of approximately 2 tidal cycles is needed to initiate the water movement in the complete model domain. The model runs start at the moment that the seaward boundary conditions start to fluctuate, which is at the same time as the start of the measurement period from the field study. Since the field study measurements started during neap tide, the model was also started at neap tide. The final grid of the model has a runtime of between 9 and 13 hours per spring-neap cycle.

5.4 Model parameters, vegetation characteristics and calibration

Adding vegetation to the model is important for the accuracy of the model. Mazda et al. (1995) suggest, based on numerical models, that the drag force caused by the mangrove forest strongly influences the water flows in the creeks. Based on Google Earth, the mangrove area of Lac Bay is determined (Figure 9). Characteristics of the mangroves are based on field data presented in Table 2 and taken uniform over the entire mangrove area. Values from the field monitoring presented in Table 2 are averaged and those average values used in the model for the vegetation can be found in Table 7. In the model, an elevation of -0.05m+LVD is needed for the vegetation to be present. By implementing this boundary condition there is no vegetation present in the creeks.

Table 7: Vegetation characteristics as used in the model

Root density (nr/m^2)	174
Root diameter (m)	0.016
Root height (m)	0.476

During the calibration, the bed roughness was adjusted. To improve the model results, the Manning bottom roughness coefficient was changed from 0.023 to 0.030. This value is based on earlier research in a mangrove forest in Thailand by Horstman et al. (2015). Including the new bottom roughness and vegetation in the model gives more accurate predictions of the water level in Awa di Lodo (Figure 41) compared to the situation without these changes (Figure 40). The tidal range in Awa di Lodo is lower due to increased drag forces exerted by the increased bottom roughness and the vegetation, which slows down the water flow to and from Awa di Lodo. Other model parameters are the default settings from Delft3D.

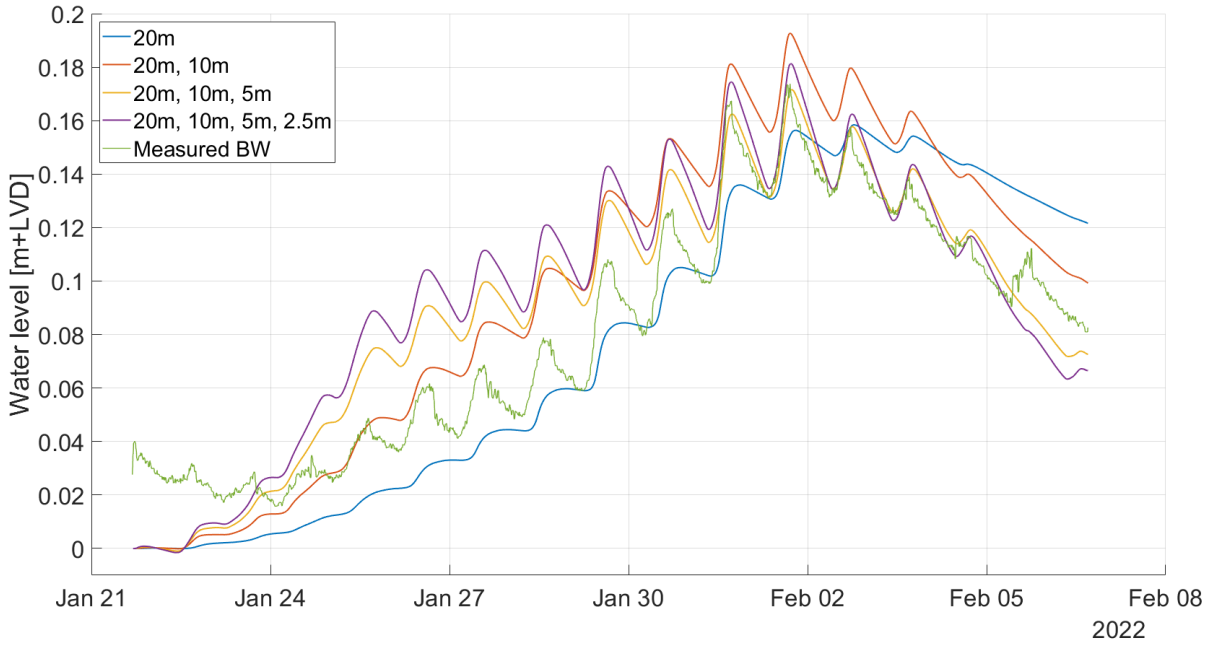

Figure 41: Water level in Awa di Lodo per grid refinement in model runs with vegetation and a Manning bottom roughness value of 0.030

5.5 Model validation

The high water event in the first spring-neap cycle simulated by the model has a good resemblance with the field data (Figure 42). The model simulations reach the maximum water level during the first period within one centimetre. Modelled water levels in Awa di Lodo increase faster than the water level from the measurements indicating that the virtual water faces not enough resistance to flow into the backwater. Declining water levels at the end of the first spring-neap cycle simulated by the model have a good resemblance with the field data. However, the model overestimates the amount of water left in Awa di Lodo resulting in higher water levels. This is probably due to the threshold of water flowing out of Awa di Lodo being too high in the model compared to the real world. The right side of Figure 42 shows that the tidal exchange (discharge into and out of Awa di Lodo) is mainly differing in flood volumes and that ebb volumes are relatively constant. When the water level in Awa di Lodo is above 0.1m+LVD, the water starts flowing out faster.

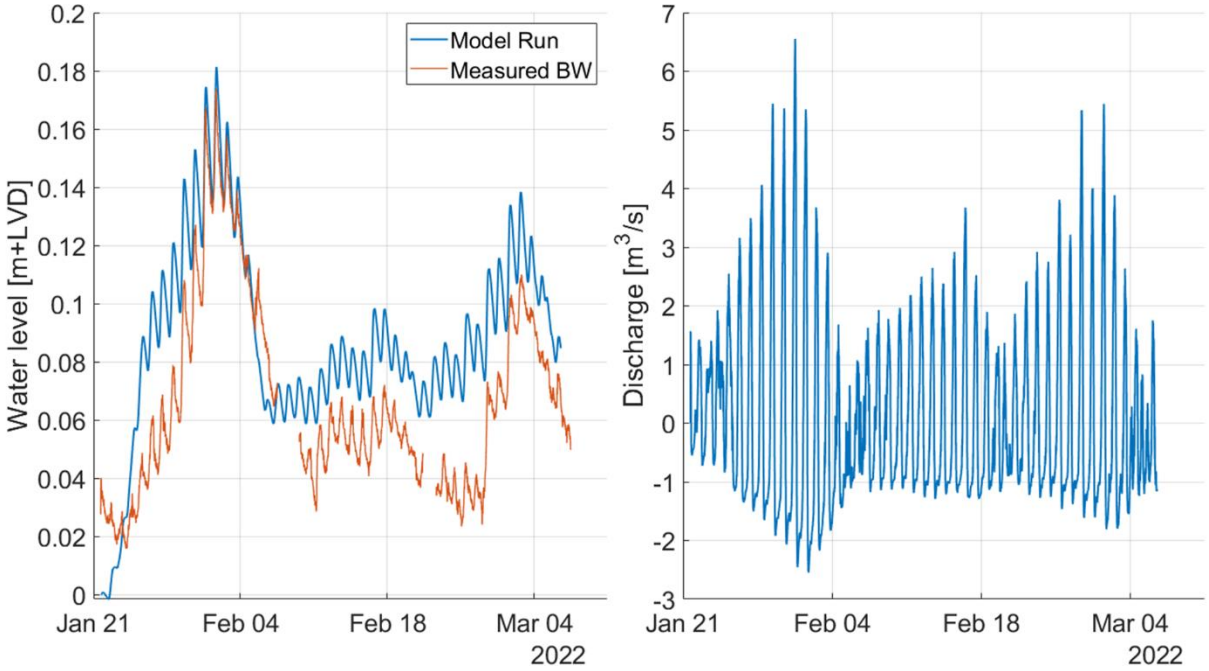

Figure 42: Water levels in Awa di Lodo for the reference situation and the measured water level (left); and the tidal exchange for the reference scenario (right) for three spring-neap cycles

For the flow velocities, WC measurements have the same order of magnitude as the model results and the timing of switching of the flow is good. Only WC fails to capture the slow ebb velocities almost completely. The modelled CC velocities have a poor representation of the flood velocities but reach the same order of magnitude for the ebb velocities. Modelled velocities at EC show a very good agreement with the field measurement.

Overall the model has a good resemblance of the water levels and flow velocities. Although the model does not perfectly represent quantitative water levels and flow velocities, the simulated water levels and tidal flow velocity patterns match qualitatively with the field observations.

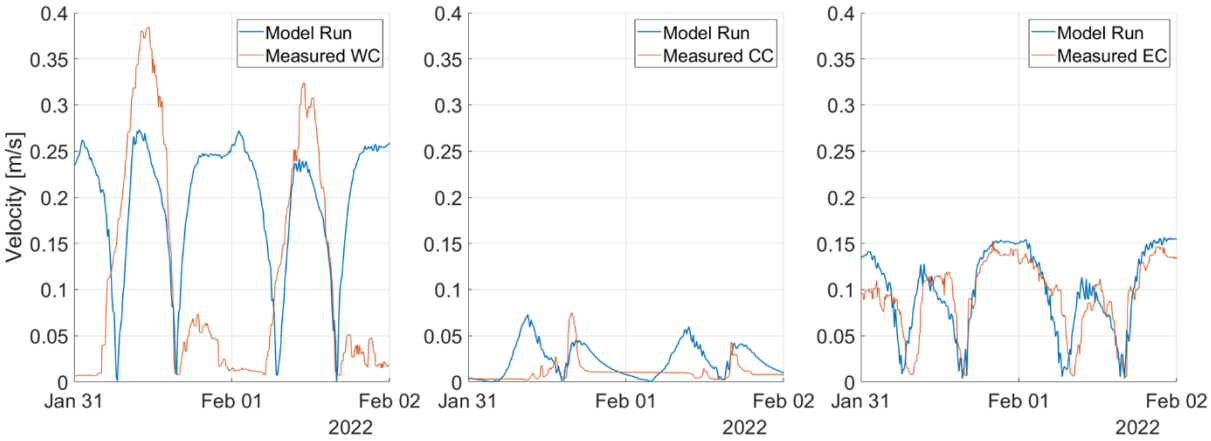

Figure 43: Measured and modelled water velocities of WC (left), CC (middle) and EC (right)

6. Contribution of creeks to the tidal exchange

In this chapter, the contribution of creeks to the tidal exchange of Awa di Lodo is investigated, including the effects of scenarios for creek restoration. The Delft3D model, as described in the previous chapter, is used to assess the change in tidal exchange, flow velocities and water level of the backwater per different creek scenario. The results of the different scenarios are compared to the reference scenario. The reference scenario includes the bathymetry and grid as described in chapter 5 (purple line in Figure 41). For the creek restoration scenarios the bathymetry is altered and if needed, local refinements of the grid are performed to be able to capture the hydrodynamic effects of for example newly created creeks. Figure 44 shows the creek profiles of the scenarios that rely on a change in the creek profile.

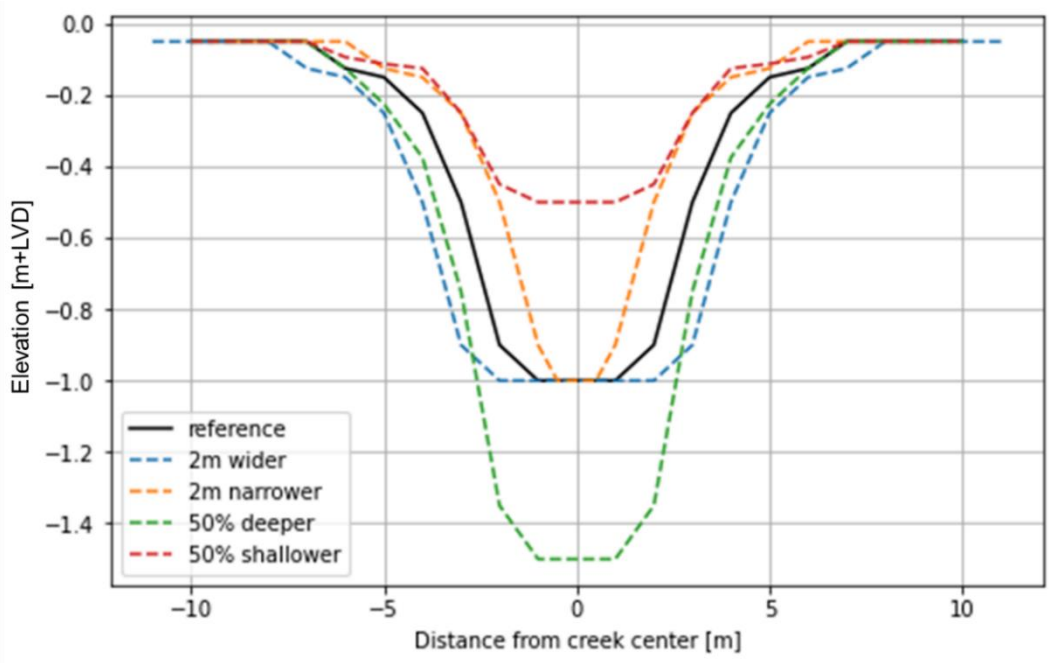

Figure 44: The reference creek profile with the adjusted creek profiles for the creek restoration scenarios

All nine scenarios are:

1. Reference scenario (section 6.2)
2. Scenario without creeks (section 6.3)
3. Scenario with a 50% increase in creek depth (section 6.4)
4. Scenario with a 50% decrease in creek depth (section 6.4)
5. Scenario with a 50% increase in creek width (section 6.5)
6. Scenario with a 50% decrease in creek width (section 6.5)
7. Scenario where the centre creek gets extended towards Awa di Lodo (section 6.6)
8. Scenario with a new creek from the forest fringe to Awa di Lodo (section 6.7)
9. Scenario where the eastern creek gets extended towards Awa di Lodo (section 6.8)

Each scenario is compared to the reference scenario. When possible, the scenarios are compared to other relevant locations in the field as well. The representative date that is used to compare values is February 1st. At this moment in time, the model has good resemblance with the field monitoring data. Besides, February 1st is during spring tide, so the tidal exchange and velocities are greater and easier to compare. To be able to quantify the tidal exchange, a transect was drawn over the islands of Lac and perpendicular over the creeks (Figure 45). By doing this the water volume surpassing that line could be computed.

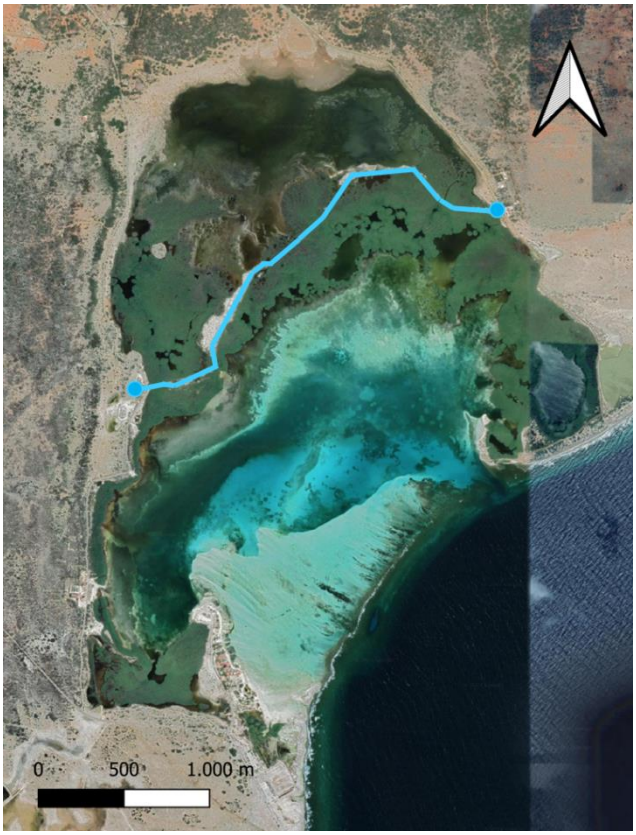

Figure 45: Manually drawn transect in blue over which the modelled tidal exchange is calculated

The cumulative discharge is represented in the form of the water level in Awa di Lodo. Figure 46 shows that this discharge and the amount of water in Awa di Lodo follow the same trend (and basically represent the same thing). Due to hypsometric effects this is not a linear relation, but because it is a large area it is close to linear. Based on Figure 46, it can be concluded that an addition of 1 cm to the water level in Awa di Lodo roughly translates to 1.8 x 10^4 m^3 of water volume crossing the cross-section. During spring tide in one tidal cycle, the tidal exchange volume is roughly 1.0 x 10^5 m^3.

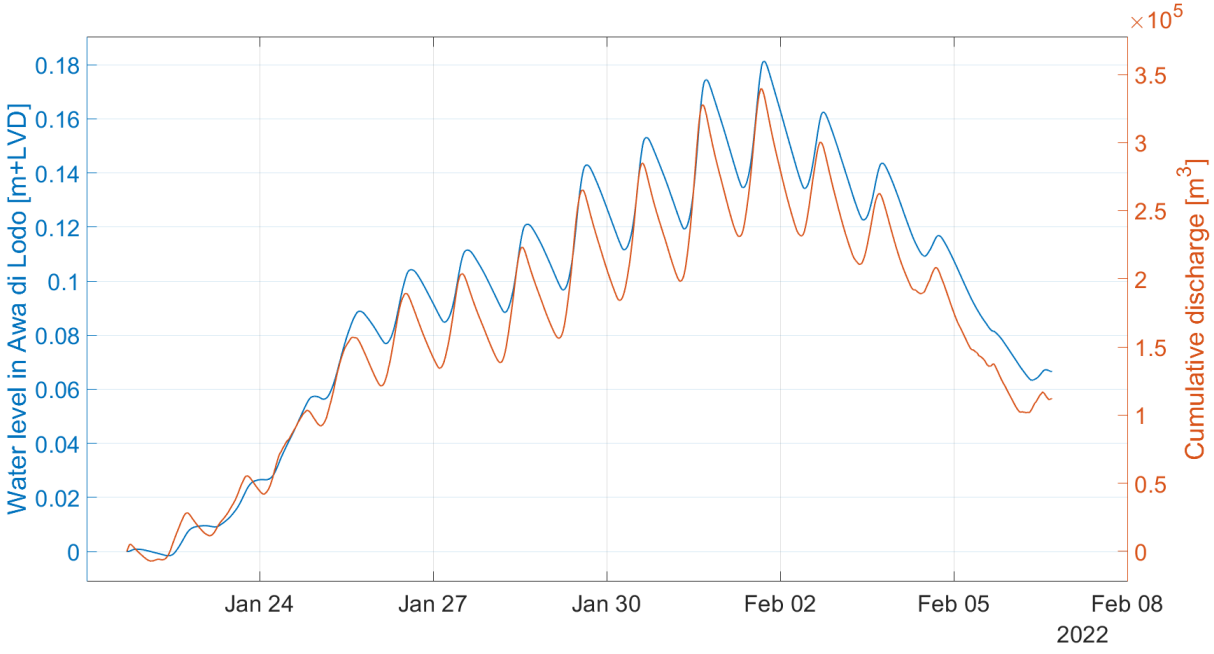

Figure 46: A comparison between the water level in Awa di Lodo and the cumulative discharge of the reference scenario

During a tidal cycle two distinct flow paths can be observed, sheet flow (flow over the vegetated forest) and creek flow (flow through the creeks) (Horstman et al., 2013). Sheet flow is responsible for the movement of a greater volume of water during high tide than during low tide. Creek flow prevails when the water level falls below the vegetated bed level and most water is transported via the creeks. Based on the model results for grid refinement in Figure 41, the importance of creeks for the tidal exchange is already visible. A greater tidal range is induced when the creeks are better represented in the model due to the flow having easier pathways (creeks) to influence the water level in Awa di Lodo. This was also observed in other mangrove forests, such as at a study site in Thailand where the tidal exchange is dominated by creek flow (Horstman et al., 2015).

6.1 Residence time

The residence time (k in days) is defined as the volume of the backwater (V in m^3) divided by the sum of the freshwater input (Q_f) and the tidal exchange volume (Q_t), both in m^3/day. Equation 7 shows this relation.

$$k = \frac{V}{Q_f + Q_t} \tag{7}$$

To decrease the residence time in Awa di Lodo, either V must decrease or Q_f or Q_t must increase. The freshwater in and outflux of the area are assumed to be relatively small and taken as 0 in the calculations. Therefore, to reduce the residence time, the tidal exchange must increase. Reducing the residence time (or increasing the refreshment rate), reduces the salinity in Awa di Lodo. For the scenarios investigated in this chapter, only Q_t is considered. Q_t is an estimation of the tidal exchange during spring tide of the first spring-neap cycle, on the 1st of February.

To be able to compute the tidal exchange, a volume for Awa di Lodo must be approximated. At timestep 1 in the model, the volume of water present in Awa di Lodo is approximately $2.4 \cdot 10^5$ m^3. The tidal exchange at spring tide is used to estimate the residence time. At the start of the 1st of February, an additional water volume of approximately $2.1 \cdot 10^5$ m^3 is added to Awa di Lodo compared to the start of the model run (Figure 46). This results in a total virtual water volume at the start of February 1 in Awa di Lodo of $4.5 \cdot 10^5$ m^3. Inaccuracies in this estimation have no major consequences as the residence time is used to compare the different scenarios.

6.2 Reference scenario

In the reference scenario, the model is made to resemble Lac Bay as much as possible. Islands, creeks and other bathymetric characteristics are combined with the vegetation for this scenario to calculate the water levels of the backwater, the tidal exchange and the flow velocities in the creeks. In the rising stage, the water level of Awa di Lodo is overestimated by the model (Figure 47). The measured water level data shows a good resemblance of the water levels during spring tide and can capture the water levels in the falling stage of the spring-neap cycle. On February 1st, the maximum flood discharge is 5.3 m^3/s and the maximum ebb discharge is 2.5 m^3/s. The modelled tidal exchange is $1.09 \cdot 10^5$ m^3 resulting in a residence time of 4.15 days.

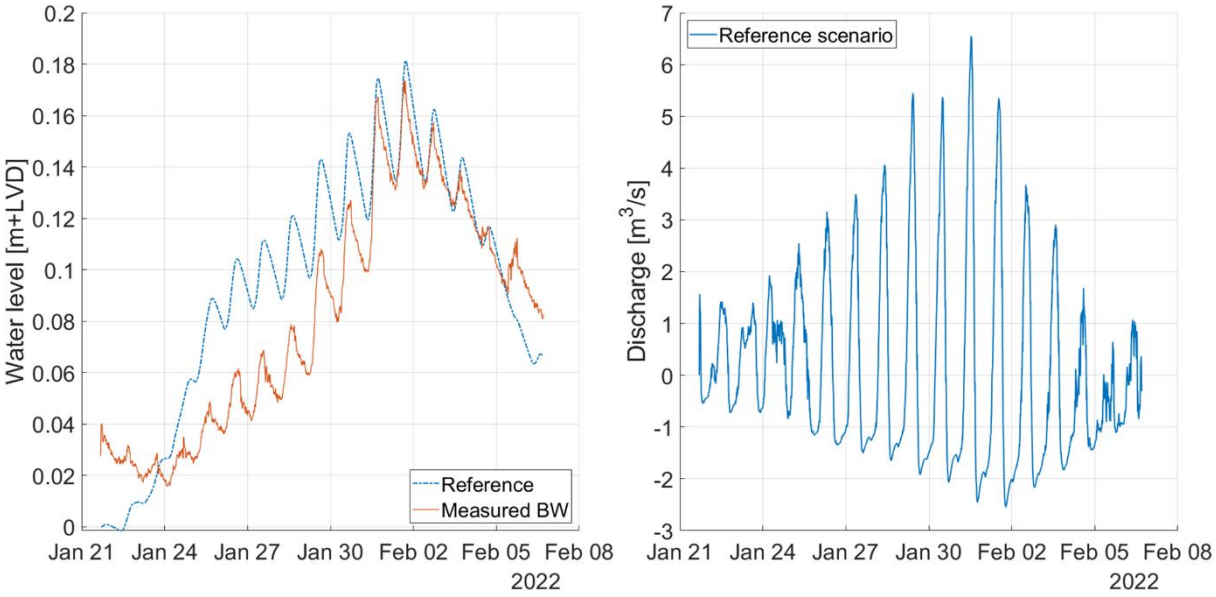

Figure 47: Water levels in Awa di Lodo for the reference situation and the measured water level (left); and the tidal exchange for the reference scenario (right)

Since the model run from the validation is the reference scenario but longer, the flow velocities from Figure 43 are representative flow speeds for the reference scenario. The modelled flow velocities are in the same order of magnitude as the monitored flow velocities. On February 1st the maximum flood speeds are 0.24, 0.06 and 0.11 m/s for the western creek (WC), centre creek (CC) and eastern creek (EC) respectively. The maximum ebb speeds are 0.27, 0.04 and 0.15 m/s for the WC, CC and EC respectively. Following the model results, the WC and EC both have an ebb dominant peak velocity asymmetry while CC has a flood dominant peak velocity asymmetry.

6.3 Effect of no creeks

Having no creeks in the system is represented in the model by removing the cross-sectional area of the creeks (Figure 48). The lagoons, islands and other bathymetric characteristics are still present. Having no creeks in the model hampers the flow of water deeper into the mangrove forest since the water is forced through the high-resistance forest. In other words, there is only sheet flow present and the water level should reach a critical height to surpass the islands. The grid is identical to that of the reference scenario. The vegetation differs compared to the reference scenario because trees can now be located where previously creeks were present.

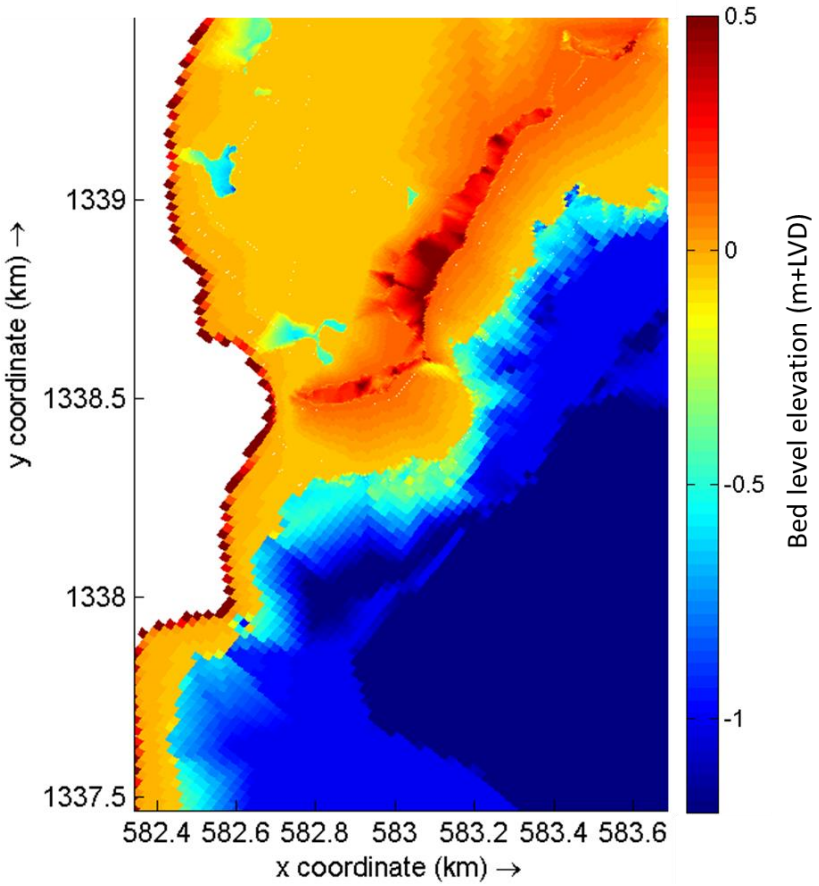

Figure 48: Snapshot of the bed level elevation in the 'no creeks' scenario

The left part of Figure 49 shows that the water level of Awa di Lodo in the 'no creeks' scenario follows a different path in reaching its highest water level and declines slower than in the reference scenario. This slower reaction of the water level is comparable to having a coarser grid where the creeks are not represented (Figure 41) due to the large grid cells. The water has no way of swiftly moving through the forest and no way to leave the forest quickly. This results in more water staying in the system over time and it will likely react as a damped system where the fluctuations are smaller due to the increased total friction. Having no creeks creates a water level in Awa di Lodo that is closer to the measured water level during the rising tides but the model fails to capture the water level when the tides are falling. The fast increase could be induced by too much water being transported via sheet flow thus increasing the tidal exchange. By elevating the bed level of the mangroves this effect is likely to become smaller.

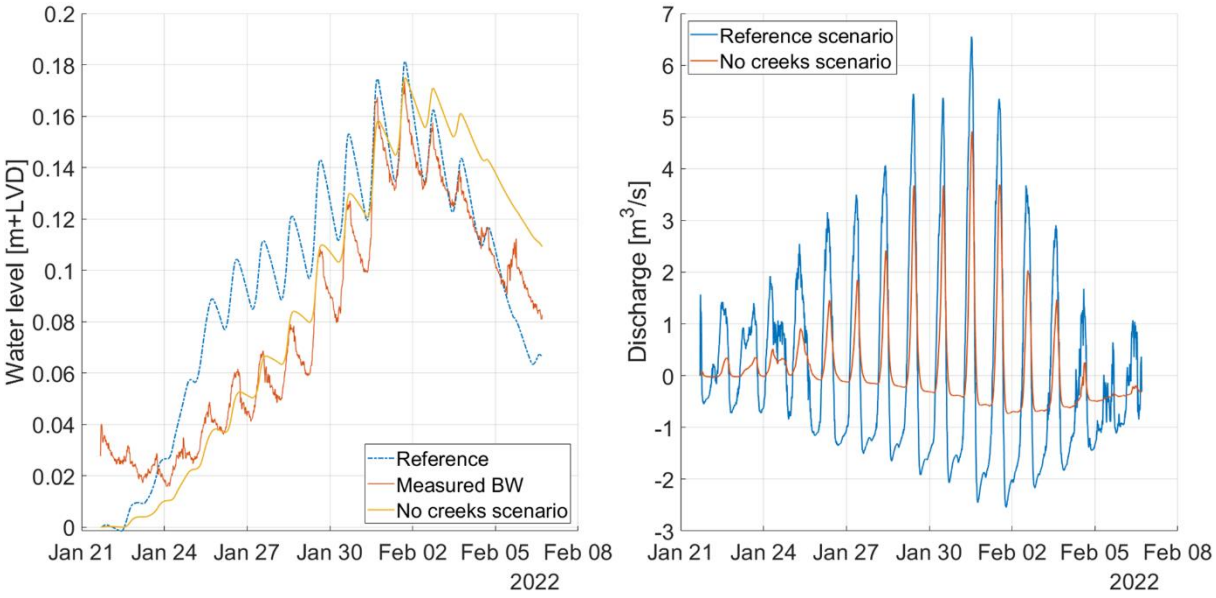

Figure 49: Water levels in Awa di Lodo for the reference situation, the 'no creeks' scenario and the measured water level (left); and the tidal exchange for the reference scenario and the 'no creeks' scenario (right)

That Awa di Lodo reacts less to the tide can also be seen in the right panel of Figure 49, where the tidal exchange is smaller in the 'no creeks' scenario. Creeks are clearly responsible for a large part of the tidal exchange in the area. Creeks especially facilitate the ebb tidal discharges, as these are reduced from 2.5 to 0.7 m^3/s when the creeks are removed (Figure 49). The flood tidal discharge is also reduced from 5.3 to 3.7 m^3/s. On the 1st of February, the modelled tidal exchange is $0.61 \bullet 10^5$ m^3 with a corresponding residence time of 7.35 days. This is an increase of 77% compared to the reference scenario, proving the importance of creeks for the tidal exchange.

Water speeds are much lower in the 'no creek' scenario than in the reference scenario and measured in the field (Figure 50). The maximum flood and ebb speeds are reduced below 0.02 m/s. This is because there are no creeks, so there are no locations in this scenario where high flow velocities are reached as they are normally reached in mangrove creeks.

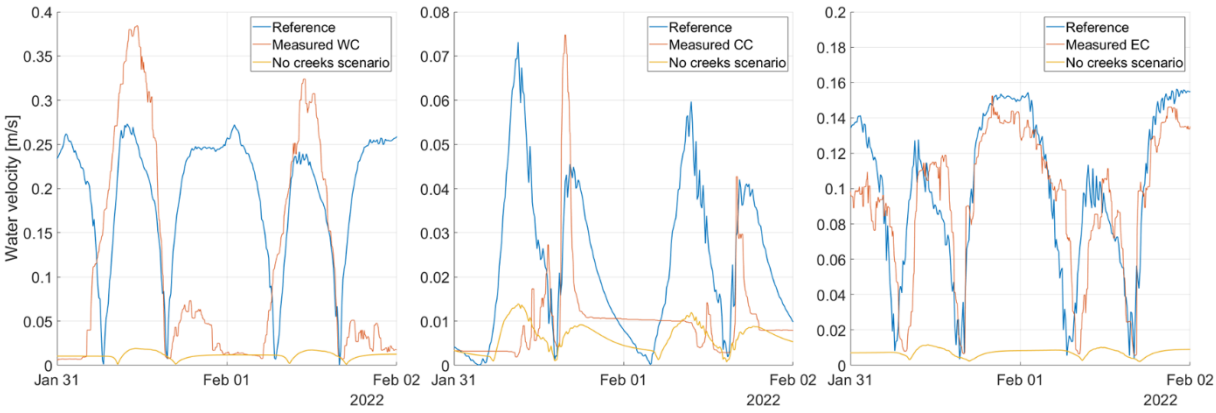

Figure 50: Water velocities of the reference scenario, measured in the field and of the 'no creeks' scenario for WC (left), CC (middle) and EC (right)

6.4 Effect of increasing and decreasing the depth of creeks

In this scenario, the existing creeks have been made 50% deeper and 50% shallower. Making the creeks deeper results in creating more space, increasing the low resistance path for the water to flow through the mangroves. The opposite is true for making the creeks shallower. The same grid is used as in the reference scenario. The only bathymetry changes are deeper and shallower creeks which does not affect vegetated bed levels. Therefore, the vegetation is the same compared to the reference scenario.

Figure 51 shows that the tidal exchange increases for the deeper creeks. On February 1st, the flood tidal exchange increased with 0.4 m^3/s to 5.7 m^3/s and the ebb tidal exchange increased with 0.4 m^3/s as well to 2.9 m^3/s. High water levels in Awa di Lodo increase faster in the deep creek scenario, but with the shallower creeks the water levels in Awa di Lodo catch up after about a week. However, the tidal exchange proceeds to be smaller for the shallow creek scenario and this eventually results in the water level dropping slower in Awa di Lodo when neap tide approaches. The tidal exchange for the increased depth scenario on February 1st is 1.20 • 10^5 m^3 with a residence time of 3.76 days. This is a 9% decrease in residence time compared to the reference scenario. For the shallower creeks, the tidal exchange is 0.92 • 10^5 m^3 with a residence time of 4.90 days. This is an increase in residence time of 18% compared to the reference scenario.

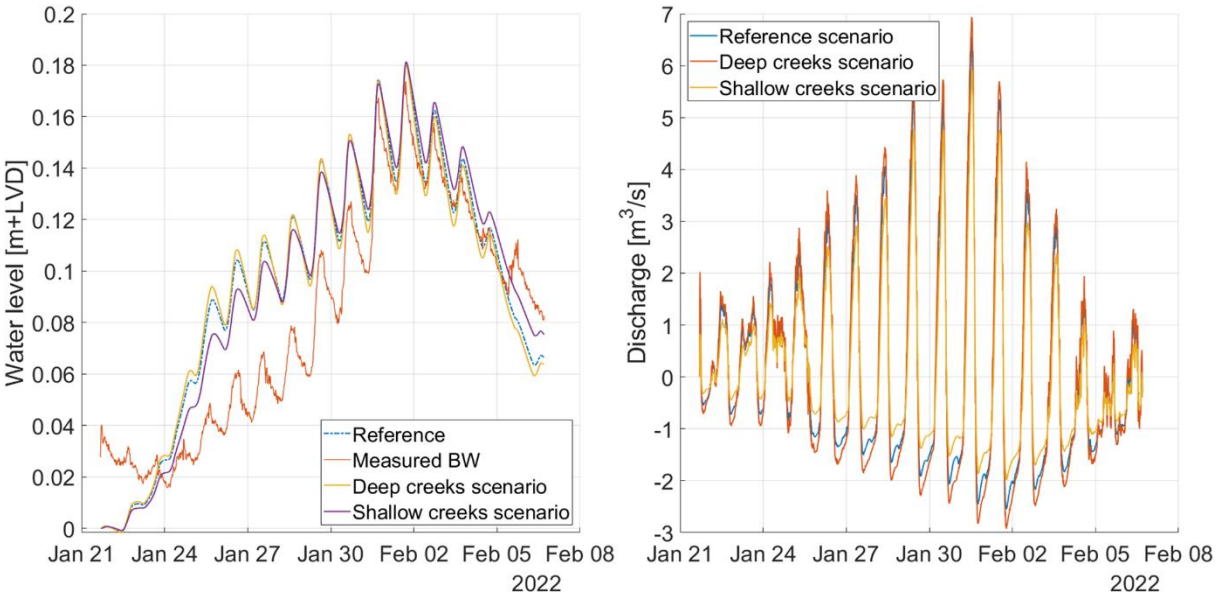

Figure 51: Water levels in Awa di Lodo for the reference situation, the 'deep creeks' scenario, the 'shallow creeks' scenario and the measured water level (left); and the tidal exchange for the reference scenario, the 'deep creeks' scenario and the 'shallow creeks' scenario (right)

Figure 52 shows that creating shallower creeks induces higher flow velocities in the creeks. The water volume has to be pushed through a smaller creek cross-section so higher flow velocities are induced. The opposite is true for the deeper creeks which result in lower flow velocities in the creeks. An overview of the velocities calculated by the model for a changing depth of the creek can be found in Table 8. The maximum ebb speeds are greater than the maximum flood speeds for both scenarios in

WC and EC thus having an ebb-dominant peak velocity asymmetry. At CC the flood speeds are greater resulting in a flood-dominant peak velocity asymmetry.

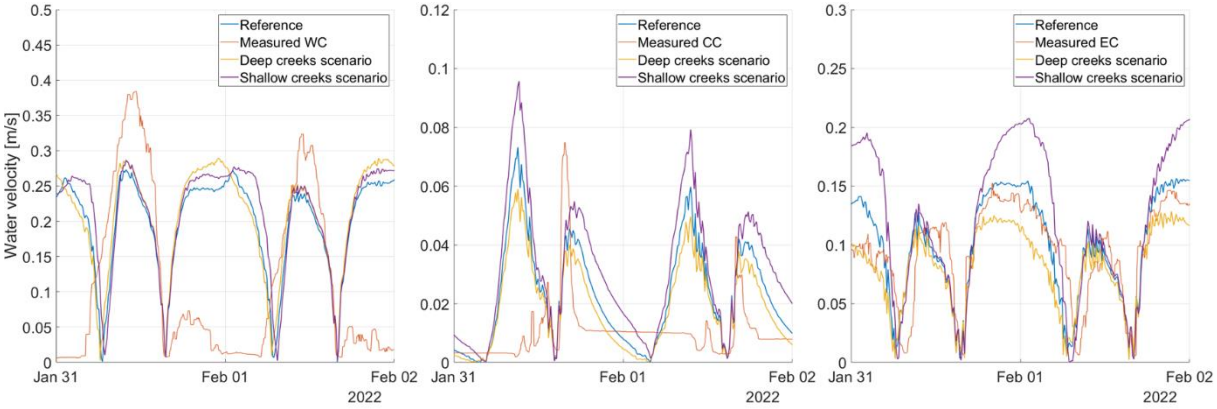

Figure 52: Water velocities of the reference scenario, measured in the field, of the 'deep creeks' scenario and of the 'shallow creeks' scenario for WC (left), CC (middle) and EC (right)

Table 8: Overview of flow speeds for the 'deep creek' and 'shallow creek' scenario for ebb and flood at WC, CC and EC

	Ebb speed for reference scenario [m/s]	Flood speed for reference scenario [m/s]	Ebb speed for deep creek scenario [m/s]	Flood speed for deep creek scenario [m/s]	Ebb speed for shallow creek scenario [m/s]	Flood speed for shallow creek scenario [m/s]
WC	0.27	0.24	0.29	0.25	0.28	0.25
CC	0.04	0.06	0.04	0.05	0.05	0.08
EC	0.15	0.11	0.13	0.10	0.21	0.12

6.5 Effect of increasing and decreasing the width of creeks

Changing the width of the creeks is in many ways similar to changing the depth because the effective cross-sectional area for water flow is made larger or smaller. In these scenarios, the creeks are made 50% wider and 50% narrower. The same grid is used as in the reference scenario. The only bathymetry changes are widening and thinning of the creeks which do affect bed levels that are vegetated in the reference scenario. The total vegetated area is slightly more/less if the creeks are widened/thinned compared to the reference scenario.

Creating a wider creek results in an increase of 0.5 m^3/s to 3.0 m^3/s for ebb tidal exchange and an increase of 0.4 m^3/s to 5.9 m^3/s for flood tidal exchange compared to the reference situation. A narrow creek limits the flood tidal exchange with 0.5 m^3/s to 4.8 m^3/s and the ebb tidal exchange with 0.6 m^3/s to 1.9 m^3/s compared to the reference situation (Figure 53). At the start of the spring-neap cycle, the scenario with wider creeks results in a slightly higher water level (a few centimetres) in Awa di Lodo. However, when spring tide is approaching, the ebb flow gets relatively more dominant in the wide creek scenario. This results in lower water levels in Awa di Lodo during spring tides for the wide creek scenario than for the narrow creek scenario. The tidal exchange for the increased width scenario on February 1st is 1.23 • 10^5 m^3 with a residence time of 3.65 days. This is a 12% decrease in residence time compared to the reference scenario. For the narrower creeks, the tidal exchange is 0.94 • 10^5 m^3 with a residence time of 4.79 days. This is an increase in residence time of 16% compared to the reference scenario.

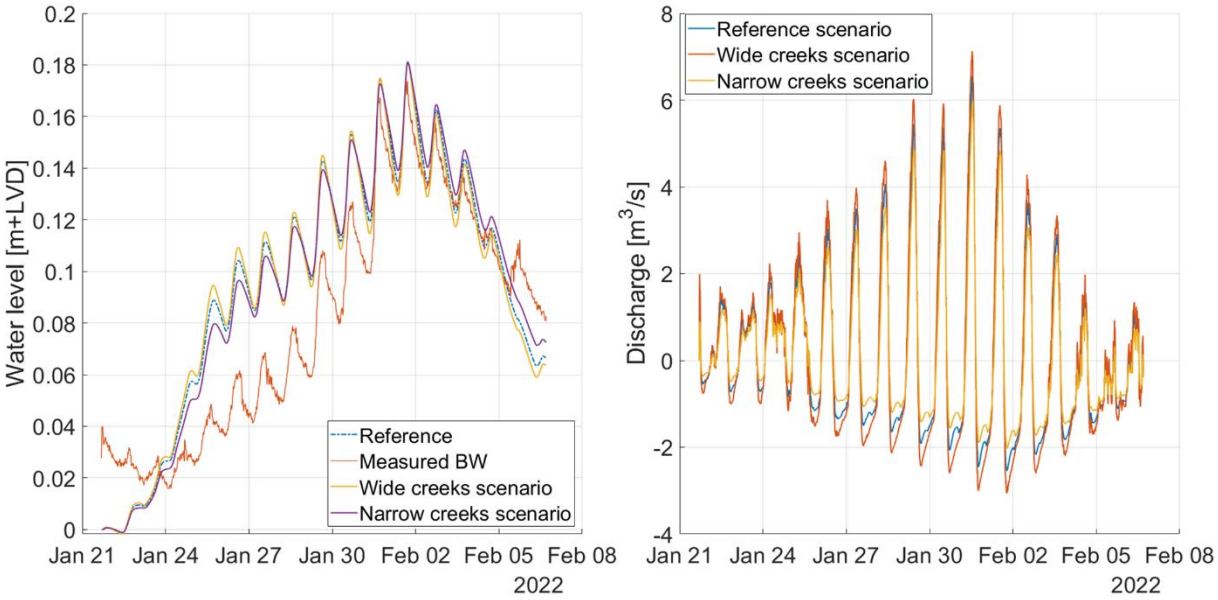

Figure 53: Water levels in Awa di Lodo for the reference situation, the 'wide creeks' scenario, the 'narrow creeks' scenario and the measured water level (left); and the tidal exchange for the reference scenario, the 'wide creeks' scenario and the 'narrow creeks' scenario (right)

Similar to the depth changes of the creeks, flow velocities in the creeks are higher when the effective flow area of the creek is smaller, and velocities are lower if the effective flow area of the creek is greater (Figure 54). An overview of the velocities calculated by the model for a changing width of the creek can be found in Table 9. Similar to the scenarios where the width has been changed, WC and EC show an ebb-dominant peak velocity asymmetry and CC has a flood-dominant peak velocity asymmetry.

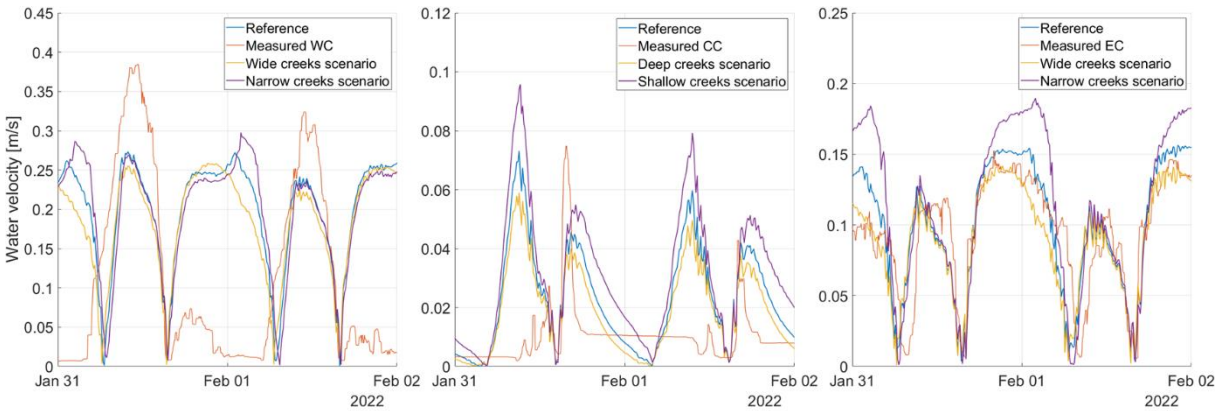

Figure 54: Water velocities of the reference scenario, measured in the field, of the 'wide creeks' scenario and of the 'narrow creeks' scenario for WC (left), CC (middle) and EC (right)

Table 9: Overview of maximum flow speeds for the 'wide creek' and 'narrow creek' scenario for ebb and flood at WC, CC and EC

	Ebb speed for reference scenario [m/s]	Flood speed for reference scenario [m/s]	Ebb speed for wide creek scenario [m/s]	Flood speed for wide creek scenario [m/s]	Ebb speed for narrow creek scenario [m/s]	Flood speed for narrow creek scenario [m/s]
WC	0.27	0.24	0.26	0.23	0.30	0.23
CC	0.04	0.06	0.04	0.05	0.05	0.07
EC	0.15	0.11	0.14	0.11	0.19	0.12

6.6 Effect of extending the centre creek

For this scenario, the extension of the centre creek is implemented with the same profile as used for the other creeks (Figure 55). While in the present situation the creek terminates before the islands, the creek is now extended to flow between Isla Fogon and Isla di Chico. By looking closely at aerial footage of that area in combination with conversations with local experts, the track of the historical creek is implemented into the bathymetry of the model. Not only the bathymetry and the vegetated area change due to the new creek, but also the grid is refined along the path of the extended creek. This is done to capture the more complex flow interactions of creeks and to be able to represent the creek bathymetry in the model.

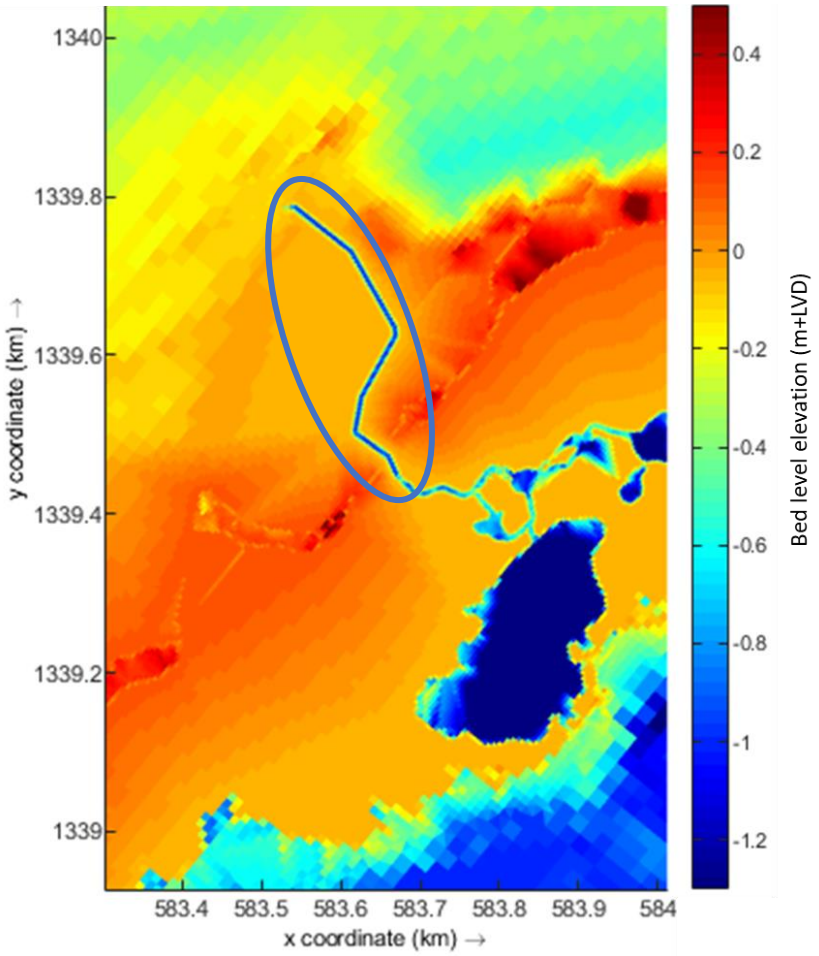

Figure 55: Bed level elevation of the Delft3D model in the 'extended centre creek' scenario

By examining Figure 56 it became clear that this scenario has got a great impact on the tidal dynamics of the area. The right panel of Figure 56 shows that the maximum ebb discharge increases by 0.7 m^3/s to 3.2 m^3/s while the maximum flood discharge increases by 0.8 m^3/s to 6.2 m^3/s. The increase in tidal exchange affects the water level in Awa di Lodo, the left panel of Figure 56, by an increased tidal range. Since the creek is made relatively deep, this creek functions mainly as a drain of Awa di Lodo while also being great in transporting water to Awa di Lodo during the rising stage of the spring-neap cycle. The tidal exchange for the extended centre creek scenario on February 1st is 1.38 • 10^5 m^3 with a residence time of 3.27 days. This is a 21% decrease in residence time compared to the reference scenario.

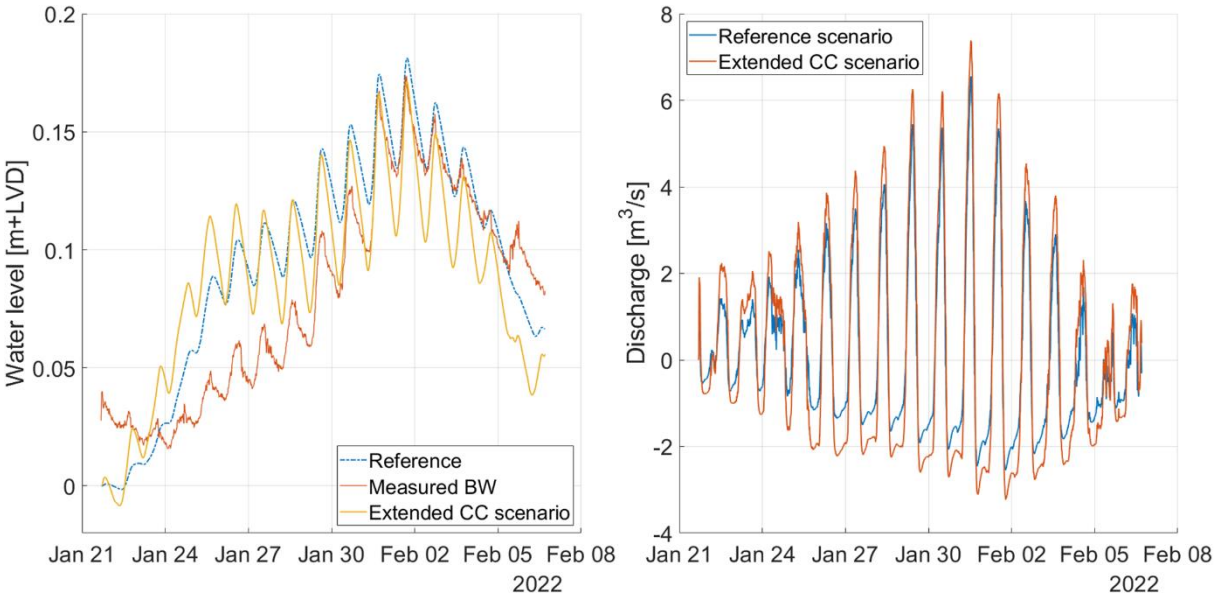

Figure 56: Water levels in Awa di Lodo for the reference situation, the 'extended centre creek' scenario and the measured water level (left); and the tidal exchange for the reference scenario and the 'extended centre creek' scenario (right)

The most obvious change in flow velocities by implementing this scenario is that at CC the simulated flow velocities are now much higher. From a maximum ebb flow velocity of 0.04 m/s at the reference scenario to 0.28 m/s in the extended centre creek scenario. The maximum flood flow velocity increased from 0.06 m/s to 0.22 m/s. Not only did these velocities increase, but CC also turned from a flood dominant creek to an ebb dominant creek.

Implementing an extension of the centre creek influences both the west creek and the east creek as well. By creating another creek for the water to flow through that area towards the open water of Lac, less water is forced through the west and east creek, resulting in lower maximum flow velocities at those locations (Figure 57). Maximum ebb speeds decreased from 0.27 m/s to 0.22 m/s at WC and from 0.15 m/s to 0.13 m/s at EC while the maximum flood speeds decreased from 0.24 m/s to 0.20 m/s at WC and from 0.11 m/s to 0.09 m/s at EC.

The middle figure of Figure 57 shows that the maximum flow velocities at CC experience a phase shift of about an hour. The maximum ebb velocities are reached an hour later than for the current situation.

The delay of the ebb tidal flow maxima is due to the water flowing into Awa di Lodo longer via the CC and because of the discharge that flows through the creek lasts longer because of its lower bed level.

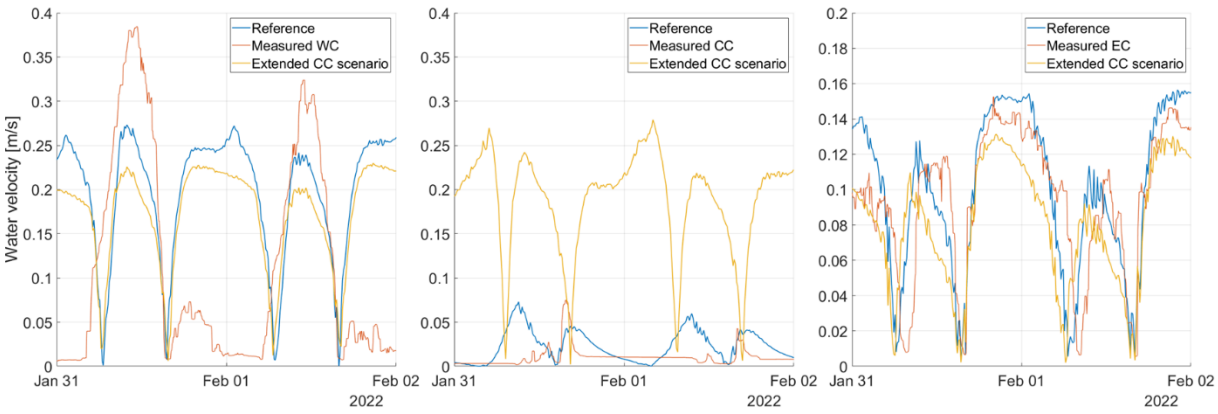

Figure 57: Water velocities of the reference scenario, measured in the field and of the 'extended centre creek' scenario for WC (left), CC (middle) and EC (right)

6.7 Effect of a new creek through the mangrove forest

For this scenario the construction of an entirely new creek is considered, connecting Awa di Lodo to the lagoon. With the same profile as used for the other creeks (Figure 44) the new creek is implemented (Figure 58). This creek is made based on conversations with local experts and by closely looking at aerial footage as it is believed this is a historical creek that has been closed over time. It is manually drawn from a notch in the forest fringe to Awa di Lodo where it flows in between Isla Rancho and Isla Fogon. Not only are the bathymetry and the vegetated area changed due to the new creek, also the grid is refined along the new creek. This is to capture the more complex flow interactions of creeks and to be able to represent the bathymetry in the model.

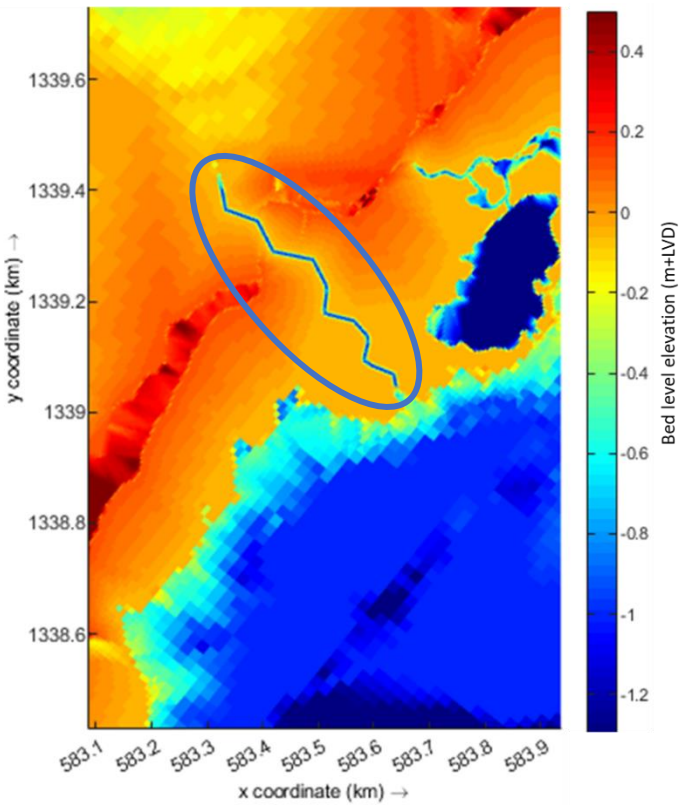

Figure 58: Bed level elevation of the Delft3D model in the 'new creek' scenario

Figure 59 shows that this scenario is comparable to the scenario of the extension of the centre creek. The right panel of Figure 59 shows that the tidal exchange increases substantially, with the maximum ebb tidal exchange increasing with 1.3 m^3/s to 3.8 m^3/s and the maximum flood tidal exchange increasing with 2.8 m^3/s to 7.5 m^3/s compared to the reference situation. The increase in maximum flood discharges is much greater than the increase in maximum ebb discharges. This is likely not only caused by the creek itself but also by the effect the implemented creek has on the bathymetry of the model. Implementing this creek causes the surrounding area to be lower as well which can be seen if the area surrounding the new creek of Figure 58 is compared to that same area in Figure 55. Lowering of the area surrounding the creek causes the tidal exchange to increase even though this is not directly induced by the creek itself.

The tidal exchange for the new creek scenario on February 1st is 1.59 • 10^5 m^3 with a residence time of 2.83 days. This is a 32% decrease in residence time compared to the reference scenario.

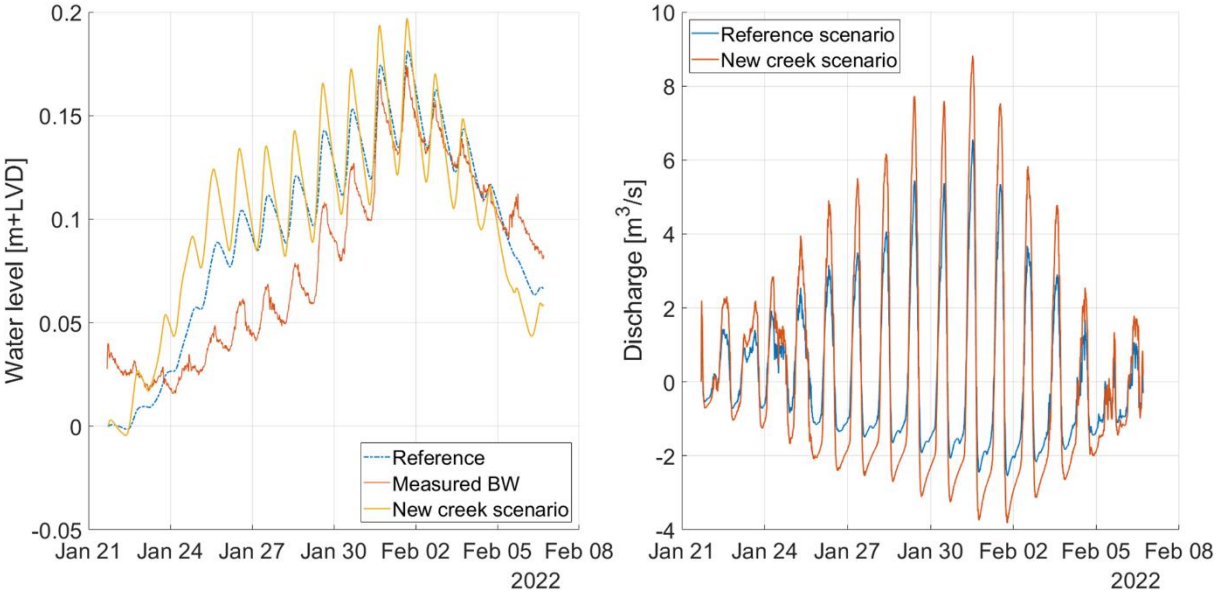

Figure 59: Water levels in Awa di Lodo for the reference situation, the 'new creek' scenario and the measured water level (left); and the tidal exchange for the reference scenario and the 'new creek' scenario (right)

All velocities in the existing creeks slightly decrease in the new creek scenario compared to the reference scenario (Figure 60). Since there is a greater total creek cross-sectional area, the water has more ways to flow back and forth between Awa di Lodo and the lagoon. The lower water velocities in the existing creeks are a logical consequence. Only small changes in maximum flood flow velocities were found for all existing creeks (changes smaller than 0.01 m/s), while the maximum ebb flow velocities decreased from 0.27 to 0.23 m/s and from 0.16 to 0.15 m/s for WC and EC respectively. Maximum ebb velocity changes at CC were also smaller than 0.01 m/s.

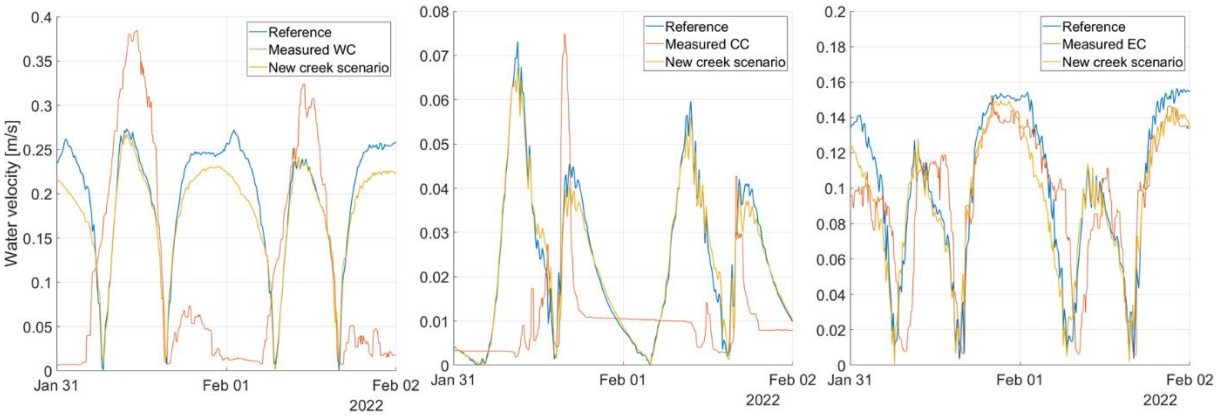

Figure 60: Water velocities of the reference scenario, measured in the field and of the 'new creek' scenario for WC (left), CC (middle) and EC (right)

Flow velocities simulated for the new creek are similar in magnitude and peak velocity asymmetry (flood dominant) to the west creek system (Figure 61). The water velocities have increased from 0.02 m/s to a maximum ebb flow velocity of 0.20 m/s and a maximum flood flow velocity of 0.28 m/s. Compared to the current situation without a creek at this location the velocities are much higher which shows the difference between the normally present sheet flow and the new creek flow. At this location in the creek, a flood dominant velocity asymmetry is visible which is similar to the west creek.

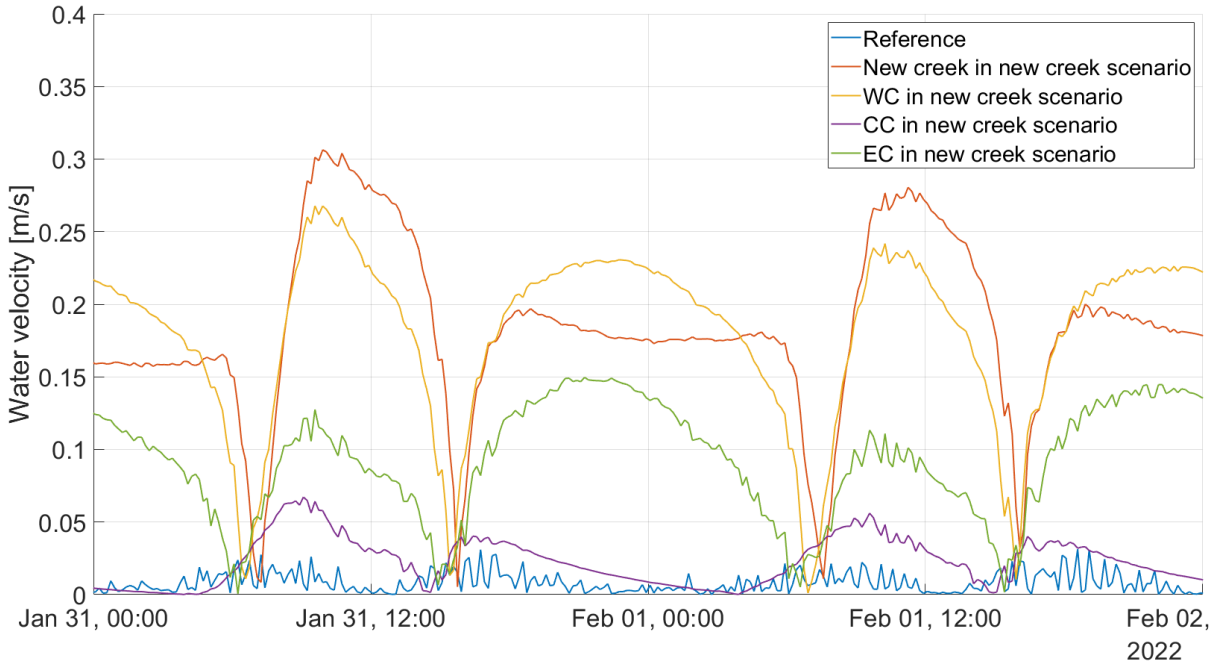

Figure 61: Flow velocities in the created creek in the reference situation and in the 'new creek' scenario

6.8 Effect of extending the eastern creek

The eastern creek was re-established in 2018 to prevent the mass die-off of fish in Awa di Lodo. This creek is of great importance to the area because it is the main connection to Awa di Lodo on the east side of Lac. The scenario discussed in this subchapter tests what happens if this creek has a greater cross-section over the last part of its trajectory before entering Awa di Lodo. At present, the northern part of the eastern creek (encircled part in Figure 62) is very shallow and narrow. This scenario is implemented in the model by making a channel at the end of the creeks as they are presented in the reference model (Figure 62). For this scenario, the bathymetry is altered and because of the deeper connection, some vegetation disappears in the creek extension. Refining the grid is also done to be able to represent the creek bathymetry and to capture the more complex flow interactions of the creeks.

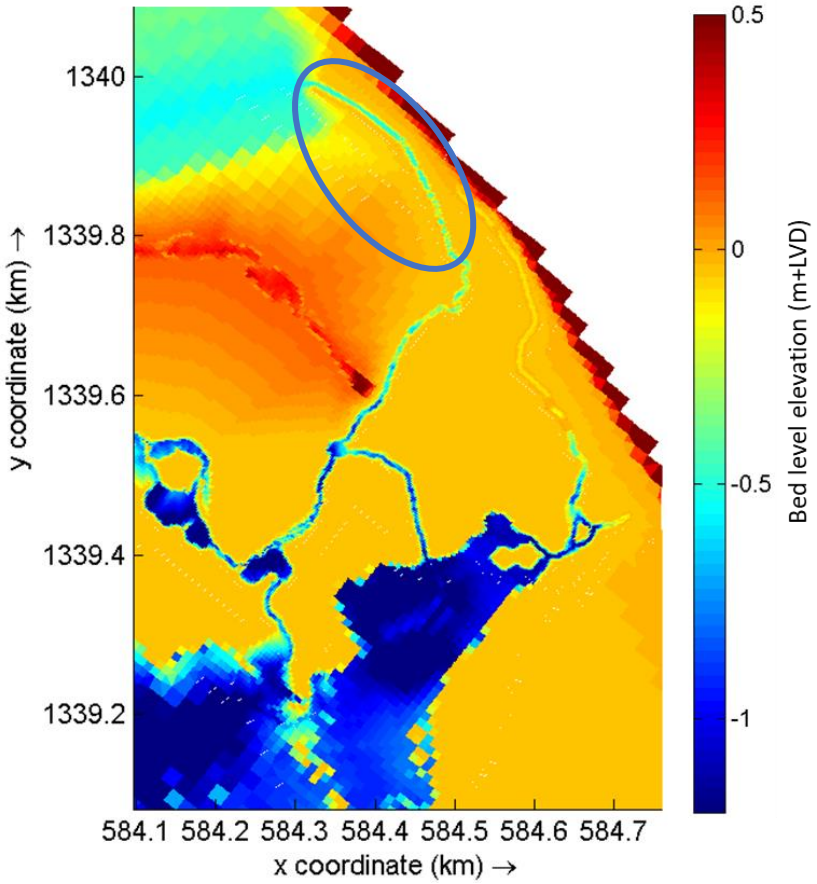

Figure 62: Bed level elevation of the Delft3D model in the 'Eastern creek extension' scenario

Having the extension of the east creek only has a marginal impact on the tidal exchange and the water levels in Awa di Lodo (Figure 63). The tidal range only increases by a few millimetres. The ebb tidal exchange increases with 0.1 m^3/s to 2.5 m^3/s and the flood tidal exchange in increased with 0.2 m^3/s to 5.5 m^3/s. The tidal exchange for the new creek scenario on February 1st is 1.13 • 10^5 m^3 with a residence time of 3.99 days. This is a 4% decrease in residence time compared to the reference scenario.

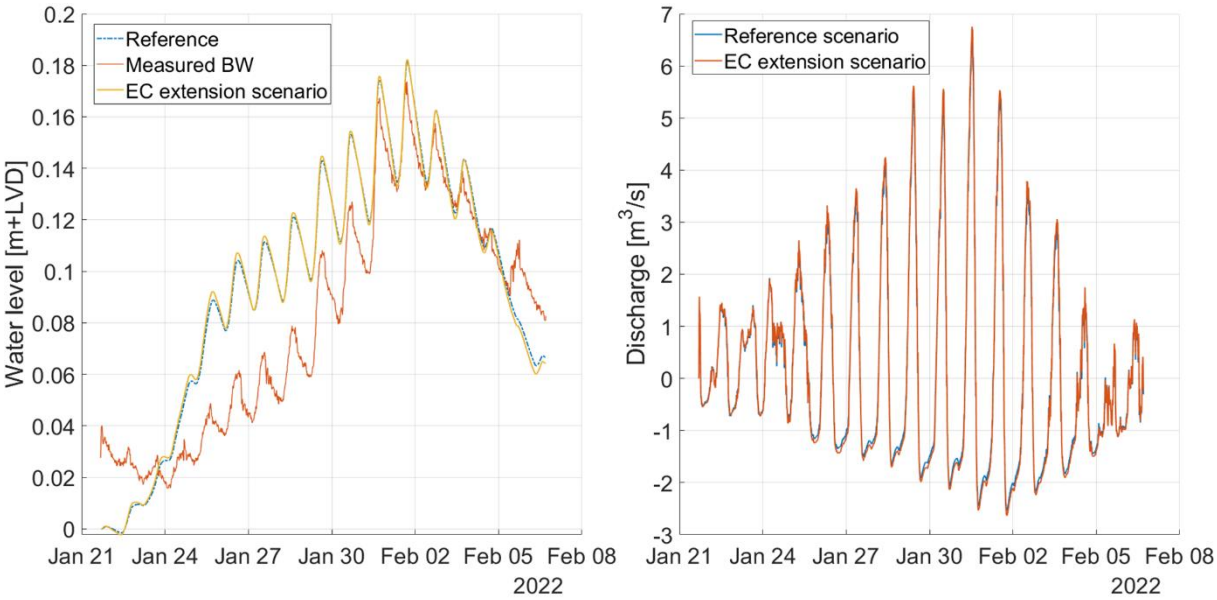

Figure 63: Water levels in Awa di Lodo for the reference situation, the 'extended eastern creek' scenario and the measured water level (left); and the tidal exchange for the reference scenario and the 'extended eastern creek' scenario (right)

Figure 64 shows that this scenario does not have a significant impact (less than 0.01 m/s change) on the flow velocities at WC and CC. It is expected that further altering this scenario would not make a large difference since this creek already forms an important flow path for water flowing in and out of Awa di Lodo.

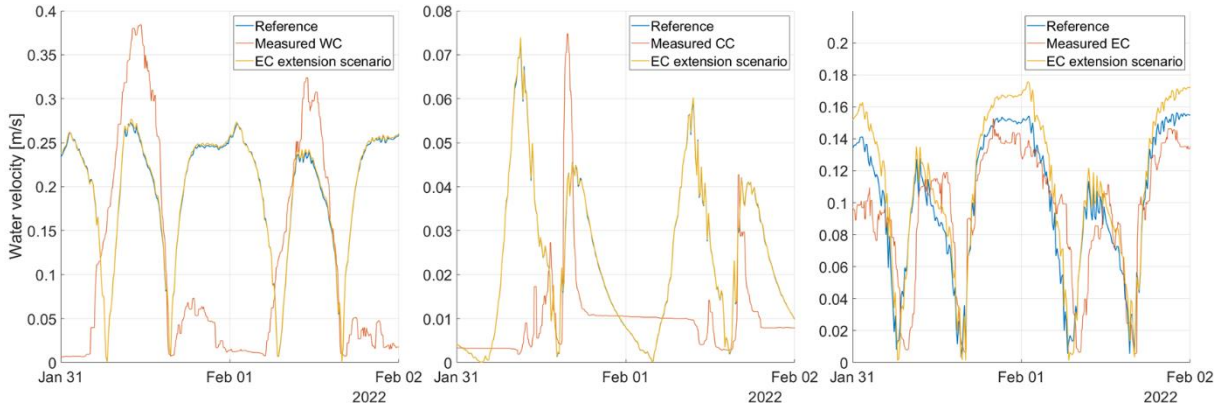

Figure 64: Flow velocities of the reference scenario, of the 'extended eastern creek' scenario and measured in the field for WC (left), CC (middle) and EC (right)

6.9 Overview of the different scenarios

A comparison of all scenarios is made to analyse their relative effects on the tidal exchange with Awa di Lodo. Figure 65 shows the water levels over the model period for all scenarios and Figure 66 considers 1 day to present the differences between the scenarios in more detail. Interestingly, the difference between the 'no creeks' scenario and the other scenarios is substantial. Having less tidal exchange causes the tidal range to be smaller and slows the flood tidal discharge into and the ebb tidal discharge out of Awa di Lodo because there are no slow-resistance water conduits through the mangroves (i.e. creeks).

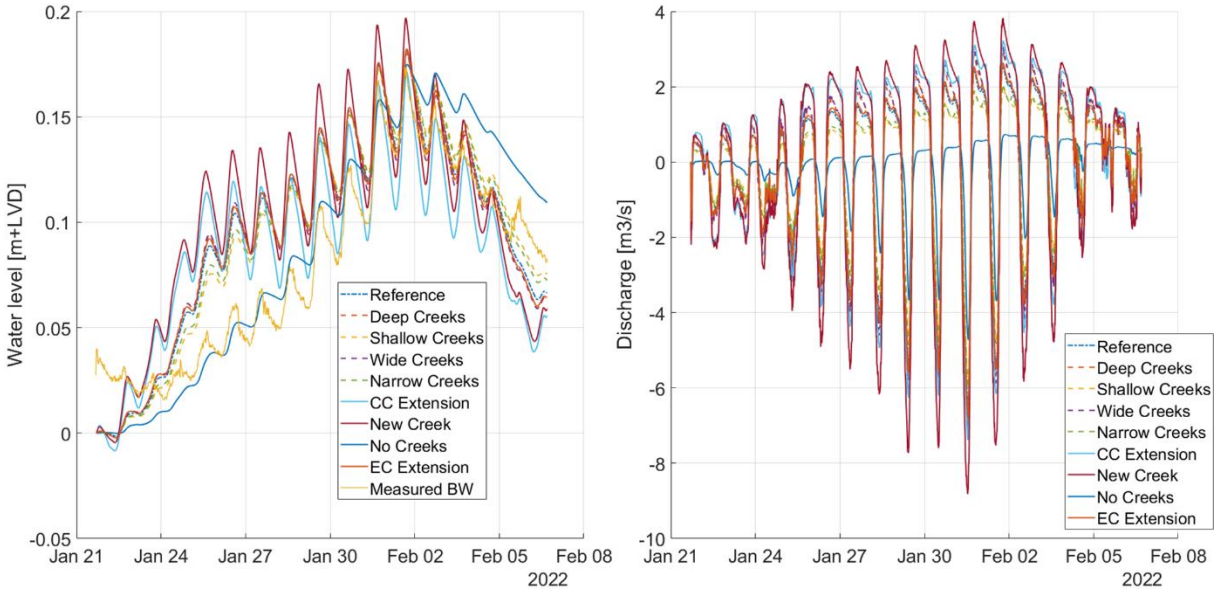

Figure 65: Water levels in Awa di Lodo for the reference situation, all scenarios and the measured water level (left); and the tidal exchange for the reference scenario and all scenarios (right)

The most effective scenario for increasing the tidal exchange, compared to the reference scenario, is creating a completely new creek from the forest fringe to Awa di Lodo followed by extending the centre creek system to Awa di Lodo(Table 10). Both scenarios effectively create a new creek connection to Awa di Lodo which results in a greater tidal exchange.

Table 10: Tidal exchange, residence time and the ratio of the residence time compared to the reference scenario of each modelled scenario. Red coloured rows indicate a decrease in tidal exchange and blue coloured rows indicate an increase in tidal exchange. A darker shade implies a greater decrease/increase.

Scenario	Tidal exchange [10^5 m^3/day]	Residence time [/day]	Ratio of change in residence time compared to reference scenario [-]
Reference	1.09	4.15	1.00
No creeks	0.61	7.35	1.77
Increasing depth	1.20	3.76	0.91
Decrease depth	0.92	4.90	1.18
Increase width	1.23	3.65	0.88
Decrease width	0.94	4.79	1.16
Extension CC	1.38	3.27	0.79
New creek	1.59	2.83	0.68
Extension EC	1.13	3.99	0.96

It was found that extending the east creek has very limited effects on the tidal exchange. That scenario does not change the current situation enough to influence the tidal dynamics. Increasing the width of the creeks has slightly more effect on the tidal exchange than increasing the depth, probably due to the reduction of vegetated area.

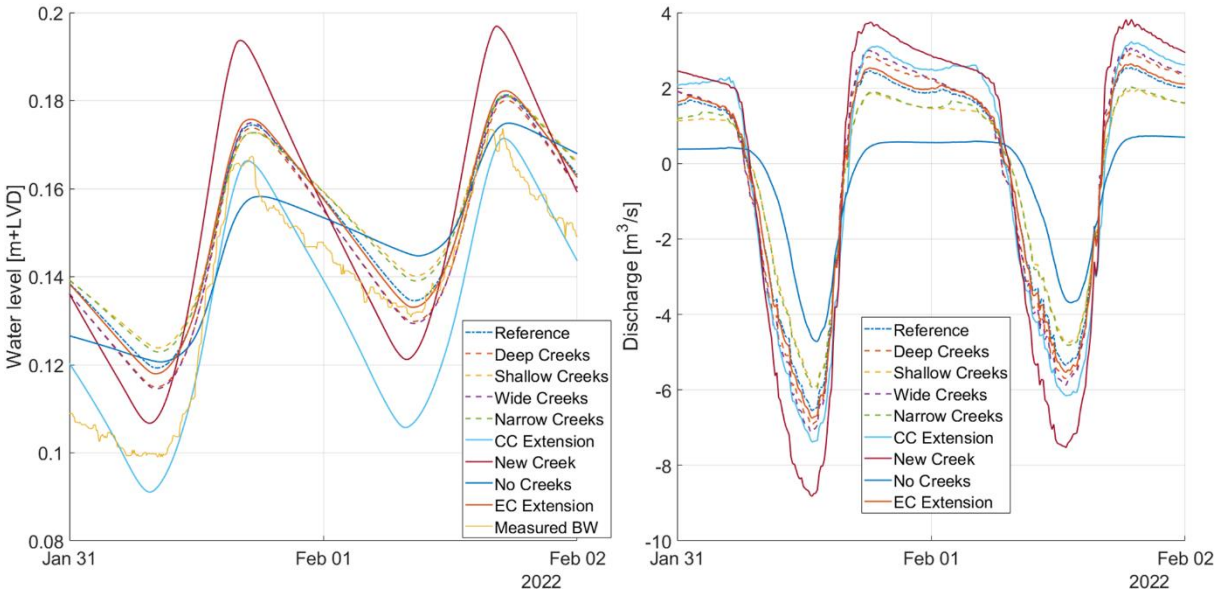

Figure 66: Water levels in Awa di Lodo for 31 January and 1 February for the reference situation, all scenarios and the measured water level (left); and the tidal exchange for the reference scenario and all scenarios (right)

For the refreshment rate of Awa di Lodo, it is not only important that water can enter the area, but also that the water leaves the area so more water with lower salinity values can flow into the area again. Therefore, it is important to look at measures that not only create more inflow into the area but also promote the outflow of the area.

7. Discussion

This chapter addresses the interpretation of, and a reflection on the results. The current situation of the area is described based on what is found during the study. The model setup and the implications of the model study are described, to emphasize the strengths and weaknesses of the model results. Lastly, uncertainties and practicalities of the field monitoring are described.

7.1 Current situation

Comparing the propagation of the tidal wave with earlier research

The findings on the delay of the tidal wave confirm the results of previous studies. For instance, Hummelinck & Roos (1969) also noted that the backwater (Awa di Lodo), had a delay of high water between 3h 45min and 4h with respect to Cai, but only with a very small tidal range in Awa di Lodo. The same research also shows that further into the mangrove forest the delay increases. Important to note is that they only did a 24 hours survey on 15/16 September 1967. Moreover, Van Moorsel & Meijer (1993) repeated these measurements. On the east side of the forest near Isla di Yunawa (Figure 3), Moorsel & Meijer (1993) found that the delay of high water is between 2h 45min and 3h 45min, close to values of Hummelinck & Roos (1969) of 2h 51min and 3h 9min. Moorsel & Meijer (1993) found a delay of 1h 25min in Awa di Lodo but only did a 12-hour survey on 14 March 1992 while there was almost no water level change in Awa di Lodo.

The result in Figure 19 shows that there is variance in the delay of high tide in and between the spring-neap cycles. Therefore, it is hard to say if there is historical development in the delay of the tidal wave by the mangrove forest. Van Moorsel & Meijer (1993) did see tidal fluctuations in Awa di Lodo through the feeder channel of Kreek di Coco. The results from this study show that it is important to do measurements ranging for at least one full spring-neap cycle (preferably more) to draw conclusions about the tidal delay in Lac Bay.

Small water level differences in the open water of Lac Bay

Water level differences between Cai and the western fringe (WF) are small, both in the measurements and in the model. The shallow water equations, shown in section 4.4, predict that the tidal wave from the entrance of Lac to the fringe propagates in a period of the order of minutes. Based on these findings, future research does not need to locate multiple water pressure sensors in the open water of Lac to measure the tidal wave. In the open water of Lac, the water level moves more or less uniformly up and down.

Connection of the west creek system from the forest fringe to Awa di Lodo

The hydrodynamic analysis showed that while the water level at the west fringe (WF) is lower than at Awa di Lodo (so the water level in Awa di Lodo is greater than in the forest fringe) is enough for the flow direction in the western creek (WC) to reverse from ebb (seaward) to flood (landward). Based on the principle that water flows from a higher elevation to a lower elevation this observation is counterintuitive. What likely happens is that the west creek system is not connected very well to Awa di Lodo and is influenced more by the mangrove vegetation surrounding Isla di Yuwana and Awa di Pedro. The water level is reacting faster to the tide in the west creek system and thus has a phase lag with the water level in Awa di Lodo. Water levels being lower already in the west creek system results in a seemingly negative water level difference, while in reality the west creek system already has lower water levels and causes the flow to change direction.

Tidal asymmetry

The dominance of the peak velocity asymmetry determines the direction of sediment fluxes. Ebb flow dominance at spring tide flushes sediments out of the system while flood flow dominance keeps them

in the system (Mazda et al., 1995). Whether the sediment will be flushed out is also dependent on the sediment and channel properties. For the eastern creek (EC), the ebb dominance during neap tide is likely to flush out sediments from the backwater towards the open water of Lac based on the current velocity data. Tidal dynamics at the western creek (WC) are more likely to push sediments into the forest and towards the backwater due to the prominent flood dominance. However, it is likely that these patterns do not prevail along the entire west creek and east creek system since tidal velocity asymmetry can vary spatiotemporally (due to e.g. hypsometric effects) (Horstman et al., 2021; Kumbier et al., 2022).

If dams or levees are removed from the catchment an increase of the inflow by runoff into Awa di Lodo will occur. This influences the peak velocity asymmetry as well as tidal duration asymmetry. With greater inflow, the peak velocity asymmetry in the creeks will become more ebb dominant. At the end of spring tide, when there is more water in Awa di Lodo, the maximum ebb and flood velocity increase and decrease respectively. This change in maximum ebb and flood velocity is caused by the increased water pressure exerted by the higher water level in Awa di Lodo. The opposite effect is present at the start of spring tide when water levels are relatively low in Awa di Lodo. Lower water levels in Awa di Lodo cause lower maximum ebb velocities and higher maximum flood flow velocities because the area has the potential for higher water levels. Tidal duration asymmetry increases in Awa di Lodo with increasing inflow from runoff. It takes longer for the water level to decrease due to the slow total discharge of water via the creeks. At the same time, the forest gets inundated during flood allowing for sheet flow through the vegetated areas. The sheet flow contribution results in faster flows into Awa di Lodo leading to a faster rise in water level.

Influence of precipitation and evaporation

The exact impact of precipitation and evaporation on the salinity of Awa di Lodo is unclear. The water fluxes of the precipitation and evaporation are great enough to have a major impact on the water level and salinity of Awa di Lodo.

The estimated volume in Awa di Lodo during spring tide is $4.5 \cdot 10^5$ m^3 (section 6.1). Assuming a month in the rainy season with average precipitation, the volume of runoff flowing into Awa di Lodo during a month is approximately $2.3 \cdot 10^5$ m^3 ($= 1.25 \cdot 10^6 \cdot 0.55 / 3$, see sections 2.3 and 2.4). If this system had nothing but precipitation it would increase the volume of Awa di Lodo by roughly 50% in the rainy season. Doing these calculations for a month in the dry season (monthly inflow of $6.3 \cdot 10^4$ m^3) the increase in total volume of Awa di Lodo would be roughly 14%. This calculation indicates the magnitude of the effect precipitation has on the water fluxes in Awa di Lodo and how the temporal variability over the year can play a role in the water level and salinity values.

On average on Bonaire, the precipitation exceeds the evaporation only in the months November to January (Wösten, 2013). The average annual potential evaporation is 2600 mm (Borst & de Haas, 2005), which equals 217 mm monthly. Awa di Lodo's evaporation likely is lower due to its hypersaline water. Nevertheless, evaporation is a significant portion of the fluxes out of Awa di Lodo. To examine the order of magnitude evaporation can have on the total water volume, an example is made. Take for the monthly evaporation a value of 200 mm (a bit lower than the potential monthly evaporation) and multiply that by the (roughly taken) area of Awa di Lodo of 0.70 km^2. The evaporated volume of that month would be $1.40 \cdot 10^5$ m^3. Compared to the estimated volume in Awa di Lodo during spring tide of $4.5 \cdot 10^5$ m^3, roughly 30% of the total volume will on average evaporate in a month. Inflow of the tidal exchange and precipitation are also present thus it is unlikely that the water volume in Awa di Lodo drastically decreases.

Although the calculations indicate that the volume of rainfall can be significant compared to the volume of the tidal exchange in Awa di Lodo, there is no visible response of the water levels of the backwater to precipitation events. This could be due to the precipitation not directly being added to Awa di Lodo or that the magnitude of these events was not great enough to make a difference to the water level. Precipitation likely has a significant impact on the water levels in Awa di Lodo but the direct effect is hard to distinguish from outflow through creeks. More studies and data on the water level of Awa di Lodo are needed to clarify the relationship between precipitation, evaporation and the water level of Awa di Lodo.

Trapped sediment in Awa di Lodo

Most of the sediment in Awa di Lodo in the present situation is not likely to be released in the Bay due to the lack of transport mechanisms. To re-create the old situation this sediment must be removed manually. It is unlikely that the sediments will flush out of Awa di Lodo and end up in the open water of Lac or other parts of the mangroves since few processes stir up and transport the sediments. The model results show that flow velocities in Awa di Lodo do not exceed 1.5 cm/s. The main process could be wind-driven flow that directs sediment to the southwest of Awa di Lodo.

Mass die-off of the fish

Lott (2001) and Van Moorsel & Meijer (1993) observed a mass die-off of fish each year in the dry season. Since the connection of the east creek to Awa di Lodo was restored in 2018, the often observed mass fish die-off has not occurred anymore (Engel (2022), pers. comm.). This indicates that this measure either decreased the stressors (water temperature, salinity, etc.) in Awa di Lodo to such a degree that the fish can survive the adjusted environment or that the otherwise dying fish can now escape the area. Increasing the tidal exchange would only further decrease the probability of mass die-off occurring again in the future because the water would be refreshed with higher quantities. In the scenarios where the creeks are extended and deepened the frequency of the refreshment is also likely to become greater.

Habitation of Awa di Lodo by mangroves

A large part of Awa di Lodo will not be inhabited by mangroves because the inundation depth is too large for the settling of the *Avicennia species* (>20 cm water depth) and too salty for the *Rhizophora* species. Along the water line, however, the possibility of mangrove trees growing increases if the tidal range increases since mangroves usually grow within the intertidal zone. On the larger mud flats in Awa di Lodo the *Avicennia* species has a great chance to re-colonize. However, if the excess supply of sediment is not addressed, the entire system will be elevated and creeks will start to clog again, likely resulting in the die-off of the mangrove trees.

7.2 Model setup

The balance between grid resolution and computational time

In model studies, the balance must be found between grid resolution and computational time. Increased model accuracy can primarily be obtained by a greater grid resolution at locations with a lot of spatial variation in bathymetry and vegetation. However, this is at the cost of an increase in computational time. Finally, a grid with sufficient accuracy and a reasonable computational time was selected. The grid can be further improved by creating a more gradual transition between the smaller and larger grid cells. The way the model is built now might not be the most optimal way as the grid cell size decreases significantly within a few steps. The RGFGRID manual states that “Adjacent grid cell sizes should vary less than 20%, although locally exceptions may be acceptable” (Deltares, 2022a, p. 113). Steps being greater can create truncation errors. If this effect is present in the model is hard to say, but if possible it is better to prevent it at the cost of extra computational time. Results on the water

levels are likely not influenced and flow velocities are more likely to be influenced but it is expected the effects are small.

Implementation of the vegetation

The difference between Figure 40 and Figure 41 of this report shows the effect of including vegetation in the Delft3D model on the simulated water levels in the model. Adding vegetation into the model induced friction in the model making it harder for the water to flow through the vegetated area. The increased vegetation presence decreases the tidal exchange and therefore the tidal range of the backwater gets also decreased.

The mangrove root characteristics that were measured during the field study are used to calculate average mangrove root characteristics values. These average mangrove root characteristics are used to represent the entire mangrove area, which is a large simplification. Especially the variation between the forest fringe, dominated by the red mangrove, and the inner forest, dominated by the black mangrove, should have variability in the root characteristics according to the monitoring data. Mangrove hydrodynamics greatly depend on the mangrove root characteristics (Mazda et al., 1997). The hydraulic resistance between the red and black mangrove differs due to their different root structures. Equation 8, adapted from Baptist et al. (2007) determines the vegetation resistance force (F_v) of the flow through an area with rigid cylinders. Assuming the same drag coefficient (C_D), fluid velocity (u) and fluid density (ρ) for each vegetation make the vegetation density (N_v), the vegetation diameter (d_v) and the vegetation height (h_v) determine the difference in vegetation resistance.

$$F_v = \frac{1}{2}\rho C_D N_v d_v h_v |u| u \qquad (8)$$

Taking the average vegetation characteristics per mangrove species from Table 2 gives the values of Table 11. The value of $N_v \bullet d_v$ is 37% greater for the black mangrove than for the red mangrove. However, the root height of the red mangrove is about 6 times higher than that of the black mangrove.

Table 11: Average mangrove root characteristics for the red and black mangrove

	Root density [/m²]	Root height [m]	Root diameter [m]	$N_v \bullet d_v$ [m/m²]	$N_v \bullet d_v \bullet h_v$ [-]
Rhizophora mangle **(red mangrove)**	104	0.663	0.022	2.284	1.515
Avicennia germinans **(black mangrove)**	428	0.118	0.007	3.136	0.369
Values used in model	174	0.474	0.016	2.784	1.320

In the forest fringe, which is dominated by the red mangrove and where the water depths are generally higher, the hydraulic resistance is overestimated by 21% when the water levels are below the root height. Due to the average $N_v \bullet d_v$ being higher than that of the red mangroves, more friction is induced. At greater water depths, this overestimation of the hydraulic resistance becomes smaller. When fully submerged, the red mangrove hydraulic resistance used in the model will be underestimated by 13% compared to the hydraulic resistance based on the monitored mangrove root characteristics. The inner forest is dominated by the black mangrove and has smaller resistance in the model compared to the measurements (12%) at water depths below 0.118 m. However, at a water depth of 0.474 m, when the modelled vegetation is fully submerged, the resistance is overestimated by 258% because of the lower height of the black mangrove roots than of the average roots.

The effect of spatial variability of the mangrove root characteristics on the tidal exchange is hard to quantify but it would increase the accuracy of the model because of the differences in the vegetation resistance forces. Based on the calculations of this section, it is likely that the water flows faster into the forest at low water levels but stays there longer due to higher friction at low water levels. With high water levels, the flow will face more resistance in the fringe, but less resistance in the inner part of the forest, resulting in the water spreading much faster via sheet flow. Because the tidal exchange into the backwater is also dependent on sheet flow, applying spatial diversification on mangrove root characteristics can have an impact on the results.

Resolution of the bathymetry of the open water part of Lac Bay

As the open water of Lac was not the focus of this study it has a relatively low grid resolution (20-by-20 m). If future studies are interested in the dynamics of that area, not only a higher grid resolution is desired, but also a higher resolution of bathymetry in open water Lac is desired. The bed level elevation accuracy is in the order of meters. A large part of Lac, e.g. the area in front of Sorobon, is very shallow which due to bottom and vegetation-induced friction has a large influence on the flow of water in the lagoon. To be able to predict the hydrodynamic properties of the shallow areas a bed level accuracy in the order of decimetres to centimetres is required.

Extending the calibration

This study used a simple model setup with limited model calibration. A more detailed calibration could improve the model and provide a more quantitative value to the results. The model can be calibrated based on important parameters like tidal asymmetry, maximum flow speeds, delay of high tide and the water levels. This model improvement could be achieved by changing the bottom roughness.

Simplifications of the model

Simplifications in the model are inevitable. Vegetation characteristics greatly vary over the area and thus the effect on the flow varies spatially as well. However, a uniform vegetation was implemented into the model for the sake of simplicity. Spatial differentiation would improve the fidelity of the model and possibly creates more accurate model results. The same holds for the creeks throughout Lac, which all have variable profiles. In reality, the profile changes for every creek and every section of the creek. In the model, only a single representative creek profile with an adjustment for the locally measured depth was applied. Figure 13 shows the different measured creek profiles and the applied representative profile. Differentiation in the creek profiles would again improve the fidelity of the model. The cross-section of the west creek system, which is a relatively wide creek, is used to represent all the creeks in the study area. An overestimation of the discharge through creeks and, as a result, an overestimation of the tidal exchange is likely the result of taking the west creek as a representative creek profile.

Located in between the creeks and the islands, most of the mangrove forest can be found. The bed level of the mangrove forest for most of the area is an interpolation between the creek profile and the RTK data along the islands of Lac Bay. Due to a lack of instruments to measure the bed level inside the mangroves, the interpolation is the best practice. A different bed level in the mangrove forest will impact the water depth in the forest which influences the drag and tidal exchange. For future research, it is advised to do measurements on the bed level elevation of the mangrove forest by e.g. placing the RTK-GPS on a measuring stick (that can be disassembled) of at least 5 meters.

Roughness and meandering of creeks

Water levels of Awa di Lodo rise and decline faster in the model than monitored in the field. Probably the roughness of the creeks, the vegetation roughness or bottom roughness in the model should be higher so the tidal exchange decreases. Increasing the roughness of the creeks would likely improve

the model output as the inaccuracy seems caused by having too much flow through the creeks. Increased roughness of the creeks might also be obtained by having spatially varying creek profiles which could impose more friction than the uniform cross-section as it is implemented now. The roughness in the field is likely also higher due to overhanging vegetation in the creeks.

Meandering of the newly created creeks in the scenarios is not represented as well as the meandering of the already existing creeks. Due to uncertainty of the possible creek paths and lack of creek profile data, the effect is hard to take into account. Meandering of the creeks will have an effect by inducing more flow obstacles and friction. Increasing the sinuosity of a channel substantially increases the flow resistance (Willets & Hardwick, 1993). The tidal exchange is therefore overestimated in this model compared to the real world due to increased friction in creeks with increased sinuosity.

Water fluxes not included in the model

Groundwater flows, rainwater and evaporation are not taken into account in the analysis of the measurements nor the model. The previous paragraph has shown that precipitation and evaporation can have a significant influence on the salinity of Lac Bay. As groundwater on Bonaire is mainly a product of rainwater this also has the potential of being of great influence in the area. Each year, mass fish die-off was observed in the dry period (Lott, 2001). This might be due to changing tides throughout the year, but it is more likely that this is the combined effect of groundwater, rainwater and evaporation. Connecting the east creek to Awa di Lodo has resulted in the prevention of the mass die-off ever since.

7.3 Creek restoration scenarios

Effect of creeks on the tidal exchange

Creeks are more important for transporting the ebb tidal exchange than the flood tidal exchange. The ‘no creek’ scenario showed this by the flood tidal exchange being much greater than the ebb tidal exchange resulting in the filling of Awa di Lodo. Increasing the depth and with of the creeks decreased the residence time of the backwater by 9% and 12% respectively. Even though an increase of 50% in width or depth of the existing creeks adds roughly the same cross-sectional creek area as creating a new creek, the new creek and the extension of the centre creek (CC) are much more effective (32% and 21% increase respectively) in decreasing the residence time. The tidal exchange of the new creek scenario is overestimated because in the model not only a creek is added but also the surrounding area has come down due to the combination of lack of bed level data in that area and the interpolation. Nevertheless creating a new connection to Awa di Lodo is still the most effective way to decrease the residence time.

Sediment transport out of Awa di Lodo

An ebb-dominant creek system can transport suspended sediment out of an area and maintain its own depth (Wolanski et al., 1990). Sediments being transported out of the mangrove area pose problems for the coral reef at the opening of the bay. If the sediment leaves the mangrove area, it can settle on the coral and smother the coral reef over time. However, mangrove systems normally function as sediment sinks for fine sediment (Furukawa & Wolanski, 1996). The ebb-dominant character of the east creek is therefore not likely to transport the sediment out of the mangrove forest. The sediment will be transported into the forest again because of the flood dominance of the mangrove forest. The east creek has been opened for some time now and this creek has an ebb dominant character, thus having the potential to move the sediments out of Awa di Lodo into the open water of Lac. Since this has not happened over time it is unlikely it will happen to other (new) creeks as well. This makes it also unlikely that the extension of the centre creek, described in section 6.6 of this report, will transport sediments into the open water of Lac Bay despite its ebb dominance peak velocity asymmetry.

Hence, the chance that the corals in front of the mangrove area would be covered by a sediment layer is rather small. Due to the sometimes high suspended sediment concentrations in Awa di Lodo, it is plausible that some of these sediments are transported through the creeks. It is expected that this sediment ends up in the creek system and eventually in the flood dominant mangrove forest itself. Due to the self-scouring of the creeks, it is unlikely that the creeks will clog up purely from the sediment but in between the mangrove trees the sediments will settle and then reduce the sheet flow through the mangrove forest. Section 6.7 shows that a new creek is likely to have a flood-dominant character which further reduces the likelihood of the sediment entering the open water of Lac.

Feasibility of the scenarios

While assessing the creek restoration scenarios, only effects on the tidal dynamics are considered. The costs, effort, ecological or other impacts are not taken into account. Experts can use these scenarios and assess the feasibility of the interventions to help with the future course of action. Based on the findings of this study, the best way of increasing the tidal exchange is to create a new connection to the backwater. Restoring the natural habitat of the mangroves requires increasing the tidal range and decreasing the salinity. Both can be achieved by increasing the tidal exchange. Widening and deepening of the creeks, which seem less work because it is easier to work in already existing creeks, does not substantially increase the tidal exchange. Also, by widening the creeks, mangroves will be lost since mangroves are densely populated around the creeks. Deepening the creek is hard at some locations due to the limestone shield below the creeks (Lott, 2001). The 'new creek' scenario is probably the hardest to realize due to the long distance that has to be covered from the forest fringe to Awa di Lodo. Extension of the central creek system seems to be the best combination of feasibility and effectiveness.

Reducing mangrove stressors by reducing the residence time

Increasing the tidal exchange through new/extended creeks results in a higher tidal range and a lower residence in Awa di Lodo since a larger volume of water moves in and out of the area. This would increase the potential habitat area for mangroves since they normally grow in the intertidal area. The reduction of the tidal range in Awa di Lodo is likely one of the causes the die-off of mangrove trees happened in the first place. A small tidal range causes either long, inundation-free periods, where the mangroves die because of drought stress and hypersalinity or long inundation periods where the aerial roots drown (Balke & Friess, 2016). One of the other stressors, the hyper salinity of Awa di Lodo, will also be less severe due to an increased tidal exchange after the creek restoration. Salt water from the sea is less salt than the hypersaline water in Awa di Lodo that results from the high evaporation in the area, thus an increased exchange with the seawater will decrease the salinity in Awa di Lodo.

Important to note is that a residence time of e.g. 4 days does not replace all the water of Awa di Lodo in 4 days. This is because one of the tidal cycles with the greatest tidal range of the first spring-neap cycle is taken for the calculation and this tidal exchange is not representative for the rest of the spring-neap cycle. During neap tide, the tidal exchange is up to 5 times as small and compared to the other monitored spring-neap cycles the first one has the greatest tidal exchange. Also, Awa di Lodo is prone to bad mixing, thus the decreased salinity due to the increased tidal exchange will not affect the backwater equally.

7.4 Field measurements

Uncertainty in the water levels and water velocities

In the analysis of the hydrodynamic properties of Lac Bay, data of the west fringe frame (WF) was used as reference time series for the water levels at the forest fringe and thus all subsequent analyses. This is done because, during the field campaign, this frame was subject to the least hydrodynamic

disturbance, thus having the least uncertainty in the water level data. Even with this approach, there are still uncertainties in the water level data because of uncertainty in the RTK data (1.5 cm) and in the manual measurements (3 cm). During neap tide, the water level differences between the backwater and the forest fringe stay below 10 cm (Figure 30) thus the uncertainty possibly has a major impact. Additional uncertainty by moving the frame creates an estimated total uncertainty in the order of 0.1 meters, greater than the (currently estimated) water level difference between Awa di Lodo and the forest fringe. Therefore, it is important to reduce the uncertainty of the water levels by not moving the frame in the field and to do multiple measurements on the instrument height to reduce the manual and RTK uncertainty.

The TCMs were attached to pavers and located on the bottom of creeks and in the open water of Lac Bay. The magnitude and direction of the flow depend on the exact location of the TCM, especially for the ones located in the creeks. Velocity deviations over the width, depth and length of the creek are present. The magnitude of the uncertainty is likely within a few cm/s. In this study, the velocities are used to assess the order of magnitude of the flow in the mangrove creeks. Thus the uncertainty has no major impact on the results and conclusions of this study.

Correction for atmospheric pressure

While in Bonaire, most instruments had to be checked every two weeks, batteries were replaced, data was extracted and later the instruments were placed back into the field. This creates gaps in the time series data. This gap is also present in the data of the HOBO that measured the air pressure. To still be able to create continuous time series of the pressure sensors deployed under water, the data missing from the HOBO is interpolated when no air pressure data is available. This results in slight inaccuracies in the eventual water depth for the other monitoring stations. Since the water pressure fluctuations are much greater than pressure fluctuations induced by the air, this inaccuracy is considered acceptable. However, in Awa di Lodo the water pressure fluctuations are much smaller and the air pressure fluctuations do create significant pressure changes. Since the air pressure HOBO and the water pressure HOBO in Awa di Lodo were installed and removed simultaneously, this correction did not influence the eventual water level data of Awa di Lodo. However, it is important to measure the atmospheric pressure since the local change in air pressure is great enough to influence the eventual computed water level derived from the pressure sensors in the water.

8. Conclusions

This study focuses on the hydrodynamic properties of Lac Bay and the contribution of creeks to the tidal exchange between the open water and the backwater (Awa di Lodo). The presence of islands in the mangrove forest and the presence of mangrove vegetation increases the flow resistance and induces complex flow patterns through the area.

*What **physical characteristics** affect the tidal dynamics of the Lac Bay mangroves?*

Lac Bay's hydrodynamics are driven by the tides. The lunisolar diurnal tidal constituent (K1) is the dominant tidal constituent, followed by the principal lunar diurnal tidal constituent (O1) and the principal lunar semi-diurnal tidal constituent (M2). Together, the tidal constituents form a diurnal tide in Lac. This diurnal tide has variations in the maximum tidal range between the different spring-neap cycles, ranging from 34 to 46 centimetres. As a result, it is important to analyse data of multiple spring-neap cycles to obtain an understanding of the hydrodynamics of the system. When the tidal wave enters and leaves Lac Bay, the open water area in front of the mangrove forest moves up and down uniformly. For the tidal wave to reach the backwater of the mangrove forest, Awa di Lodo, it has to surpass the islands and overcome the increased drag of the mangrove trees. Because of this increased flow resistance, the occurrence of high tide in Awa di Lodo has an average delay of more than 4 hours with respect to the high tides at the forest fringe.

*What are the **spatial and temporal effects** of the tidal dynamics in the Lac Bay mangroves?*

Awa di Lodo itself behaves like a bathtub, it gets filled by the flood tide and rainwater, and drains due to the ebb tide and evaporation. Ebb tidal discharge out of the area is slower than flood tidal discharge into the area. This occurs because during high water, water flows into Awa di Lodo via sheet and creek flow, while during low water it mainly leaves the area via creek flow. If the tidal range is large enough (during spring tide), the water level in Awa di Lodo does not drop to the low water level because of this delayed discharge and it gets filled further during consecutive tides. During neap tides, the tidal range is not large enough and Awa di Lodo continues to drain. When the water level at the forest fringe is 5-8 cm higher than the water level in Awa di Lodo, the flow direction in the east creek system reverses from the ebb direction into the flood direction. The west creek system is poorly connected to Awa di Lodo and reversed the flow direction when the water level difference is between -10 and 0 cm. This water level difference can be negative due to the poor connection of the west creek system to Awa di Lodo. In general, the magnitude of the flow velocity in the creeks depends on the water level difference between the open water and Awa di Lodo, meaning that a larger water level difference induces larger flow velocities.

Awa di Lodo is subject to a flood dominant tidal duration asymmetry: the water level rises faster than it declines due to the contribution of sheet flow during flood. It was found that the west creek shows a flood dominant peak velocity asymmetry, while the east creek faces a change of the peak velocity asymmetry over the spring-neap cycle. During neap tide, the measurement station located in the east creak showed an ebb dominant peak velocity asymmetry, while during spring tide the peak velocity asymmetry was mostly flood dominant. It is shown to be important to take measurements lasting multiple spring-neap cycles because effects like the movement of the tidal wave, tidal asymmetry and most other characteristics of the tidal dynamics differ between spring-neap cycles. Smothering of the coral reef, located at the opening of the bay, because the sediments wash out from Awa di Lodo over time, is unlikely to happen. The sediments are more likely to end up on the vegetated, flood dominant, vegetated bed of the mangrove forest.

*To what extent do **creeks** contribute to the **tidal exchange** in the Lac Bay mangroves and can the tidal exchange be increased by creek restoration?*

The model simulations of the tidal dynamics in Lac Bay in which creeks were removed, clearly showed the importance of the creeks for the tidal exchange and the water levels in Awa di Lodo. A 77% reduction in tidal exchange is observed when there are no creeks present in the model. In other model simulations with creek adaptation, it was found that changing the depth of the creeks has a similar effect on the tidal exchange between the bay and Awa di Lodo as changing the width of the creeks. Moreover, extending the east creek system had limited effect on the modelled tidal exchange. The most effective measure to increase the tidal exchange across the mangroves is to restore creek connections into Awa di Lodo that are currently not present. The creation of a completely new creek decreased the residence time by 32% from 4.15 to 2.38 days, but it would also be the most labour and cost-intensive intervention. The extension of the centre creek is the second-best alternative in terms of decreasing the residence time (a 21% decrease from 4.15 to 3.27 days) and would be less labour and cost-intensive than the construction of an entirely new creek. This would make the intervention to extend the centre creek the most viable option to increase the tidal exchange substantially.

9. Recommendations

Based on the findings of this thesis, some recommendations are made regarding future research and interventions to increase the tidal exchange in Lac Bay.

Increase of the tidal exchange

Based on the model results of the creek restoration scenarios, the best way to increase the tidal exchange in the mangroves of Lac Bay is to restore old creeks or open new creeks to connect with Awa di Lodo with the open water in the bay. Recreating the 'new creek' scenario would require digging a new creek over a large distance, which would be a time-consuming effort. The faster approach would be to extend the centre creek towards Awa di Lodo. If this connection is made, the sediment concentrations in the creek should be monitored. Based on the results of this study, it is unlikely that the sediments from Awa di Lodo will flush out to the open water of Lac Bay. The sediment concentrations in the creek should be monitored to make sure the sediment does not flush out to the open water of Lac Bay and smothers the coral reef over time. It was found that extending the east creek system likely has a limited effect on the tidal exchange. Widening and deepening the creeks does increase the tidal exchange, but has a smaller effect than creating a new connection to Awa di Lodo.

Suggestions for model improvement

The model results can be improved by the inclusion of more processes and by increasing the accuracy and spatial resolution of the bed level and vegetation data in the model. Creeks are now implemented into the model by using one cross-section for the entire area. Spatial variations in creek dimensions will enhance the flow resistance in the creeks and can improve the accuracy of the model as the discharge through creeks and thus the tidal exchange is currently overestimated. Processes that also could be included to have a more complete water balance in the model are precipitation, evaporation, and precipitation-induced runoff and groundwater flows. An average annual potential evaporation of 2600 mm creates a significant outflow of Awa di Lodo influencing the salinity and water levels. All water from the catchment flowing into Lac coming directly or indirectly from precipitation is likely also an important factor in the salinity values of Awa di Lodo.

More data on the bed level of the mangrove forest would also increase the accuracy of the model since a few decimetres of change of the bed level can create large deviations in the local water depth and hence the tidal exchange. The tidal exchange during the rising stage of the first spring-neap cycle is overestimated since the simulated water level within Awa di Lodo rises much faster than the water level measured during the field study. Increasing the bed level of the mangrove forest is advised as this would decrease the volume of water flowing into Awa di Lodo while likely keeping the same values for the water flowing out of Awa di Lodo, as ebb flows are mostly directed through the creeks (and the model already showed good resemblance on this aspect with the measurement data).

The Delft3D model used in this study can be further improved to create more accurate results. Calibrating the model would increase the accuracy of the model. Calibrating can be done for parameters like tidal asymmetry, the maximum flow speeds, the delay of high tide and water levels by changing the bottom roughness. Calibrating for the water levels is the most useful since increasing the tidal exchange is the most important factor and can easily be linked to the water level in Awa di Lodo (chapter 6). Changing the vegetation parameters has proven to be important for the tidal exchange. Making a spatial differentiation of the vegetation characteristics is recommended because the variations of different trees and species and their impacts on the hydrodynamics vary greatly across the area.

One of the bottlenecks in using this model effectively is the computational time. A balance has to be found between grid refinement and the computational time. Using subgrid modelling, which parameterizes the effects of certain dynamics on smaller scales based on the values of larger scales via statistical relations (Herring, 1979), decreases the computational time of the model without losing much accuracy.

Suggestions for future field monitoring

In future monitoring efforts on the hydrodynamics of Lac Bay, the following suggestions could be considered. In the open water of Lac, only one pressure sensor is required to monitor the water level, since the water level moves more or less uniformly up and down. Along the creeks, multiple TCMs could be deployed to observe characteristics like tidal asymmetry, propagation of the tidal wave and peak velocities throughout the creeks. Especially monitoring of flow velocities of sheet flow inside the mangrove forest would greatly increase the insights into the hydrodynamics of Lac. These measurements could contribute to the calibration of the model. Other locations of interest for TCM and HOBO sensors could be in between the islands within the mangroves. By doing these estimations an approximation of how much water actually moves into Awa di Lodo can be made which will support an assessment of the tidal exchange.

On top of the instruments used in this study, salinity measurements throughout Lac during at least two spring-neap tidal cycles would be valuable. This will show the extent of the reduced salinity by the tidal exchange through the creeks in Awa di Lodo, will show the effect of precipitation events and will provide more insight into one of the most important stressors for mangrove vegetation: salinity. By taking multiple measurements in Awa di Lodo, the circulation through Lac will become clear as well. It is known that there is poor mixing in Awa di Lodo and that the creeks have a limited area of influence in Awa di Lodo. Therefore, increasing the tidal exchange may still have a limited effect. To see if the circulation increases or decreases during certain tidal cycles would help create future strategies to eventually increase the circulation in Lac Bay. Measuring the salinity during the rainy season and the dry season creates further insights into the temporal changes in the dynamics of the area.

Sediment transport depends on sediment characteristics, fluid characteristics and flow characteristics (Nakato, 1990). With the use of sediment transport formulas, the critical threshold of sediment movement can be estimated. Using our knowledge of the creeks, an indication can be given if sediment transport is expected to happen in the mangrove creeks of Lac Bay for various creek restoration scenarios. Sediment and channel properties can be analysed to see if the current velocity is great enough reach to the thresholds of transport. For this analysis, the sediment characteristics must be known. If these are known, sediment dynamics can also be added to the Delft3D model, allowing for model simulations of the sediment fluxes throughout Lac. This will help to support claims on the movement of sediments in the different creek restoration scenarios.

10. References

Adame, M. F., Connolly, R. M., Turschwell, M. P., Lovelock, C. E., Fatoyinbo, T., Lagomasino, D., Goldberg, L. A., Holdorf, J., Friess, D. A., Sasmito, S. D., Sanderman, J., Sievers, M., Buelow, C., Kauffman, J. B., Bryan-Brown, D., & Brown, C. J. (2021). Future carbon emissions from global mangrove forest loss. *Global Change Biology*, *27*(12), 2856–2866. https://doi.org/10.1111/gcb.15571

Alongi, D. M. (2009). *The Energetics of Mangrove Forests*. Springer Netherlands. https://doi.org/10.1007/978-1-4020-4271-3

Ashton, E. C., & Macintosh, D. J. (2002). *Preliminary assessment of the plant diversity and community ecology of the Sematan mangrove forest, Sarawak, Malaysia*.

Augustinus, P. G. E. F. (2005). *Een voorstudie van de te verwachten milieueffecten naar aanleiding van de bouw en exploitatie van een hotelschool, annex hotel, langs de westoever van het Lac, Bonaire*.

Balke, T., & Friess, D. A. (2016). Geomorphic knowledge for mangrove restoration: A pan-tropical categorization. *Earth Surface Processes and Landforms*, *41*(2), 231–239. https://doi.org/10.1002/esp.3841

Baptist, M. J., Babovic, V., Uthurburu, J. R., Keijzer, M., Uittenbogaard, R. E., Mynett, A., & Verwey, A. (2007). On inducing equations for vegetation resistance. *Journal of Hydraulic Research*, *45*(4), 435–450. https://doi.org/10.1080/00221686.2007.9521778

Bennett, E. L., & Reynolds, C. J. (1993). The value of a mangrove area in Sarawak. In *Biodiversity and Conservation* (Vol. 2).

Borst, L., & de Haas, S. A. (2005). *Hydrological Research Bonaire: A hydrogeological investigation of Bonaire's watersystem* . https://www.dcbd.nl/document/hydrological-research-bonaire

Cannon, D., Kibler, K., Donnelly, M., McClenachan, G., Walters, L., Roddenberry, A., & Phagan, J. (2020). Hydrodynamic habitat thresholds for mangrove vegetation on the shorelines of a microtidal estuarine lagoon. *Ecological Engineering*, *158*, 106070. https://doi.org/10.1016/j.ecoleng.2020.106070

Davaasuren, N., & Meesters, E. H. W. G. (2012). *Extent and health of mangroves in Lac Bay Bonaire using satellite data*. www.imares.wur.nl

Debrot, A. O., Slijkerman, D., & Meesters, E. (2010). *Lac Bonaire- Restoration action spear points*. https://www.researchgate.net/publication/48185028

Debrot, A. O., Wentink, C., & Wulfsen, A. (2012). *Baseline survey of anthropogenic pressures for the Lac Bay ecosystem, Bonaire*. www.imares.wur.nl

Deltares. (2022a). *Delft3D FM Suite, RGFGRID User Manual*. https://content.oss.deltares.nl/delft3d/manuals/RGFGRID_User_Manual.pdf

Deltares. (2022b). *Delft3D 3D/2D modelling suite for integral water solutions User Manual QUICKIN*.

Dronkers, J. (1986). Tidal asymmetry and estuarine morphology. *Netherlands Journal of Sea Research*, *20*(3), 117–131.

Duke, N. C. (2017). Mangrove Floristics and Biogeography Revisited: Further Deductions from Biodiversity Hot Spots, Ancestral Discontinuities, and Common Evolutionary Processes. In

Mangrove Ecosystems: A Global Biogeographic Perspective (pp. 17–53). Springer International Publishing. https://doi.org/10.1007/978-3-319-62206-4_2

Engel, S. (2017). *Lac bay depths (GIS)*. https://www.dcbd.nl/document/lac-bay-depths-gis

Erdmann, W., & Scheffers, A. (2006). *Mangrove Population of Lac (Bonaire) 1961 and 1996*. https://www.dcbd.nl/document/mangrove-population-lac-bay-bonaire-1961-1996

Friess, D. A., Yando, E. S., Alemu, J. B., Wong, L.-W., Soto, S. D., & Bhatia, N. (2020). Ecosystem services and disservices of mangrove forests and salt marshes. *Oceanography and Marine Biology*.

Furukawa, K., & Wolanski, E. (1996). Sedimentation in Mangrove Forests. *Mangroves and Salt Marshes*, *1*(1), 3–10. https://doi.org/10.1023/A:1025973426404

Garmin. (2022, April 30). *eTrex® 10*. https://www.garmin.com/nl-NL/p/87768

Gijsman, R., Horstman, E. M., van der Wal, D., Friess, D. A., Swales, A., & Wijnberg, K. M. (2021). Nature-Based Engineering: A Review on Reducing Coastal Flood Risk With Mangroves. In *Frontiers in Marine Science* (Vol. 8). Frontiers Media S.A. https://doi.org/10.3389/fmars.2021.702412

Grontmij, & Sogreah. (1968). *Water and land resources development plan for the islands of Aruba, Bonaire and Curaçao*.

Guo, L., Wang, Z. B., Townend, I., & He, Q. (2019). Quantification of Tidal Asymmetry and Its Nonstationary Variations. *Journal of Geophysical Research: Oceans*, *124*(1), 773–787. https://doi.org/10.1029/2018JC014372

Herring, J. R. (1979). Subgrid Scale Modeling — An Introduction and Overview. In B. E. and S. F. W. and W. J. H. Durst Franz and Launder (Ed.), *Turbulent Shear Flows I* (pp. 347–352). Springer Berlin Heidelberg.

Horstman, E. M., Bryan, K. R., & Mullarney, J. C. (2021). Drag variations, tidal asymmetry and tidal range changes in a mangrove creek system. *Earth Surface Processes and Landforms*, *46*(9), 1828–1846. https://doi.org/10.1002/esp.5124

Horstman, E. M., Dohmen-Janssen, C. M., Bouma, T. J., & Hulscher, S. J. M. H. (2015). Tidal-scale flow routing and sedimentation in mangrove forests: Combining field data and numerical modelling. *Geomorphology*, *228*, 244–262. https://doi.org/10.1016/j.geomorph.2014.08.011

Horstman, E. M., Dohmen-Janssen, C. M., & Hulscher, S. J. M. H. (2013). Flow routing in mangrove forests: A field study in Trang province, Thailand. *Continental Shelf Research*, *71*, 52–67.

Hummelinck, P. W., & Roos, P. J. (1969). Een natuurwetenschappelijk onderzoek gericht op het behoud van het Lac op Bonaire. *Nieuwe West-Indische Gids/New West Indian Guide*, 1–28.

Jennerjahn, T. C., Gilman, E., Krauss, K. W., Lacerda, L. D., Nordhaus, I., & Wolanski, E. (2017). Mangrove Ecosystems under Climate Change. In *Mangrove Ecosystems: A Global Biogeographic Perspective* (pp. 211–244). Springer International Publishing. https://doi.org/10.1007/978-3-319-62206-4_7

KNMI. (2022). *Uurgegevens van het Caribisch gebied*. https://www.knmi.nl/nederland-nu/klimatologie/uurgegevens_Caribisch_gebied

Kumbier, K., Hughes, M. G., Carvalho, R. C., & Woodroffe, C. D. (2022). Intertidal wetland geomorphology influences main channel hydrodynamics in a mature barrier estuary. *Estuarine, Coastal and Shelf Science*, *267*. https://doi.org/10.1016/j.ecss.2022.107783

Lee, S. Y. (1999). Tropical mangrove ecology: Physical and biotic factors influencing ecosystem structure and function. *Australian Journal of Ecology*, *24*, 355–366.

Leica Geosystems. (2022, April 30). *Leica Viva GS14*. https://leica-geosystems.com/nl-nl/products/gnss-systems/smart-antennas/leica-viva-gs14

Lodder, T. S. C. (2013). *Identifying the niche of four mangrove species along environmental gradients*. WUR.

Lott, C. E. (2001). *Lac Bay: Then and Now…*. https://www.dcbd.nl/document/lac-bay-then-and-now%E2%80%A6-historical-interpretation-environmental-change-during-1900s-site

Lowell Instruments LLC. (2022, April 30). *TCM-4 Shallow Water Tilt Current Meter*. https://lowellinstruments.com/products/tcm-4-tilt-current-meter/

Lucas, R., Lule, A. V., Rodríguez, M. T., Kamal, M., Thomas, N., Asbridge, E., & Kuenzer, C. (2017). Spatial Ecology of Mangrove Forests: A Remote Sensing Perspective. In *Mangrove Ecosystems: A Global Biogeographic Perspective* (pp. 87–112). Springer International Publishing. https://doi.org/10.1007/978-3-319-62206-4_4

MacRae, D., & de Meyer, K. (2006). *Bonaire National Marine Park Management Plan*. https://www.dcbd.nl/document/bonaire-national-marine-park-management-plan-2006#:~:text=The%20plan%20specifies%20management%20goals,of%20current%20and%20future%20generations.

Mazda, Y., Kanazawa, N., & Wolanski, E. (1995). Tidal asymmetry in mangrove creeks. *Hydrobiologia*, *295*(1–3), 51–58. https://doi.org/10.1007/BF00029110

Mazda, Y., Wolanski, E., King, B., Sase, A., Ohtsuka, D., & Magi, M. (1997). Drag force due to vegetation in mangrove swamps. *Mangroves and Salt Marshes*, *1*(3), 193–199.

Nakato, T. (1990). Tests of Selected Sediment-Transport Formulas. *Journal of Hydraulic Engineering*, *116*(3), 362–379. https://doi.org/10.1061/(ASCE)0733-9429(1990)116:3(362)

Onset. (2022, April 30). *HOBO Water Level (13 ft) Data Logger*. https://www.onsetcomp.com/products/data-loggers/u20l-04/

Ramsar. (2022). *Annotated List of Wetlands of International Importance*. https://rsis.ramsar.org/ris/199

rbr-global. (2022a, April 30). *RBRsolo^3 | Single Channel Logger*. https://rbr-global.com/products/compact-loggers/rbrsolo

rbr-global. (2022b, April 30). *Standard | Tide & Wave Loggers*. https://rbr-global.com/products/standard-loggers/standard-tide-wave

Regensburg, T. (2013). *How channel dimensions relate to the erosivity of tidal flows in mangrove channels in Lac Bay, Bonaire*. https://www.dcbd.nl/document/how-channel-dimensions-relate-erosivity-tidal-flows-mangrove-channels-lac-bay-bonaire-bsc

Rønde, V. (2013). *Investigation of subsurface freshwater flow from southern Bonaire into Lac bay*. https://www.dcbd.nl/document/investigation-subsurface-freshwater-flow-southern-bonaire-lac-bay

Senger, D. F., Saavedra Hortua, D. A., Engel, S., Schnurawa, M., Moosdorf, N., & Gillis, L. G. (2021). Impacts of wetland dieback on carbon dynamics: A comparison between intact and degraded mangroves. *Science of the Total Environment*, *753*. https://doi.org/10.1016/j.scitotenv.2020.141817

Slijkerman, D., Peachey, R., & Hausmann, P. (2011). *Eutrophication status of Lac, Bonaire, Dutch Caribbean Including proposals for measures*. www.imares.wur.nl

Smithsonian. (2018, April). *Mangroves*. https://ocean.si.edu/ocean-life/plants-algae/mangroves

Snedaker, S. C. (1982). *Mangrove species zonation: why?* (pp. 111–125). https://doi.org/10.1007/978-94-009-8037-2_8

STINAPA. (2014). *Ecologisch herstel Lac gebied en overig zuidelijk kustgebied*.

Taylor, N. G., Grillas, P., Smith, R. K., & Sutherland, W. J. (2021). *Marsh and Swamp Conservation Global evidence for the effects of interventions to conserve marsh and swamp vegetation CONSERVATION EVIDENCE SERIES SYNOPSES*. https://www.conservationevidence.com/

Teledyne Marine. (2022, April 30). *Streampro ADCP*. http://www.teledynemarine.com/streampro

van Loon, A. F., te Brake, B., van Huijgevoort, M. H. J., & Dijksma, R. (2016). Hydrological classification, a practical tool for mangrove restoration. *PLoS ONE*, *11*(3). https://doi.org/10.1371/journal.pone.0150302

van Moorsel, G., & Meijer, M. (1993). *Base-line ecological study van het Lac op Bonaire*. https://www.researchgate.net/publication/328007211

van Winsen, S. (2013). *Hydrology and Quantitative Water Management*.

van Zee, R. (2022). *Hydraulic circulation of the tides in Lac Bay, Bonaire [Unpublished manuscript]*.

Vreugdenhil, I. (2013). *Modelling Mangrove growth and salinity: a semi-arid case study*. https://www.dcbd.nl/document/modelling-mangrove-growth-and-salinity-semi-arid-case-study

Wentink, C., & Wulfsen, A. (2011). Recreational and land use survey for Lac Bay Bonaire. *Institute for Marine Resources & Ecosystem Studies Report, Wageningen UR*. https://www.dcbd.nl/document/recreational-and-land-use-survey-lac-bay-bonaire-study-towards-mapping-human-activities-lac

Willets, B. B., & Hardwick, R. I. (1993). Stage dependency for overbank flow in meandering channels. *Proceedings of the Institution of Civil Engineers - Water, Maritime and Energy*, *101*(1), 45–54. https://doi.org/10.1680/iwtme.1993.22989

Wösten, J. H. M. (2013). *Ecological rehabilitation of Lac Bonaire by wise management of water and sediments*. https://www.dcbd.nl/document/ecological-rehabilitation-lac-bonaire-wise-management-water-and-sediments